The Field of Neighbourhood (FON) - ein phänomenologischer Modellansatz zur Beschreibung von Nachbarschaftsbeziehungen sessiler Organismen

Hanno Hildenbrandt

Vorgelegt dem Fachbereich 2 (Biologie/Chemie) der Universität Bremen als Dissertation
zur Erlangung des Grades eines Doktors der Naturwissenschaften (Dr. rer. Nat.).

Bremen 2002

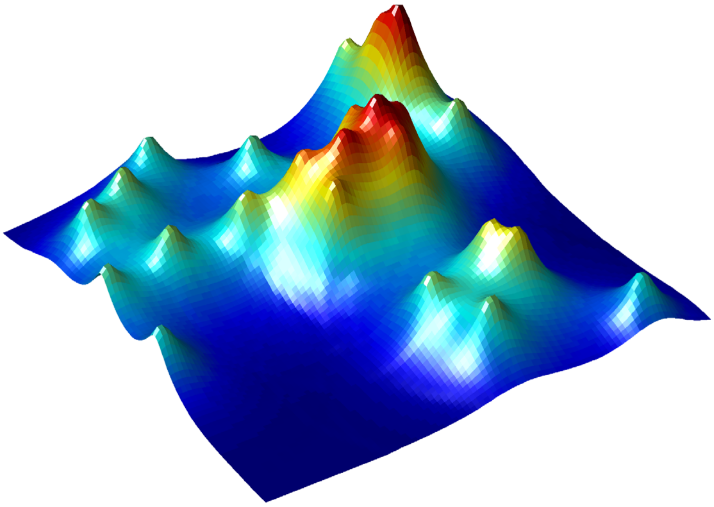

Tag des öffentlichen Kolloquiums: 24.07.2003

Erster Gutachter: Prof. Dr. Ulrich Saint-Paul

Zweiter Gutachter: Prof. Dr. Christian Wissel

Vorwort

Im Rahmen des deutsch-brasilianischem Kooperations-Projektes MADAM (Mangrove Dynamics and Management) (Berger et al., 1999; Lara et al., 1999; Thüllen & Berger, 2000) wurde der „Field of Neighbourhood“-Ansatz, kurz FON, von uns ursprünglich als Basis für ein Modell entwickelt, das der Untersuchung der Dynamik von Mangrovenwäldern dient. Der Ansatz ermöglichte uns eine phänomenologische Beschreibung lokaler intra- wie interspezifischer Konkurrenz zwischen den einzelnen Mangrovenbäumen. Es stellte sich dann heraus, dass FON ein überraschend großes Potential für die individuen-basierte, räumlich explizite Modellierung in einem weiter gefassten Kontext aufweist. Diese kumulative Dissertation besteht aus fünf Publikationen, die sich mit dem neuen Ansatz befassen, seine Vor- und Nachteile gegenüber bestehenden Ansätzen untersuchen und Anwendungsmöglichkeiten aufzeigen.

Kapitel I gibt eine kurze methodische Einführung in die praktische Anwendung des „Field of Neighbourhood“-Ansatzes und richtet sich vor allem an Leser, die eigene Modelle auf FON-Basis entwickeln wollen und daher genauer wissen müssen, worin sich FON von den bekannten Ansätzen unterscheidet.

In Kapitel II,1 wird der „Field of Neighbourhood“-Ansatz und das darauf aufsetzende Simulationsmodell KiWi im Detail vorgestellt. Der Artikel geht auf die Gründe ein, die uns dazu bewogen haben, nicht auf bestehende und etablierte Ansätze zurück zu greifen. Für die näherungsweise Berechnung der im „Field of Neighbourhood“-Ansatz auftretenden Integrale präsentieren wir einen generischen Algorithmus, der in vielen Fällen als Grundlage für die Umsetzung von FON in ein Computerprogramm genügen sollte.

In der in dieser Arbeit verwendeten Fassung ist das Simulationsmodell KiWi ein zwar funktionierendes, zugleich aber minimales Referenz-Modell, das primär als Testumgebung für den „Field of Neighbourhood“-Ansatz entworfen wurde. Dennoch können wir zeigen, dass die Kombination FON/KiWi ein geeignetes Werkzeug für die Modellierung dynamischer Prozesse in (Mangroven-) Wäldern und für die Untersuchung von Waldstrukturen ist. Hauptargument dafür sind die realistischen Biomasse-Dichte-Trajektorien, die wir bei der Simulation von Selbstausdünnungs-Prozessen (Entwicklung von Baumkohorten) aufnehmen konnten. Um Trajektorien zu erhalten, die theoretischen Überlegungen und empirischen Untersuchungen standhalten, muss das Modell vieles richtig und darf nur wenig falsch machen: entscheidend ist ein stimmiges Zusammenspiel zwischen räumlicher Anordnung, Wachstum und Mortalität. Ohne ein „gutes“ Konkurrenzmodell ist dies nicht zu erreichen (Berger, Hildenbrandt, 2000).

Kapitel II,2 greift die Selbstausdünnungs-Thematik auf und vertieft die Diskussion der am Modell aufgenommenen Biomasse-Dichte-Trajektorien. Uns gelingt die Verknüpfung zweier wichtiger ökologischer Muster: das des Verlaufs der Biomasse-Dichte-Trajektorie und das der für ein bestimmtes Entwicklungsstadium charakteristischen Größenverteilung (bzw. deren Schiefe) innerhalb einer Baumkohorte. Aus empirischer Sicht ist dies besonders interessant, weil hier ein dynamisches Muster (die Trajektorie) mit einem statischen (der Größenverteilung) verbunden wird. Als bestimmend für die Ausprägung beider Muster können wir – im Modell-Kontext - die individuelle Konkurrenzstärke ausmachen (Berger, Hildenbrandt, 2001).

Mit der Möglichkeit, die gesamte Biomasse-Dichte-Trajektorie als Ergebnis eines dynamischen Selbstausdünnungs-Prozesses zu beschreiben, fanden wir uns mitten in einer der am kontroversesten geführten Diskussionen in der Ökologie wieder: die Auseinandersetzung um die Frage, ob es ein „Gesetz der Selbstausdünnung“ gibt und wenn ja, wie es auszusehen hat. Kurz zusammengefasst geht es darum, dass bei vielen höheren Pflanzen ein linearer Zusammenhang zwischen den Logarithmen der mittleren Biomasse und der Bestandsdichte festgestellt wurde, beide also über ein einfaches Potenzgesetz verknüpft sind. Da der empirische Wert des Exponenten häufig ungefähr -3/2 erreicht, wurde dieser Zusammenhang als „*-3/2 power law of self-thinning*“ bekannt (Yoda et al., 1963). Yoda begründete sein „Gesetz“ durch geometrische Überlegungen, die im Grenzfall, d.h. bei optimaler Raumausnutzung durch nahezu gleich große Pflanzen, zu einem theoretischen Exponenten von -3/2 führen (s.a. Lonsdale, 1990). Ein anderer theoretischer Exponent von -4/3 wurde später allometrisch motiviert, wiederum im Grenzfall, diesmal bei optimaler Ressourcenausnutzung durch die Pflanzen (White, 1981; Enquist et al., 1999; Enquist & Niklas, 2001). So oft ein bestimmter linearer Zusammenhang zwischen Biomasse und Bestandsdichte empirisch belegt werden konnte, so oft wurde er auch wiederlegt (Weller, 1987; Osawa et al., 1989). Extrem große negative Exponenten von bis zu -∞ wurden z.B. bei Arten gefunden, die fast ausschließlich in vertikaler Richtung wachsen, also eine eher unübliche Morphologie aufweisen (Miyanishi et al. 1979; Ellison, 1989). Obwohl z.T. heftig verteidigt, kann offenbar keines der diskutierten Selbstausdünnungs-„Gesetze“ die erhoffte universelle Gültigkeit für sich beanspruchen.

In Kapitel II,3 nähern wir uns der theoretischen Fragestellung von einer anderen Seite. Nicht von „oben“ (dem optimalen Grenzfall), sondern von „unten“ mit einem Modell (FON/KiWi), das die Dynamik der Selbstausdünnungs-Prozesse nachbildet. Auf den Ergebnissen von Kapitel II,2 aufbauend zeigen wir, wie die Steigung der Biomasse-Dichte-Trajektorie vom Entwicklungsstadium der Kohorte abhängt und dort, wo überhaupt ein konstantes Potenzgesetz erwartet werden kann, der Exponent mit der Konkurrenzstärke der modellierten Pflanzen variiert. Die Suche nach einem universellen Potenzgesetz erscheint dadurch müßig. Dagegen können die in der Natur gefundenen Trajektorien plausibel durch die Dynamik des Selbstausdünnungs-Prozesses erklärt werden und die Varianz der empirischen Exponenten auf unterschiedliche Konkurrenzstärken zurückgeführt werden. Das ist ein wichtiger Schritt hin zu einer einheitlichen „Theorie der Selbstausdünnung“, die allein auf der Hypothese lokaler Konkurrenz aufbaut. Tatsächlich ist lokale Konkurrenz unter Nachbarn etwas, was allen selbstausdünnenden Pflanzenpopulationen unterstellt werden kann (Berger & Hildenbrandt, 2002).

Kapitel II,4 geht der Frage nach, in wie weit FON ein geeignetes Werkzeug für die Untersuchung bzw. Darstellung unterschiedlicher Konkurrenz-Modi (symmetrisch, asymmetrisch) ist. Asymmetrische Konkurrenz wird für die

Ausbildung der Größen- und Biomassenverteilungen in Pflanzenpopulationen verantwortlich gemacht und hat auch sonst einen erheblichen Einfluss auf die Populationsdynamik (Weiner, 1990). Der Zusammenhang wird aber überlagert durch andere Einflüsse wie die der räumlichen Anordnung, Dichte, Ressourcen-Verfügbarkeit und Mortalität. Die theoretische Untersuchung asymmetrischer Konkurrenz ist eine Domäne der ZOI-Modelle („Zone of Influence“). Grundidee ist bei diesen Modellen, die vorhandenen Ressourcen geeignet unter den Individuen aufzuteilen, sobald sich deren Einflusszonen überlappen. Mit der Wahl einer geeigneten Aufteilung wird der Konkurrenz-Modus festgelegt: z.B. impliziert „der Größere bekommt alles“ asymmetrische Konkurrenz und „die Ressourcen werden unabhängig von der Größe gleichmäßig aufgeteilt“ symmetrische Konkurrenz. In letzter Zeit kamen Zweifel auf, ob es überhaupt Sinn macht, die Ausprägungen von Konkurrenz-Modi mit Modellen zu untersuchen, die einen Konkurrenz-Modus implizit vorgeben (Schwinning & Weiner, 1998).

Der Artikel zeigt, dass im „Field of Neighbourhood“-Ansatz der Konkurrenz-Modus nicht vorgegeben werden muss[1], und sich das Bild asymmetrischer Konkurrenz aus der Interaktion benachbarter Individuen ergibt. Zudem wird gezeigt, wie Konkurrenzstärke durch die Form der Nachbarschaftsfelder eingestellt werden kann. In dem Beitrag wird eine jüngst entwickelte Metrik zur quantitativen Bestimmung asymmetrischer Konkurrenz angewandt, mit dessen Hilfe die Ergebnisse abgestützt werden konnten (Bauer, Wyzomirski, Berger, Hildenbrandt, Grimm, 2002).

Kapitel II,5 positioniert den „Field of Neighbourhood“-Ansatz in die gegenwärtige Landschaft der individuen-basierten Modellierung von Pflanzenpopulationen. Durch die einfache Anwendung von FON wie durch die Erfolge bei der Beschreibung und Erklärung der Selbstausdünnung ermuntert, erlauben wir uns, FON als möglichen Standard der individuen-basierten Modellierung von Pflanzenpopulationen vorzuschlagen (Berger, Hildenbrandt, Grimm, 2002).

---

[1] Die Anzahl möglicher Nachbarschaftsfelder ist prinzipiell unbegrenzt. Wir möchten daher nicht ausschließen, dass es Felder gibt, mit denen sich auch Konkurrenz-Modi vorgeben lassen. Untersucht wurden hier Felder, die ihre Form mit der Individuen-Größe nur über die Fläche ändern, auf der sie definiert sind.

BERGER U., HILDENBRANDT H., 2000: *A new approach to spatially explicit modelling of forest dynamics: spacing, ageing and neighbourhood competition of mangrove trees*; Ecological Modelling 132:287-302.

Der „Field of Neighbourhood"-Ansatz wurde von mir auf Anregung von Uta Berger entwickelt, das Simulationsmodell KiWi von mir und Uta Berger in etwa gleichen Teilen. Der Artikel wurde von Uta Berger und mir gemeinsam konzipiert und verfasst (Kapitel II,1).

BERGER U., HILDENBRANDT H., 2001: *Nachbarschaftsfelder zur Untersuchung ökologischer Interferenzen – vom Anfang und Ende der Selbstausdünnung*; In: F. Jopp & G. Wiegmann (eds.), Rolle und Bedeutung von Modellen für den Erkenntnisprozeß in der Ökologie. Theorie in der Ökologie Band 4, 19-30.

Dieser Artikel wurde von Uta Berger und mir gemeinsam konzipiert und verfasst (Kapitel II,2).

BERGER U., HILDENBRANDT H., 2002: *About the competition strength of individual trees and its influence on the curvature of the biomass-density-trajectory of the whole cohort*; Plant Ecology, in press.

Der Beitrag wurde von Uta Berger und mir gemeinsam konzipiert und verfasst (Kapitel II,3).

BAUER S., WYSZOMIRSKI T., BERGER U., HILDENBRANDT H., GRIMM V. 2002: *Asymmetric competition as a natural outcome of neighbour interactions among plants: results from the field-of-neighbourhood modelling approach*; Plant Ecology, in press.

Modell und Experimente wurden von Silke Bauer entworfen. Die Methode zur qualitativen Bestimmung asymmetrischer Konkurrenz stammt von Tomasz Wyszomirski. Konzipiert und verfasst wurde der Artikel vornehmlich von Silke Bauer und Volker Grimm. Mein Beitrag beschränkt sich neben dem Modellansatz auf die Implementierung des Modell-Kerns (Kapitel II,4).

BERGER U., HILDENBRANDT H., GRIMM V. 2002: *Towards a standard for the individual-based modeling of plant populations: self-thinning and the field-of-neighborhood approach*. Natural Resource Modeling 15:39-54.

Von Volker Grimm stammt die Idee, den Ansatz im Zusammenhang mit „Standards" für individuenbasierte Modelle zu diskutieren. Der Beitrag wurde zu gleichen Teilen von den Autoren konzipiert und verfasst (Kapitel II,5).

Inhalt

I Einleitung

Die Mangrove ist ein ungewöhnlich dynamisches und heterogenes Ökosystem zwischen Land und Meer. Im Mangrovenwald nahe Bragança im Norden Brasiliens, dem Untersuchungsgebiet des Forschungsprojektes MADAM, wechseln sich Gebiete mit unterschiedlichster Struktur und Artenzusammensetzung scheinbar regellos ab. Größere zusammenhängende Flächen, denen man eine Art „Gleichgewichtszustand" zuordnen könnte, sind selten - aber eben doch vorhanden. Dazwischen finden sich immer wieder degenerierte Flächen, die keinen oder nur Sekundärbewuchs aufzeigen. Zudem weisen Mangroven eine hohe morphologische Plastizität auf. Je nach Standort finden sich Bestände von mächtigen Bäumen mit einer Höhe von bis zu 30m oder kleinwüchsige Gruppen, die über eine Höhe von wenigen Metern nicht hinauskommen. Der Versuch einer Erklärung des Zustandekommens dieser vielfältigen räumlicher Muster ist eine Herausforderung an alle Beteiligten im MADAM-Projekt. Unser Modell zur Populationsdynamik in Mangrovenwäldern trägt dazu bei, die interdisziplinär gewonnenen Erkenntnisse zu integrieren und Hypothesen bezüglich der Entstehung der räumlichen Muster zu testen.

Bevor wir uns auf die Besonderheiten der Mangrove konzentrieren konnten, benötigen wir zunächst einen Modellansatz, der die Gemeinsamkeiten zu terrestrischen Wäldern abdeckt: wie auch immer die Prozesse aussehen mögen, die zu der Ausprägung der unterschiedlichen Muster führen, werden sie doch von einer „normalen" Populationsdynamik überlagert. Diese ist in der Mangrove, wie in terrestrischen Wäldern, von der Konkurrenz unter den einzelnen Pflanzen geprägt. Gesucht wurde hierfür ein flexibler Ansatz, der einfach zu handhaben, schnell zu berechnen und orthogonal zu den zu testenden Hypothesen sein sollte.

FON kombiniert Schlüsselelemente verschiedener Ansätze zur Beschreibung intra- wie interspezifischer Konkurrenz unter Pflanzen – und verwirft andere. Auf die Frage nach dem Warum gehen die in Kapitel II aufgeführten Artikel an verschiedenen Stellen ein. Diese Informationen sollen im folgendem gesammelt und wo nötig ergänzt werden.

1. Die Wurzeln von FON

Um der hohen individuelle Variabilität der Mangrovenpflanzen und der Kommunikation innerhalb eines interdisziplinärem Forschungsprojektes gerecht zu werden, wurde eine individuen-basierte Form der Modellierung gewählt (Huston et al., 1988; DeAngelis & Gross, 1992; Uchmanski & Grimm, 1996; Grimm, 1999). Individuen-basiert heißt hier, das jede einzelne Pflanze eine explizit zugewiesene Position erhält und ihre Zustandsvariablen wie Stammdurchmesser, Höhe, Alter usw. mit sich führt. Wesentlich beeinflusst wurde die Entwicklung von FON so vor allem durch zwei individuen-basierte und räumlich explizite Ansätzen, die beide einen kontinuierlichen Raum in Betracht ziehen: dem „Zone of Influence“-Ansatz und der „Ecological Field Theory“.

1.1 Zone of Influence (ZOI)

ZOI-Modelle umgeben die Pflanzen mit einer konzentrischen, kreisrunden Einflusszone (der „Zone of Influence“) um ihre Position, dessen Radius mit der Größe der Pflanze in Beziehung gesetzt wird, also die physikalische Ausdehnung der Pflanze reflektiert. Die Fläche der Einflusszone stellt die für die Pflanze verfügbaren Ressourcen dar. Zwei oder mehrere Pflanzen konkurrieren um Ressourcen, sobald sich ihre Einflusszonen überlappen. Wie die Ressourcen in solchen Überlappungsgebieten aufgeteilt werden, entscheiden so genannte Kollisionsregeln, die je nach betrachteter Ressource unterschiedlich kompliziert ausfallen (Gates & Westcott, 1978; Gates, 1982; Czaran & Bartha, 1992; Czaran, 1998). Eine der häufiger verwendeten „einfachen“ Kollisionsregeln ist die der gleichmäßigen Aufteilung der Ressourcen unter den beteiligten Nachbarn, die zur Beschreibung symmetrischer Konkurrenz verwendet wird (Weiner et al., 2001): wird ein Gebiet nur von einer Pflanze überdeckt, so bekommt diese alle Ressourcen; bei zwei oder mehr Pflanzen werden die Ressourcen zu gleichen Teilen aufgeteilt. Angewandt auf die Situation in Abb.1, können wir für die k-te Pflanze die Ressourcen berechnen, die ihr zukommen:

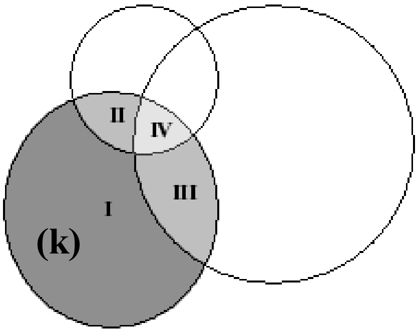

Abb. 1: Der „Zone of Influence“-Ansatz: Pflanzen bekommen die Ressourcen innerhalb ihrer Einflusszone zugewiesen (I). Kollisionen bei Mehrfachüberlappung (II, III, IV) werden durch gesonderte Regeln aufgelöst.

$$R_k = R_0 \cdot A_I + \frac{R_0}{2}(A_{II} + A_{III}) + \frac{R_0}{3} \cdot A_{IV} \,. \tag{1}$$

Dabei bezeichnet R_0 die Ressourcen, die an jedem Ort verfügbar sind, A_I bis A_{IV} die Flächen der in Abb. 1 hervorgehobenen Gebiete. R_k wird entweder direkt für die Wachstums-Berechnung herangezogen oder normiert als Konkurrenz-Maß (Competition Index) verwendet, z.B.:

$$CI_{ZOI} = 1 - \frac{R_k}{R_0 \cdot A_k} \; ; \; CI_{ZOI} = [0,1]; \text{ mit } A_k\text{: ZOI-Fläche.} \qquad (2)$$

Hat CI_{ZOI} den Wert „0“, ist die Pflanze keinerlei Konkurrenz ausgesetzt. Eine „1“ würde anzeigen, dass alle Ressourcen auf die Nachbarn verteilt wurden, die betrachtete Pflanze also leer ausgeht (ein Fall, der bei der gewählten Kollisionsregel nicht auftreten kann).

Der ZOI-Ansatz ist konzeptionell sehr einfach, hat aber leider auch einige Probleme. Größe, Abstand und sogar die Anzahl der Nachbarn gehen in die Ressourcen-Bilanz nur über die erzielte Überlappungsfläche ein. Das macht ZOI „blind“ gegenüber räumlichen Konfigurationen. In allen in Abb. 2 gezeigten Situationen erhalten wir z.B. für die große Pflanze immer den gleichen Wert für CI_{ZOI} (0.08), „nur“ weil die überlappten Flächen in allen Fällen gleich groß sind. Ursächlich wird dies durch die Annahme einer homogene Ressourcen-Aufnahme bedingt, die innerhalb der Einflusszone unabhängig vom Abstand zum Mittelpunkt überall gleich behandelt wird. Das ist besonders problematisch bei kleinen Pflanzen, die komplett innerhalb der Einflusszone einer größeren stehen. In solchen Fällen verliert ZOI jegliche Differenzierung der Abstände zwischen den Pflanzen.

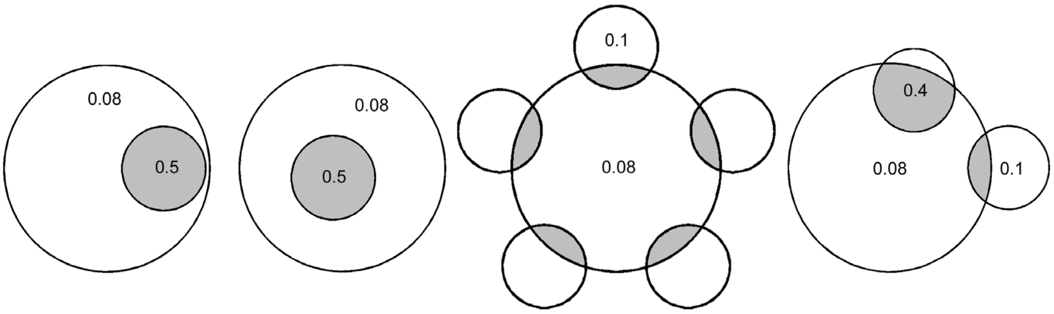

Abb. 2: ZOI unterscheidet nicht zwischen unterschiedlichen räumlichen Konfigurationen, sobald die Überlappungsflächen gleich groß sind (s. Text). Die Zahlen geben die CI_{ZOI}-Werte nach Gleichung (2) an.

1.2 Ecological Field Theory (EF)

Der offensichtlich unrealistischen Annahme einer homogenen Ressourcen-Aufnahme begegnet die „Ecological Field Theory“ (Wu et al. 1985; Walker et al. 1986). EF ordnet jeder einzelnen Pflanze eine oder mehrere ortsabhängige Funktionen (skalare Felder) zu, die angeben, wie die Pflanze eine ursprünglich als homogen angenommene Ressourcen-Verteilung beeinflusst:

$$R_k(x,y) = R_0 \cdot \{1 - \varphi_k(x,y)\} \; ; \; \varphi_k = [0,1]; \qquad (3)$$

wobei R_k die Ressourcen-Verfügbarkeit am Ort (x,y) angibt, nachdem der Einfluss φ_k der k-ten Pflanze berücksichtigt wurde, also gewissermaßen das, was die

Pflanze übrig lässt. Sind mehr als nur eine Pflanze zu berücksichtigen, dann ergibt sich die Ressourcen-Verfügbarkeit durch einen iterativen Prozess. Mit $R_0=1$:

$$R(x,y)=\{1-\varphi_k(x,y)\}\times R_{k-1}(x,y)\,;\quad k=1,\ldots,n. \tag{4}$$

Die Transformation 1-$R(x,y)$ wird „Ecological Interference Potential“ genannt und ist als Maß geeignet, die Konkurrenz am Ort (x,y) zu beschreiben. Beträgt es „0“, dann ist die Ressourcen-Verfügbarkeit uneingeschränkt (von keiner Pflanze beeinflusst), bei einem Wert von „1“ sind an diesem Ort keine Ressourcen mehr verfügbar. Auffallend ist der eher ungewöhnliche multiplikative Charakter der Berechnung: kommt ein weiterer Konkurrent dazu, so verringert er die Ressourcen-Verfügbarkeit weniger, als ein Vorgänger mit gleichem Einfluss auf den Ort (x,y)[2]. Geeignet ist die multiplikative Überlagerung der Einfluss-Felder besonders dann, wenn wir die Ressource „Licht“ beschreiben wollen, wobei dann φ die ortsabhängigen Transmissions-Koeffizienten angibt[3]. Für andere Ressourcen müssen kompliziertere Überlagerungen der Felder gefunden werden, die lokale Limitierungseffekte berücksichtigen. Solche Überlagerungen sind meist nicht mehr „geschlossen“ zu berechnen und müssen in Form von Regeln formuliert werden, ähnlich den Kollisionsregeln in ZOI.

Ressourcen-Verfügbarkeit und das „Ecological Interference Potential“ kann für die gesamte Fläche berechnet werden, auf der eine Pflanze Ressourcen aufnimmt. Die Integration liefert für eine Pflanze die gleichen Informationen über ihre Konkurrenz-Situation wie 1-R für einen Ort:

$$CI_{EF}=\iint\limits_{\varphi_k\neq 0}\bigl(1-R(x,y)\bigr)dxdy\,;\quad CI_{EF}=[0,1]. \tag{5}$$

In CI_{EF} geht die räumliche Verteilung der Nachbarn, deren Größe, Anzahl und Abstand ein – deutlich feiner aufgelöst, als mit dem ZOI-Ansatz möglich ist. Prinzipiell ist die „Ecological Field Theory“ in der Lage, die Ressourcen-Aufteilung unter konkurrierenden Pflanzen realistisch zu beschreiben. Wu et al. schlagen vor, unterschiedliche Ressourcen und die verschiedenen Kompartments einer Pflanze getrennt zu behandeln und dafür jeweils eigene Einfluss-Felder und Überlagerungs-Regeln auf zu stellen (Wu et al., 1985; Walker et al. 1986). Ob der postulierte Grad an Realismus erreichbar ist, erscheint jedoch mehr als fraglich, da für die meisten Ressourcen bis heute weder die Einfluss-Felder noch deren Überlagerung aus empirischen Daten hergeleitet werden konnten (Pukkala, 1989; Miina & Pukkala, 2000). Die gleichen Autoren bescheinigen dem Konkurrenz-Maß aus Gleichung (5) gleichwohl ein sehr gutes Zeugnis, weil es u.a. räumliche Konfigurationen auflösen kann. Dabei verwenden sie ein phänomenologisches, durch trail-and-error gefundenes Einfluss-Feld, dass an der Stammposition „1“ erreicht und nach außen hin exponentiell abfällt.

---

[2] Ein Effekt, den wir auch bei der gewählten Kollisionsregel für den ZOI-Ansatz beobachten können (Gleichung (1)).

[3] Die Pflanzen müssen dabei zusätzlich nach ihrer Höhe (Nähe zur Lichtquelle) sortiert werden.

1.3 Field of Neighbourhood (FON)

Für unsere Mangroven konnten und können wir auf eine realistische Darstellung im „Ressourcen-Bild“ der „Ecological Field Theory“ nicht hoffen. Dazu liegen empirische Untersuchungen mit dem erforderlichen Detaillierungsgrad nicht vor. Eine technische Limitierung hat letztlich den Einsatz von EF auch mit phänomenologischen Einfluss-Felder verhindert: die numerische Berechnung von Gleichung (5) ist sehr umständlich und äußerst rechenintensiv! Selbst im einfachsten Fall eines konstanten Einfluss-Feldes, wird in der Praxis ein feines Rechengitter verwendet, auf dem für jede Zelle 1-$R(x,y)$ getrennt berechnet wird (s. z.B. das Supplementary zu Enquist et al., 2001). Für ein Modell auf Populationsebene, d.h. einer Computersimulation, die diese Operation zigtausendmal pro Zeitschritt aus zu führen hat, ein zu zeitaufwändiges Verfahren.

Wie lässt sich der EF-Ansatz so optimieren, dass er in einem Populationsmodell verwendbar ist, ohne die unbestrittene Güte des Konkurrenz-Maßes CI_{EF} zu verwässern? Unsere Antwort darauf: durch Verzicht auf das Ressourcen-Bild. Dies scheint uns schon aus methodischer Sicht angezeigt: sobald wir mit phänomenologischen Einfluss-Feldern arbeiten, können wir keine reale Ressource benennen, auf deren Verfügbarkeit sich die Einfluss-Felder auswirken sollten. Dann macht es auch keinen Sinn, zunächst den Einfluss der Pflanzen auf die Verfügbarkeit einer fiktiven Ressource zu berechnen (Gleichung (4)) um daraus den wechselseitigen Einfluss der Pflanzen aufeinander zu bestimmen (Gleichung (5)).

FON verwendet statt dessen Einfluss-Felder, die direkt den Einfluss einer Pflanze auf ihre Nachbarn beschreiben. Je größer die (physikalische) „Präsenz“ einer Pflanze, desto höher der Feldwert an diesem Ort. Basalflächen von Pflanzen können z.B. derart ausgezeichnet werden, indem ihnen der maximale Feldwert zugeordnet wird. Diese Nachbarschafts-Felder sind auf den Einflusszonen der Pflanzen (s. ZOI) definiert und überlagern sich dort, wo sich Einflusszonen überlappen. Das Gesamtfeld an einem Ort (x,y) ergibt sich dann durch Superpositionierung der Nachbarschafts-Felder aller N Pflanzen:

$$F(x,y) = \sum_N FON_n(x,y); \qquad (6)$$

$F(x,y)$ korrespondiert mit dem „Ecological Interference Potential“ und liefert Informationen über die Nachbarschafts-Situation an jedem beliebigen Ort. Zu beachten ist die additive und Überlagerung der Nachbarschafts-Felder: die doppelte Anzahl gleich großer Pflanzen im gleichem Abstand zu (x,y) bewirkt den doppelten Einfluss. Diese Art der Überlagerung scheint uns die „natürlichere“ zu sein (s. auch Adler, 1996) und lässt uns mehr Freiheiten bei der Wahl der Feldformen. So ist $FON_n(x,y)$ und $F(x,y)$ nicht notwendigerweise auf [0,1] beschränkt. Durch Feldwerten kleiner Null können gleichzeitig positive Effekte von Nachbarschaft (z.B. Wind- und Lichtschutz) beschrieben werden. Durch aufsummieren ergibt sich der entgültige Mischeffekt.

Als Maß für die Konkurrenz, der eine Pflanze ausgesetzt ist, wird der Mittelwert des Gesamtfeldes definiert, das durch alle anderen Pflanzen innerhalb der Einflusszone der betrachteten Pflanze erzeugt wird. Für die k-te Pflanze:

$$F_A^k = \frac{1}{A_k} \int_{A_k} F^*(x,y)\,da \quad = \frac{1}{A_k} \int_{A_k} \sum_{n\#k} FON_n(x,y)\,da\,. \tag{7}$$

Mit der Annahme FON_n=[0,1] können wir auch F_A auf diesen Wertebereich einschränken:

$$\begin{aligned} CI_{FON} &= F_A && ;\text{ falls } F_A \leq 1 \\ CI_{FON} &= 1 && ;\text{ sonst.} \end{aligned} \tag{8}$$

Wieder bedeutet CI_{FON} = 0 keinen Einfluss durch die Nachbarn und CI_{FON} = 1 maximalen Einfluss (setzten wir z.B. im Stammbereich von Bäumen das Nachbarschafts-Feld auf „1“, dann würde CI_{FON} = 1 bedeuten, dass sich der betrachtete Baum innerhalb des Stammes eines anderen befindet...). CI_{FON} ist als Konkurrenz-Maß CI_{EF} mindestens ebenbürtig und löst räumliche Konfigurationen sehr viel besser auf, als CI_{ZOI} (Abb. 3).

FON erfüllt die Anforderungen an die Modellierung der Interaktion zwischen Nachbarn in Pflanzenpopulationen, die Stoll & Weiner (2000) formuliert haben: den Pflanzen wird eine explizite Position im Raum und eine (begrenzte) Einflusszone zugeordnet, auf der sich die Interaktionen abspielen; eine möglicherweise exklusive Basalfläche kann einbezogen werden; Größe und Abstand der Nachbarn werden berücksichtigt.

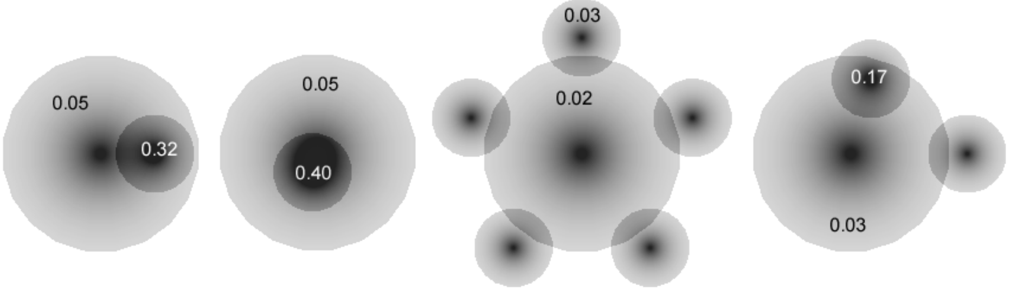

Abb. 3: FON löst räumliche Konfigurationen deutlich besser auf, als ZOI (vgl. Abb. 2). Die Feldform entspricht der für *Rhizophora mangle* angenommenen: das Nachbarschaftsfeld erreicht „1“ im Stammbereich und fällt exponential auf „0.01“ zum Rand der Einflusszone hin ab (s. Kapitel II,1). Die Zahlen geben den CI_{FON}-Wert nach Gleichung (8) an.

Darüber hinaus vermeidet FON technische Limitierungen, von denen die Gefahr droht, dass Modellierungs-Projekte am Ende doch noch scheitern, nur weil die Laufzeiten der Computer-Simulationen zu hoch ausfallen. Auf den ersten Blick ist nicht ersichtlich, was mit den Gleichungen (8) und (7) gegenüber Gleichung (5) bezüglich der Berechenbarkeit gewonnen ist. Gleichung (7) erlaubt es, Summation und Integration zu vertauschen! Äquivalent zu Gleichung (7) ist daher:

$$F_A^k = \frac{1}{A_k} \sum_{n \# k} \int_{A_k} FON_n(x, y)\, da \,. \tag{9}$$

Die Flächenintegrale müssen nun nur noch für paarweise auftretende Überlappungen berechnet werden. Das ist mathematisch vergleichsweise übersichtlich und von einem Computerprogramm um Größenordnungen schneller zu berechnen als Gleichung (5).

2. Eignung für große Individuenzahlen

Die bisher von uns mit Hilfe des „Field of Neighbourhood“-Ansatz untersuchten Modellszenarien spielten sich auf der Fläche eines Hektars ab. Die Anzahl der betrachteten Individuen überstieg selten einige tausend. In vielen Fällen durchaus ausreichend und im üblichen Rahmen derartiger Modelle. Für den Einsatz als Integrations-Werkzeug innerhalb des MADAM-Projekts sind jedoch Szenarien geplant, die bis zu 100 Hektar umfassen. Bei gleicher Dichte erwarten wir also Individuenzahlen von einigen hunderttausend. Ähnliche, oder noch höhere Individuenzahlen ergeben sich schon auf kleinerer Fläche bei Einbeziehung der Mangroven-Keimlinge oder der Diasporen-Ausbreitung in das Modell. Die Frage ist berechtigt, ob dies mit einer Computersimulation auf normaler PC-Basis überhaupt – in endlicher Zeit - machbar ist.

Es geht. Der zu betreibende Aufwand ist jedoch erheblich. Wie beschrieben, wurde diesem Punkt schon bei der Formulierung von FON einige Beachtung entgegen gebracht. Bei der Implementierung treten jedoch einige weitere Implikationen auf, die bei kleinen Individuenzahlen keine Rolle spielen. Besondere Aufmerksamkeit muss der Laufzeit-Effizienz der verwendeten Algorithmen gewidmet werden, da ein einziger falsch gewählter Algorithmus zu Ausführungszeiten führen kann, die jedes vernünftige Maß sprengen.

Laufzeit-Effizienz sagt etwas über die Ausführungsdauer eines Algorithmus in Abhängigkeit von der Anzahl der zu behandelnden Elemente (Individuen in unserem Fall). Sie hat nichts mit cleverer, optimierender Implementierung ein und des selben Algorithmus zu tun. Die Laufzeit-Effizienz ändert sich dadurch genau so wenig wie durch die Ausführung auf schnellerer Hardware. Eine gängige Konvention zur Bezeichnung der Laufzeit-Effizienz ist die „Groß-O“-Notation $O(f(N))$. „$O(1)$“ bedeutet, dass die Dauer unabhängig von der Anzahl der Elemente konstant bleibt. „$O(N)$“ bedeutet eine zur Anzahl der Elemente proportionale Dauer. Daneben finden sich $O(\log(N))$, $O(N \cdot \log(N))$, $O(N^2)$ usw. mit entsprechenden Bedeutungen. Konstante Faktoren werden ignoriert, so dass $O(k \cdot N)$ weiterhin als $O(N)$ bezeichnet wird und $O(\log_b(N))$ als $O(\log(N))$.

Wichtig für die Modellierung einer großen Anzahl Individuen ist nun, dass *kein* Algorithmus, der pro Zeitschritt alle Individuen behandeln muss, schlechter als $O(N \cdot \log(N))$ sein darf. Alles andere führt zu exponentiellem Anstieg der Laufzeiten, die damit nur zu leicht inakzeptabel hoch ausfallen.

2.1 Die Effizienz der F_A-Berechnung

Als Beispiel soll der Algorithmus dienen, den wir selber in Kapitel II,1 „*A new approach to spatially explicit modelling of forest dynamics ...*“ für die Berechnung von F_A vorschlagen. Im FON-Ansatz spielt F_A die entscheidende Rolle, daher lohnt sich ein kritischer Blick auf diesen Algorithmus.

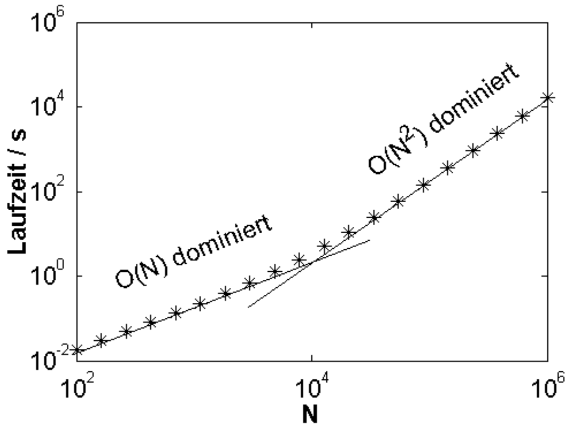

Abb. 4: Laufzeiten des Algorithmus zur Berechnung von F_A (doppelt-logarithmische Skala). FON wie in KiWi; für alle N gleichbleibende Dichte bei entsprechend vergrößertem Areal. Gemessen auf einem 1GHz PIII – PC; 512MB RAM.

Das Simulationsprogramm KiWi berechnet in jedem Zeitschritt für alle Individuen den zugeordnete F_A-Wert. Auf unserem Entwicklungsrechner benötigt der genannte Algorithmus dafür 0,2 Sekunden bei 1.000 Individuen, 4 Sekunden bei 10.000, 3 Minuten bei 100.000 und schließlich 4:30 Stunden bei 1.000.000 Individuen[4] (s. Abb 4). Für einen durchschnittlichen Simulationslauf über 1.000 Zeitschritte ergeben sich entsprechende Laufzeiten von wenigen Minuten, einer Stunde, zwei Tagen bzw. sechs Monaten.

Abb. 4 zeigt, dass sich der Algorithmus bei „kleinen“ Individuenzahlen (N<10.000) wie O(N), bei „großen“ aber wie O(N^2) verhält. Anscheinend addieren sich hier die Laufzeiten zweier Teil-Algorithmen. Der eine führt eine rechenintensive Operation mit O(N) aus, der andere bearbeitet eine „billige“ Operation mit O(N^2):

$$T \approx \tau_1 \cdot N + \tau_2 \cdot N^2; \qquad \text{mit } \tau_1 >> \tau_2.$$

Für genügend großes N dominiert der quadratische Term, gleichgültig wie das Verhältnis von τ_1 zu τ_2 ausfällt. In unserem Fall gehört τ_1 zur eigentlichen Berechnung der Flächenintegrale, die zwar aufwändig ist aber pro Individuum nur für seine Nachbarn ausführt werden muss. Da die Dichte in dem Testprogramm mit N nicht verändert wurde, ist die Anzahl der Nachbarn unabhängig von N und im Mittel konstant, so dass sich eine Laufzeit-Effizienz von N·O(1)=O(N) ergibt.

Bleibt als zweiter Teil-Algorithmus die Suche nach den Nachbarn. Der verwendete Algorithmus ist denkbar einfach: für ein gegebenes Individuum werden nacheinander alle anderen auf Überlappung mit seiner Einflusszone getestet. Das ist eine klassische „lineare Suche“ mit der Laufzeit-Effizienz von

---

[4] Ließe es der Speicherausbau zu, könnten wir ab etwa N=40.000.000 „Echtzeit“-Bedingungen erreichen. Dann würde die Berechnung eines Zeitschrittes genau so lange dauern, wie der simulierte Zeitschritt – ein Jahr.

O(N). Die Effizienz der Suche nach den Nachbarn aller Individuen ist also $N \cdot O(N) = O(N^2)$. Im Pseudocode:

```
(1) for each Tree in Trees
(2)   for each Tree' in Trees  // Zeile wird N mal ausgeführt
(3)     if Tree.Overlap(Tree') then           // N·N
(4)       ComputeArealIntegral(Tree, Tree')   // k·N
```

Der Test in Zeile (3), ob sich zwei Einflusszonen überlappen (der Abstand der Mittelpunkte muss kleiner sein als die Summe der beiden Radien) ist extrem schnell: gerade einmal 16 Taktzyklen benötigt unser Testrechner dafür. Bei einer Taktrate von 1 GHz ergibt sich τ_2 = 16ns. Das Verhältnis von τ_1 zu τ_2 beträgt tatsächlich etwa 15.000:1. Trotzdem wird bei großen N praktisch alle verfügbare Rechenleistung für diesen simplen Test verbraucht (s. Abb. 5), der noch dazu fast immer fehlschlägt.

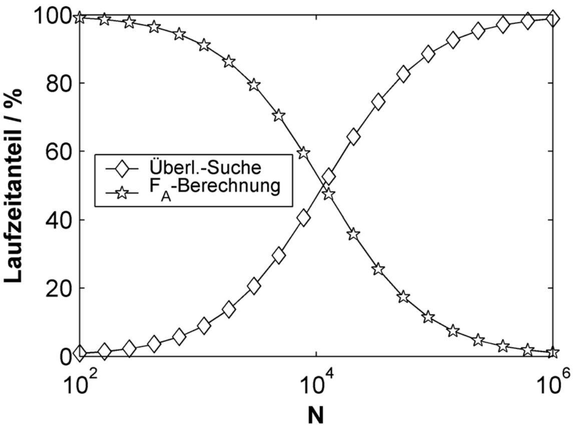

Abb. 5: Aufteilung der Rechenleistung auf die beiden Teil-Algorithmen.

Als vorläufiges Fazit müssen wir festhalten, dass unser Algorithmus zwar für kleine Individuenzahlen sehr schnell ist, die Performance bei großen Individuenzahlen allerdings derart einbricht, dass eine sinnvolle Arbeit damit unmöglich wird. Der Grund dafür ist nicht die rechenintensive numerische Integration, sondern die Implementierung der Überlappungs-Suche mit Hilfe einer linearen Suche.

2.2 Räumliche Abfragen mit O(log(N))

Verwandte Probleme treten bei räumlich expliziter Modellierung häufig auf. Sei es die Bestimmung der nächsten Nachbarn, die Suche nach Interaktionspartnern oder auch nur die Feststellung der Dichte in einem beliebigen Teilgebiet. Alles Beispiele für „räumliche Abfragen“ (spatial queries). Auch auf der Auswertungs-Seite sind räumliche Abfragen allgegenwärtig. So beruhen

Programme im Bereich der räumlichen Statistik massiv auf räumlichen Abfragen. Um so erstaunlicher, dass auch dort vielfach mit linearer Suche gearbeitet wird[5].

Dabei sind Algorithmen und Datenstrukturen, die räumliche Abfragen mit deutlich besserer Effizienz als O(N) erlauben, seit langem verfügbar. Die bekanntesten sind vielleicht der Quad-Tree, der K-D-Tree, der S-D-Tree, und Multi-Resolution-Maps. Bei Punkt-Daten sind damit Abfragen mit O(log(N)) möglich. Für räumlich ausgedehnte Objekte, wie unsere Einflusszonen, sind sie leider nicht oder nur bedingt geeignet (Samet, 1990). Speziell für Überlappungsabfragen mit O(log(N)) entworfen sind dagegen die Mitglieder der R-Tree Familie (Guttman, 1984; Sellis at al., 1989; Beckmann et al., 1990). Ideale Kandidaten also, wenn unsere Einflusszonen nicht eine weitere unangenehme Eigenschaft hätten – sie *wachsen*. Das vertragen R-Trees gar nicht gut, weil es ihre ausgeklügelte Balance zerstört (Kamel & Faloutsos, 1993). Als Ausweg bleibt nur der komplette Neuaufbau (Rebuild) der Datenstruktur, eine kostspielige Operation mit $O(N^2)$, die den Vorteil der sehr guten Abfrage-Effizienz wieder zunichte macht.

Die Suche nach einer für unsere Zwecke optimalen Lösung führte schließlich zu einer speziell angepassten Implementierung des „Hilbert R-Tree“, einem „*improved R-Tree using fractals*“ (Kamel & Faloutsos, 1994). Wir nehmen an, dass nicht nur unter den Modellierern, die den FON-Ansatz erwägen, ein erheblicher Bedarf an einer solchen Lösung besteht. Wir stellen sie daher in Form einer C++-Bibliothek jedem Interessierten zur Verfügung[6]. Die „R-Tree Library“ ist ausführlich dokumentiert, so dass wir uns die Details der Implementierung ersparen können. Im Ergebnis bekommt der Anwender eine Laufzeit-Effizienz von O(log(N)) für räumliche Abfragen mit Punkt- oder räumlich ausgedehnten Daten in zwei und drei Dimensionen. Die wichtigste Verbesserung gegenüber bisher verfügbaren Bibliotheken ist der schnelle Rebuild der Datenstruktur mit $O(N \cdot \log(N))$.

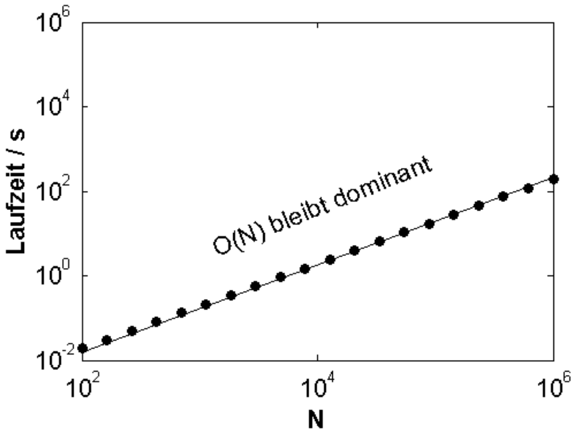

Abb. 6: Laufzeiten des Algorithmus zur Berechnung von F_A (doppelt-logarithmische Skala) bei Verwendung der „R-Tree Library“ (vergl. Abb. 4).

---

[5] Wenn der Quellcode nicht vorliegt, lässt sich dies am Laufzeit-Verhalten festmachen (s.o.).

[6] Ein Link zur „R-Tree Library“ findet sich z.Z. unter http://www.zmt.uni-bremen.de

Mit der „R-Tree Library“ wurde das Ziel erreicht, den $O(N^2)$-Anteil in unserem Algorithmus zur F_A-Berechnung zu eliminieren (Abb. 6). Auf die absolute Laufzeit wirkt sich das für große N entsprechend günstig aus. Ein Simulationslauf über 1.000 Zeitschritte benötigt bei 100.000 Individuen nur noch fünf Stunden (statt bisher zwei Tage) und bei 1.000.000 Individuen gut zwei Tage (statt bisher ein halbes Jahr). Der Laufzeit-Anteil der Suche nach Überlappungen liegt nun im gesamten Bereich unter 3%. Die verfügbare Rechenleistung kommt nun endlich der F_A-Berechnung zugute – und die ist tatsächlich sehr schnell.

Zusammenfassung

Zunächst aus der Not geboren, entpuppte sich die phänomenologische Beschreibung von Nachbarschaftskonkurrenz, die mit dem „Field of Neighbourhood“-Ansatz beschritten wurde, als seine größte Stärke. Mit phänomenologisch meinen wir, dass der FON-Ansatz nur bedingt durch mechanistischen Prinzipien motiviert ist oder darauf aufbaut. Das heißt nicht, dass FON die Existenz fundamentaler Mechanismen verneint. FON setzt da an, wo Details über die Ressourcennutzung fehlen oder zu kompliziert sind, um darauf ein mechanistisches Modell aufzubauen.

Im Gegensatz zu gitter-basierten-, ZOI- oder EF-Modellen erlaubt der FON-Ansatz eine wenig aufwändige ad-hoc Parametrisierung. Funktionierende Prototypen können schon in frühen Phasen der Modellentwicklung eingesetzt werden. Das auf FON aufbauende Simulationsmodell KiWi reproduzierte etwa schon mit einer vorläufigen und z.T. unvollständigen Parametrisierung eine Vielzahl ökologisch relevanter Muster. Im Abgleich mit den in der Natur beobachteten Ausprägungen der Mustern konnte die Parametrisierung im Nachhinein interaktiv verbessert werden (Grimm & Berger, 2002). Die realistische Darstellung und Erklärung vieler solcher Muster in Kapitel II,1-5 werten wir als guten Erfolg. Dies um so mehr, als keines dieser Muster in den Modellentwurf „hineingesteckt“ wurde.

Die unkomplizierte Modellanbindung motivierte auch die Entwicklung von spezialisierten, abstrakten Modellen, die für die theoretische Untersuchung eines Sachverhalts entworfen sind. Ein Beispiel hierfür ist das in Kapitel II,4 verwendete Modell zur Untersuchung asymmetrischer Konkurrenz. Andere widmen sich der altersbedingten Abnahme der Produktivität in Wäldern (Berger & Hildenbrandt, 2002) und der Ausbildung von Zyklen in Pflanzenpopulationen (Bauer, Berger, Hildenbrandt, Grimm, 2002). Wiederum ist es die Vielzahl der produzierten Muster, die uns vor dem Vorwurf bewahrt, diese Modelle seien tautologisch in dem Sinne, dass nur herauskommt, was hineingesteckt wurde.

Nicht zuletzt ist der Implementierungsaufwand, der für den FON-Ansatz geleistet werden muss, vergleichsweise gering. Der in Kapitel II,1 vorgeschlagene Algorithmus zur Berechnung der auftretenden Integrale ist auf alle rotationssymmetrischen Nachbarschaftsfelder anwendbar, für die sich wenigstens die Integrale über konzentrische Teilkreisringe berechnen lassen. Der Algorithmus sollte in den meisten Fällen wiederverwendbar sein. Eine einheitliche Code-Basis für viele Anwendungen kommt der Stabilität zugute, vereinfacht die Wartung und hilft, Fehler zu vermeiden.

FON versucht, die Vorteile bestehender Ansätze zu kombinieren ohne deren Nachteile zu übernehmen. Dabei bleibt FON sowohl in der Konzeption als auch in der Anwendung einfach. Weil sich über geeignete Nachbarschaftsfelder auch viele andere Effekte der Interaktion unter Nachbarn beschreiben lassen, ist FON nicht auf die Modellierung von Baum- und Pflanzenpopulationen beschränkt. Insbesonders benthische Lebensgemeinschaften erscheint uns eine vielver-

sprechende Domäne. Wir hoffen, dass sich der „Field of Neighbourhood“-Ansatz als Alternative in der individuen-basierten, räumlich expliziten Modellierung etablieren wird.

Referenzen

ADLER F.R. 1996. *A model of self-thinning through local competition*. Proceedings National Academy of Science USA 93: 9980-9984.

BAUER S., BERGER U., HILDENBRANDT H., EISINGER D., GRIMM V. 2001. *Modellierung von Nachbarschaftskonkurrenz in Pflanzenpopulationen: Test eines neuen Ansatzes*. pp. 31-42. In: Jopp F, Weigmann G. (eds.) Theorie in der Ökologie - Band 3. Peter Lang, Frankfurt/M.

BAUER S., BERGER U., HILDENBRANDT H., GRIMM V. 2002. *Cyclic Dynamics in Plant Populations*. Proceedings of the Royal Society, London, Ser. B., in press.

BAUER S., WYSZOMIRSKI T., BERGER U., HILDENBRANDT H. & GRIMM V. 2002. *Asymmetric competition as natural outcome of neighbour interactions among plants: results from the field-of-neighbourhood modelling approach*. Plant Ecology (in press).

BECKMANN N., KRIEGEL H.P., SCHNEIDER R., SEEGER B. 1990. *The R*-Tree: An Efficient and Robust Access Method for Points and Rectangles*. Proceedings of the 1990 ACM SIGMOD International Conference on Management of Data, SIGMOD Record 2, ACM Press, New York 322-331.

BEGON M., HARPER J.L. & TOWNSEND C.R. 1991. *Ökologie: Individuen, Populationen und Lebensgemeinschaften*. Basel: Birkhäuser Verlag.

BERGER U. HILDENBRANDT H. 2000. *A new approach to spatially explicit modelling of forest dynamics: spacing, ageing and neighbourhood competition of mangrove trees*. Ecological Modelling 132: 287 - 302.

BERGER U., HILDENBRANDT H. 2001. *Nachbarschaftsfelder zur Untersuchung ökologischer Interferenzen – vom Anfang und Ende der Selbstausdünnung*; In: F. Jopp & G. Wiegmann (eds.), Rolle und Bedeutung von Modellen für den Erkenntnisprozeß in der Ökologie. Theorie in der Ökologie Band 4, 19-30.

BERGER U., HILDENBRANDT H. 2002. *About the competition strength of individual trees and its influence on the curvature of the biomass-density-trajectory of the whole cohort*; Plant Ecology, in press.

BERGER U., HILDENBRANDT H., GRIMM V. 2002. *Towards a standard for the individual-based modeling of plant populations: self-thinning and the field-of-neighborhood approach*. Natural Resource Modeling 15: 39-54.

CHEN R. & TWILLEY R. 1998. *A gap dynamic model of mangrove forest development along gradients of soil salinity and nutrient resources*. Journal of Ecology 86: 37-51.

CINTRON G. & SCHAEFFER NOVELLI Y. 1985. *Caracteristicas y desarrollo estructural de los manglares de norte y sur america*. Cienca Interamericana 25: 4-15.

CZARAN T, BARTHA S. 1992. *Spatiotemporal Dynamic Models of Plant Populations and Communities*, Trends in Ecology & Evolution 7, 38-42.

CZARAN T. 1998. *Spatiotemporal Models of Population and Community dynamics*. Chapman & Hall, London.

DEANGELIS D.L., GROSS L.J. 1992. *Individual-Based Models and Approaches in ecology*. Chapman and Hall, London.

ENQUIST B.J., BROWN J.H. & WEST G.B. 1998. *Allometric scaling of plant energetics*. Nature 395: 163.

ENQUIST B.J., NICKLAS K.J. 2001. *Invariant scaling relations across tree-dominated communities*. Nature 410: 655-660.

ELLISON A.M. 1989. *Morphological determinants of self-thinning in plant monocultures an a proposal concerning the role of self-thinning in plant evolution*. OIKOS 54: 287-293.

FROMARD F., PUIG H., MOUGIN E., MARTY G., BÉTOULLE J.L. & CADAMURO L. 1998. *Structure, above-ground biomass and dynamics of mangrove ecosystems: new data from French Guiana*. Oecologia 115: 39-53.

GATES D.J. 1982. *Competition and Skewness in Plantation*, J. Theoret. Biology 94, 909 922.

GATES D.J., WESTCOTT M. 1978. *Zone of Influence Models for Competition in Plantations*, Adv. in Appl. Probab. 10, 299 537.

GRIMM V. 1999. *Ten years of individual-based modelling in ecology: what have we learned, and what could we learn in the future*? Ecol. Model. 115, 129–148.

GRIMM V., BERGER U. 2002. *Seeing the wood for the trees and vice versa. Pattern-oriented modelling*. In Seuront L, Strutton PG (eds) Scales in aquatic systems: measurement, analysis, simulation. CRC Press.

GUTTMAN A. 1984. *R-Trees: A Dynamic Index Structure for Spatial Searching*. Proceedings of the 1984 ACM SIGMOD International Conference on Management of Data, SIGMOD Record 2, ACM Press, New York, 1984, 47-57.

HUSTON M., DEANGELIS D., POST, W., 1988. *New computer models unify ecological theory*. BioScience 38, 682–691.

KAMEL I., FALOUTSOS C. 1994. *On Packing R-trees*. Proc. of the CIKM, 490-499

KAMEL I., FALOUTSOS C. 1994. Hilbert R-tree: An improved R-tree using fractals. Proceedings of the Twentieth International Conference on Very Large Databases.

LONSDALE W.M. 1990. *The self-thinning rule: dead or alive*? Ecology 71: 1373-1388.

MIINA J. PUKKALA T. 2002. *Application of ecological field theory in distance-dependent growth modelling.* Forest Ecology and Management 161,101-107.

MIYANISHY K., HOY A.R. AND CAVERS P.B. 1979. *A generalized law of self-thinning in plant populations*. Journal of Theoretical Biology 78, 439-442.

OSAWA A. & SUGITA S. 1989. *The self-thinning rule: another interpretation of Weller's results*. Ecology 70:279-283.

PUKKALA T. 1989. *Methods to describe the competition process in a tree stand.* Scand. J. For. Res.. 4,187-202.

SELLIS T.K., ROUSSOPOULOS N., FALOUTSOS C. 1987: *The* R^+*-Tree: A Dynamic Index for Multi-Dimensional Objects*. VLDB 507-518

STOLL, P. & WEINER, J. 2000. *A neighborhood view of interactions among individual plants*. pp.11-27. In: Dieckmann, U., Law, R., and Metz, J. A. J. (eds.), The Geometry of Ecological Interactions - Simplifying spatial complexity. Cambridge University Press, Cambridge.

SCHWINNING S. & WEINER J. 1998. *Mechanisms determining the degree of size asymmetry in competition among plants*. Oecologia 113, 447-455.

UCHMANSKI J., GRIMM V. 1996. *Individual-based modelling in ecology: what makes the difference*? Trends Ecol. Evol. 11,437–441.

WALKER, J., SHARPE, P. J. H., PENRIDGE, L. K. & WU, H. 1986. *Ecological field theory: the concept and field tests*. Vegetatio 83:81-95.

WEINER J. 1990. *Asymmetric competition in plant populations*. Trends in Ecology and Evolution 5: 360-364.

WEINER, J., P. STOLL, H. MULLER-LANDAU et al. 2001. *Spatial pattern, competitive symmetry and size variability in a spatially-explicit, individual-based plant competition model*. American Naturalist, 158, 438-450.

WELLER D.E. 1987. *A reevaluation of the -3/2 power rule of plant self-thinning*. Ecological Monographs 57: 23-43.

WHITE J. 1981. *The allometric interpretation of the self-thinning rule*. Journal of Theoretical Biology 89: 475- 500.

WU, H., SHARPE, P. J. H., WALKER, J. & PENRIDGE, L. K. 1985. *Ecological field theory: a spatial analysis of resource interference among plants*. Ecological Modelling 29:215-243.

YODA K., KIRA T., OGAWA H. & HOZUMI K. 1963. *Intraspecific competition among higher plants. XI: Self-thinning in overcrowded pure stands under cultivated and natural conditions*. Journal of Osaka City University Institute of Polytechnics D 14: 107-129.

Kapitel II,1

A new approach to spatially explicit modelling of forest dynamics: spacing, ageing and neighbourhood competition of mangrove trees

UTA BERGER[1], HANNO HILDENBRANDT[1]

[1] Center for Tropical Marine Ecology (ZMT), Bremen, Germany

Ecological Modelling 132:287-302 (2000)

ELSEVIER

Ecological Modelling 132 (2000) 287–302

ECOLOGICAL MODELLING

www.elsevier.com/locate/ecolmodel

A new approach to spatially explicit modelling of forest dynamics: spacing, ageing and neighbourhood competition of mangrove trees

Uta Berger *, Hanno Hildenbrandt

Center for Tropical Marine Ecology (ZMT), Fahrenheitstraße 1, D-28359 Bremen, Germany

Received 21 September 1999; received in revised form 5 April 2000; accepted 18 April 2000

Abstract

This paper presents a new approach to spatially explicit modelling that enables the influence of neighbourhood effects on the dynamics of forests and plant communities to be analysed. We refer to this approach as 'field of neighbourhood' (FON). It combines the 'neighbourhood philosophy' of grid-based models with the description of individual spacing in the 'zone of influence' (ZOI) approach. The novel feature of FON is that modelling of local competition between neighbouring trees is based on the notion of a field of neighbourhood exerted by each tree. This field is defined only on the ZOI of a tree and depends on the distance to the stemming point. For the demonstration of FON's power, a simulation model (KiWi) was implemented that focuses on the dynamic of mangrove forests. The realistic self-thinning behaviour of modelled stands of *Avicennia germinans* and *Rhizophora mangle* confirms the suitability of the FON approach for the description of intra- and inter-specific competition. In KiWi, mortality is modelled in terms of a 'memory function', i.e. the yearly stem increment of each tree is stored in its 'memory' over a certain time period and determines — as a sign of vitality — tree mortality. The results of KiWi demonstrate that this description is sufficient to keep the maximum age of the trees within a reasonable limit. The model thus manages without a description of individual tree age. This is an important feature considering the fact that a direct relationship between tree age and mortality is questioned and there is no established method as yet for determining the age of mangrove trees. © 2000 Elsevier Science B.V. All rights reserved.

Keywords: Spatially explicit modeling; Individual-based model; Local interactions; Competition; Self-thinning; Mangrove forest; *Avicennia germinans*; *Rhizophora mangle*

1. Introduction

Ecology is spatial, but theoretical ecology has ignored this dimension for decades, or has taken it into account only in an indirect or highly idealised manner. Only since computers became powerful and inexpensive enough to be generally

---

* Corresponding author. Tel.: +49-421-2380031; fax: +49-421-2208330.

E-mail addresses: uberger@zmt.uni-bremen.de (U. Berger), hildenbr@uni-bremen.de (H. Hildenbrandt).

PII: S0304-3800(00)00298-2

available has space been an explicit issue in theoretical ecology and ecological modelling. Once these computers were available one model type in particular helped to establish the spatially explicit approach in ecology, namely grid-based models in which space is divided into quadratic or other grid cells of the same size (Zeigler, 1977; Wolfram, 1984; Green et al., 1985; Turner, 1987; Hogeweg, 1988; Baker, 1992; Jeltsch, 1992; Silvertown et al., 1992; Wissel, 1992; Jeltsch and Wissel, 1994; Jeltsch et al., 1996, 1997; Berger et al., 1999a; Grimm, 1999; Jeltsch et al., 1999). Cell size is chosen to represent the smallest spatial unit of interest in relation to the problem addressed by the model, e.g. canopies of mature trees, territories, local forest stands, sampling units, etc. Within the cells, spatial effects are ignored; spatial interactions occur only between neighbouring cells.

Although grid-based models have proved to be extremely powerful and have been applied to almost all kinds of ecological systems and to scales ranging from square metres to entire continents, there are still questions and systems for which the grid-based approach is unsuitable. We became aware of these limitations of the grid-based approach when we tried to develop a spatially explicit model of mangrove forests. The development of such a model is one of the tasks of our Brazilian–German project MADAM. The name MADAM stands for 'Mangrove Dynamics and Management' and explains the focus of the scientific program (Berger et al., 1999b). The model should allow the dynamic of the mangrove forest to be analysed. Although we had to consider the specific environmental conditions exposed at our study area near Braganca (northern Brazil), we looked for a modelling approach being adequate for the description of mangrove stands in a more general sense.

To our knowledge there is only one spatially explicit mangrove model FORMAN (see Chen and Twilley (1998) for an overview of other, non-spatial mangrove models), a gap model (Chen and Twilley, 1998). FORMAN demonstrates the existence of different successional stages. In a three-species forest consisting of *Avicennia germinans*, *Rhizophora mangle*, and *Laguncularia racemosa*, the abundance of *A. germinans* increases over time. If large-scale disturbances are absent this species will dominate the forest not only at higher salinities, but also under benign conditions, i.e. lower salinities. These results show that FORMAN is a powerful tool for investigating mangrove dynamics, but a number of important questions remain unanswered: the influence of site-specific establishment rates, the role of seedlings dispersal, the influence of small scale heterogeneities of environmental factors on tree growth, and the process of species replacement by competition.

Some of these limitations are common to both gap models and the grid-based approach. The main problem with these vegetation models is that they do not permit the consistent application of an individual-based approach (Huston et al., 1988; DeAngelis and Gross, 1992; Uchmanski and Grimm, 1996; Grimm, 1999) in which individuals of all possible size are considered at their very locations. We, therefore, developed a new approach to the spatial modelling of vegetation dynamics. Our approach, which we will refer to as the field of neighbourhood (FON) approach, combines the advantages of the grid-based and the zone of influence (ZOI) approaches (Czárán, 1998). Although we developed this new approach as a means of modelling mangrove forest dynamics, we believe it can be used to model communities of any sessile organisms, i.e. plant and benthic communities.

The purpose of this paper is to introduce the FON approach. First, we will explain the limitations of the grid-based and other approaches and how these limitations led us to our own approach. We will then introduce the FON approach; a detailed and easily applied algorithm is provided in the Appendix A so that our approach can be easily implemented and tested by others. Then, as an sample application, we will develop the mangrove model KiWi in order to apply FON to some aspects of mangrove dynamics that have not yet been modelled: self-thinning and inter-specific competition leading to different outcomes under different initial conditions. Finally, we will discuss both the potentials of the FON approach to modelling vegetation dynamics and the potential of

FON and KiWi to advance theoretical synthesis within mangrove research.

2. Why a new approach to spatially explicit modelling of mangroves?

The fixed cell size used in grid-based models, e.g. canopy size of mature trees, is not suitable for modelling mangrove forests. Mangrove tree architecture and maximum trunk diameter are highly variable, and depend on several stress factors such as pore water salinity or water logging. A grid-based model of mangrove forests would, therefore, need an adaptive grid size with different sets of model rules for each grid size. Besides the problem of sufficient empirical knowledge being available to formulate all these rules, the resultant number of model rules would be so high that the grid-based approach would lose its key advantage, namely the representation of quantitative and qualitative ecological knowledge by a small number of simple rules that can be easily formulated and implemented.

Furthermore, grid-based models are often particularly successful when they are combined with the strategy of 'pattern-oriented modelling' (Grimm, 1994; Grimm et al., 1996), in which both model construction and validation are focused on distinguishing patterns observable in the system being studied. However, in grid-based forest models with cells representing the canopy size of mature trees, trees would be 'forced' to adopt an artificial, regular distribution. Besides this drawback, a suitable approach to modelling mangroves should focus on explicit description of the small-scale processes that generate patterns on both small and larger scales. To this end, our new approach has to give explicit consideration to the position of each tree within a continuous space.

There are two recent modelling approaches which explicitly consider the exact position of individuals — the 'tessellation' and the 'zone of influence' approach. Since there is no community model based on these approaches, we examined their suitability for multi-species systems. Tessellations are used in single-species plant models to study intraspecific competition for different spatial arrangements of the plants (Czárán, 1998). The performance, e.g. growth, of each individual depends on the area of its Voronoi polygon, which is determined by the number, size, location and, in particular, the proximity of its neighbours. A dynamic tessellation model for an even-aged tree monoculture was developed by Galitsky (1990)). This model enables self-thinning processes in plant communities to be analysed.

Nevertheless, the tessellation approach is difficult to extend to multi-species systems. Although the differences in architecture between the various species could be taken into account by weighted distances (Okabe et al., 1992), the implementation of different growth rates is not straightforward. Furthermore, the tessellation approach usually considers death as the only demographic process, yet establishment would also be necessary for the analysis of mangrove forest dynamics. Moreover, the tessellation approach does not permit the superimposed influence of several trees to be represented at a given location. Yet precisely this 'local density' seems to be decisive for tree growth and for sapling establishment, especially. In summary, the tessellation approach is not suitable for modelling mangrove forests.

The 'zone of influence' (ZOI) approach is based on the notion that each individual exploits resources within a circular zone around its stemming point (Czárán, 1998). Resource competition occurs wherever the zones of influence of individuals overlap. The strength of competition depends on the fraction of zones overlapped (Gates and Westcott, 1978). However, the ZOI of a tree describes only the area used by a tree but does not consider that the influence of a tree, e.g. the intensity of exploitation, will usually vary with the distance from the stem. Hence, as soon as the ZOI of one tree is completely superimposed by the ZOI of another tree, the specific distance between the two trees and their actual sizes become irrelevant, which seems to be rather unrealistic, especially in the case of sapling establishment.

In summary, what we need in order to model mangrove forests is an approach which combines the advantages of the grid-based and the ZOI approach while avoiding their limitations. The strength of grid-based models is the simple but powerful consideration of local interactions, i.e. neighbourhood effects such as competition; whereas the strength of the ZOI approach is that it enables modelling of individuals of all sizes at their real, exact location (Wyszomirski, 1983; Wyszomirski et al., 1999). The FON approach is designed to combine these advantages. Another important aim of our approach is that it avoids spatial effects at the local scale being ignored, as is the case with grid-based models. In this way, we hope to show how the strategy of 'pattern oriented modelling' at the local scale can be applied to the modelling of mangrove forests.

3. The FON approach

Consider a single, isolated tree. If abiotic conditions are benign, the tree will grow at maximum growth rate and achieve a maximum final size. Now consider a second tree. As long as this tree is not too close to the first, both trees will grow at the maximum growth rate. However, if the two trees stand closer to each other than a certain, critical distance, they will disturb each other, resulting in a reduced growth rate for both trees. This is true in general and does not depend on the particular mechanism and level of interaction, e.g. root competition, competition for light in the canopy, or whatever. The extent to which a tree's growth rate is reduced depends on the 'strength' and distance of its neighbour(s).

In order to model this general phenomenon of local competition a tree is firstly characterised by its stem position and a circular ZOI around this position. The radius R of the ZOI depends on the size of the tree. In our demonstration model KiWi (see the following section below) we use the simple relationship:

$$R = a\sqrt{\mathrm{rbh}} \quad (\mathrm{m}), \qquad A = \pi a^2 \mathrm{rbh} \quad (\mathrm{m}^2) \tag{1}$$

where rbh is the half diameter at breast height (dbh), a is a scaling parameter, and A is the area of the ZOI.

The ZOI, however, defines only the neighbourhood of a plant: two plants are, by definition, neighbours whenever their ZOIs overlap. ZOIs do not provide any weighting of the neighbourhood in terms of tree distances, despite the fact that a remote tree will certainly exert a smaller competition on a focal tree than a tree in the vicinity. To model this distance-dependent intensity of neighbourhood, we introduce a scalar field (the FON) on the ZOI. This field of neighbourhood indicates at any point within the ZOI the strength of competition or the 'degree' of neighbourhood that the focal tree would exert at that point. FON corresponds with the competition function used by Adler (1996), and Davie (1999). Its interpretation is not limited to a particular mechanism of competition, such as resource competition; in any case, it is not necessary to know such mechanisms in detail.

In KiWi, we chose the following field it amounts to 1 at the stem, decreases exponentially with increasing distance to a small value $F_{\min}$ at the borderline of the ZOI, and it is 0 outside the ZOI (Fig. 1):

$$\begin{aligned} &\mathrm{FON}(r) = 1; \quad \text{for } 0 \le r < \mathrm{rbh}, \\ &\mathrm{FON}(r) = \mathrm{e}^{-c(r-\mathrm{rbh})}, \\ &R \text{ from Eq. (1); } \quad \text{for } \mathrm{rbh} \le r \le R, \\ &\mathrm{FON}(r) = 0 \quad \text{otherwise.} \end{aligned} \tag{2}$$

Now, the basic assumption of our approach is that the FON's of all trees superimpose. At a given location (x, y), the aggregate field strength $F(x, y)$ of all trees is, therefore, given by the sum of their single field intensities. Hence, in the case of N trees $F(x,y)$ is:

$$F(x,y) = \sum_{N} \mathrm{FON}_n(x,y). \tag{3}$$

The specific, dimensionless value of $F(x, y)$ depends on the local configuration of all neighbouring trees (Fig. 1). It represents the local neighbourhood situation and takes into account the number, the weighted distance and the individual size of the neighbouring trees. A location influenced by some smaller trees can be characterised by the same $F(x, y)$ value as a location influenced by a single, larger tree. A location which is not influenced by any tree has an aggregate field strength $F(x, y)$ of 0.

For the description of the neighbourhood situation of a tree, we assume that a tree 'perceives' the aggregate field strength F on its entire ZOI. Consequently, we compute the mean value F_A of the aggregate field strength F produced by all other trees on the tree's area A (Eq. (1)). For example, F_A for kth of N trees is:

$$F_A^k = \frac{1}{A}\int_A F'(x,y)\,\mathrm{d}a = \frac{1}{A}\int_A \sum_{n \neq k} \mathrm{FON}_n(x,y)\,\mathrm{d}a = \frac{1}{A}\sum_{n \neq k}\int_{A'} \mathrm{FON}_n(x,y)\,\mathrm{d}a'. \quad (4)$$

In this case, F' corresponds to the total field F without the contribution of the kth tree (a tree is not its own neighbour). A′ Is the overlapping area of the FONs of the nth and the kth tree.

Computing F_A as a mean has three advantages: first, it makes sense biologically to scale the influence of all neighbours by the ZOI of the focal tree; second, F_A is a dimensionless variable and third, changing the sequence of integration and summation in Eq. (4) enables a very simple algorithm for calculating F_A to be used, because integrals now have to be taken only over overlapping ZOIs in pairs (see Appendix A for a detailed description of the algorithm for calculating F_A).

F_A supplies the same information for a tree as $F(x, y)$ for a point: the description of the neighbourhood strength depending on the number, size, and proximity of its neighbours. F_A can cause growth depression as well as the deformation of a tree. Because FON is the 'neighbourhood field' exerted by a tree and not the tree itself, it cannot be deformed.

4. Using the FON approach: the KiWi model

In this section we present the KiWi model based on the FON approach. KiWi was developed in order to analyse demographic processes of mangrove forests according to abiotic environmental factors, individual tree spacing, and intra- and inter-species competition.

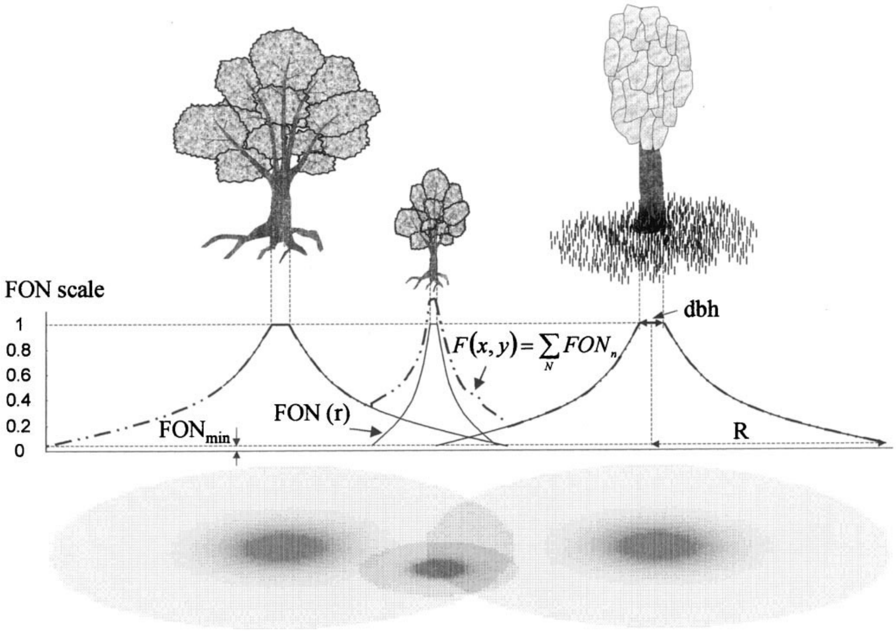

Fig. 1. The principal components of the FON approach describing the competition strength of an individual in its environment (see text for explanations).

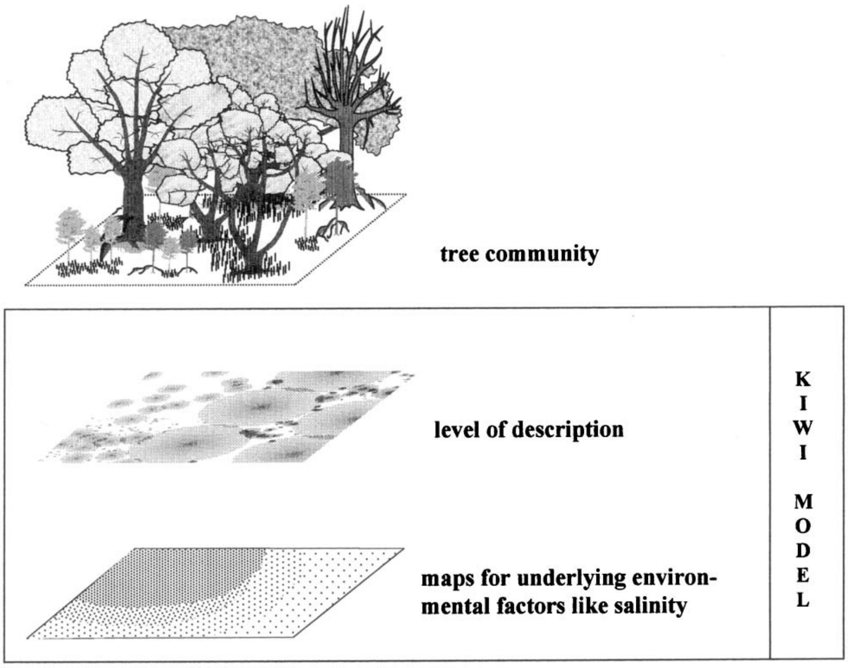

Fig. 2. Architecture of the KiWi model. There are only two levels of description: one for the life history of the trees and one for the abiotic factors.

Fig. 2 shows the basic structure of the model. It requires only one 'biotic' level for describing the trees, because modelling of growth, mortality and sapling establishment is based on a single module, the FON module. The FON approach permits this compact handling of the demographic processes, because all plant-to-plant interactions are expressed in terms of FON. Sapling establishment depends on $F(x, y)$ (see below). Tree competition is influenced by F_A.

The second level of the model describes the abiotic factors influencing the demographic processes. Since the primary focus of this paper is to introduce FON we limited the complexity of the model and considered pore water salinity only. We implemented the spatial distribution of pore water salinity as a bitmap in which the particular colour strength (e.g., a value between 0 and 256) defines salinity at a given position. In this way it is possible to specify a simple, artificial salinity distribution as well as distribution maps based on field studies. The dynamics of the salinity distribution can be taken into account by specifying different bitmaps at different time steps. Extending KiWi by including other abiotic factors such as nutrients or water level can be done in the same manner as described for salinity. A time step in KiWi corresponds to 1 year. The salinity distribution used for the simulations presented below was homogeneous. The concrete value never exceeded 50‰.

4.1. Setting the FON

We apply Eqs. (1) and (2). The parameters a in Eq. (1) and $F_{\min}$ in Eq. (2) are species-specific (Table 1). In general, there is no simple method for specifying the parameters or the functional relationships in Eqs. (1) and (2). As long as no detailed field studies exist which would deliver information about these relationships one has to work with biologically reasonable ad hoc assumptions which are then tested and fine-tuned by comparing model output with patterns in the real system (Grimm, 1994; Grimm et al., 1996).

4.2. Growth

For the description of optimal tree growth we need a sigmoid function to define the growth rate in relation to actual tree size and the upper limit of tree height. The depression of the growth rate under less than optimal conditions (e.g. at higher pore water salinities, or with a strong competition of neighbouring trees) is taken into account by including a multiplier for correcting the 'optimal' function. This multiplier should range between 0 (pessimal conditions) and 1 (optimal conditions).

KiWi uses the time-discrete ($\Delta t = 1$ year) form of the growth function for optimal conditions and the correction factor for salt stress already provided and well documented for the FORMAN model (Chen and Twilley, 1998):

$$\frac{\Delta \mathrm{dbh}}{\Delta t} = \left[\frac{G\cdot\mathrm{dbh}\cdot(1-\mathrm{dbh}\cdot H/\mathrm{dbh}_{\mathrm{max}}\cdot H_{\mathrm{max}})}{274+3b_2\cdot\mathrm{dbh}-4b_3\cdot\mathrm{dbh}^2}\right]\cdot S(U)\cdot C(F_{\mathrm{A}})$$

with

$$H = 137 + b_2\cdot\mathrm{dbh} - b_3\cdot\mathrm{dbh}^2$$

(height of the tree) (5)

and

$$S(U) = \frac{1}{1+\exp[d(U_i - U)]} \quad \text{(salt stress factor)} \qquad (6)$$

H and dbh are indicated here in cm. The species-specific parameters G, $\mathrm{dbh}_{\mathrm{max}}$, H_{max}, b_2, b_3, d and U_i are provided for *Avicennia germinans*, *Rhizophora mangle*, and *Laguncularia racemosa* by Chen and Twilley (1998) (Table 1). The value U specifies the salinity at the stem position of the tree.

The second factor, $C(F_{\mathrm{A}})$, considers tree-to-tree competition. We assume that growth is impossible if the 'strength of neighbourhood' F_{A} (Eq. (3)) exceeds 0.5. Below this threshold, $C(F_{\mathrm{A}})$ must be 1 if the tree has no competing neighbours, and must decrease with the 'stress factor' F_{A}. Thus, $C(F_{\mathrm{A}})$ is given by:

$$C(F_{\mathrm{A}}) = (1 - 2\cdot F_{\mathrm{A}}) \qquad (7)$$

4.3. Mortality

Doubts exist as to any direct relationship between tree mortality and tree age in the case of mangrove trees, because, as in some terrestrial forests, trees which have been exposed to the highest stress may become the oldest trees. Moreover, the age of mangrove trees is generally unknown. In the FORMAN model Chen and Twilley (1998) handle this problem by using different mortality functions. KiWi abandons any

Table 1
Species-specific parameters for *A. germinans* and *R. mangle* used in the KiWi model

Parameters	Description	*A. germinans*	*R. mangle*	References
a	Scaling factor in Eq. (1)	10	10	Assumed
F_{min}	Min. value of the FON (Eq. (2))	0.1	0.1	Assumed
G	Grow constant	162	267	Chen and Twilley (1998)
D_{max}	Maximum dbh (cm)	140	100	Chen and Twilley (1998)
H_{max}	Maximum height (cm)	3500	3000	Chen and Twilley (1998)
$\mathrm{age}_{\mathrm{max}}$	Maximum age (year)	300	250	Chen and Twilley (1998)
b_2	Constant in height to dbh relationship	48.04	77.26	Chen and Twilley (1998)
b_3	Constant in height to dbh relationship	0.172	0.396	Chen and Twilley (1998)
d	Constant for salt effect on growth	−0.18	−0.25	Chen and Twilley (1998)
U_I	Salt effect on growth (g kg^{-1})	72.0	58.0	Chen and Twilley (1998)
ε	Additional yearly mortality	1/600	1/500	Assumed

relationship between age and mortality. Instead, we assume that the probability of dying increases after continuous periods of growth depression. In the model growth depression is effected by the two stress factors pore water salinity and competition. For the calculation of growth depression we do not differentiate between these particular causes. We only consider the effect on the yearly increment of the stem diameter, Δdbh. If Δdbh decreases in time the probability that the tree will die increases. However, it is unrealistic to assume that a tree reacts immediately to bad environmental conditions. As is known from field studies a tree can survive with a certain probability even when it does not grow during a certain time period. We thus included a 'memory effect' — each tree 'remembers' the growth increment Δdbh over a specified time range (5 years in KiWi). A tree dies if the mean over this time range, $\overline{\Delta \text{dbh}}$, is less than 1/2 of the average stem diameter increment under optimal conditions, $D_{\max}/\text{age}_{\max}$ (Table 1). The use of $\text{age}_{\max}$ to define the value '1/2' is optional. Field measurements focusing on the varying mortality of mangrove trees under different stress regimes were able to validate this value. Note that $\overline{\Delta \text{dbh}}$ decreases the more the stem diameter approaches its maximum, or the more the environmental conditions, both abiotic and biotic, deteriorate in consecutive years. The tree 'revives' if the stress period is followed by better years in which $\overline{\Delta \text{dbh}}$ increases. This happens, for example, when pore water salinity decreases or when neighbouring trees die. To consider other sources of tree mortality we use a small, additional yearly mortality ε. Altogether, the mortality submodel assures a moderate maximum age of a single tree.

4.4. Sapling establishment

Saplings are distributed randomly at the beginning of a simulation year. Whether a sapling establishes or not is dependent on the environmental conditions at the sapling's position. The probability of establishment at a given position is taken to be:

$$P_{\text{Sap}}(x,y) = (1 - 2 \cdot F(x,y)) \tag{8}$$

Biologically, Eq. (8) expresses how the probability of establishment depends on the competition strength of the older trees influencing the sapling. $P_{\text{Sap}}(x, y)$ is analogous to the correction factor $C(F_{\text{A}})$ (Eq. (7)). The rationale behind this analogy is that, under conditions which prevent tree growth, it should also be impossible that a sapling becomes established. The influence of pore water salinity on sapling establishment is not considered directly. But an established sapling will die in the same year if this factor prevents its growth, i.e. the establishment module is run first, then the growth module.

4.5. Output variables

In order to analyse the output from the model, we use the relationship between dbh and the crown diameter of *R. mangle* trees and the relation between dbh and the biomass of *R. mangle* and *A. germinans* trees, respectively. The biomass calculation has been approximated by Fromard et al. (1998). It is expressed for *A. germinans* as:

$$\text{BIOM} = 1.2 - 1.3 \cdot D + 0.5 \cdot D^2$$
$$(R^2 = 0.9) \quad \text{for } 1 < \text{dbh} < 4 \text{ cm} \tag{9}$$

and

$$\text{BIOM} = 63.3 - 17.1 \cdot D + 1.2 \cdot D^2$$
$$(R^2 = 0.9) \quad \text{for } 4 \text{ cm} < \text{dbh} \tag{10}$$

and for *R. mangle* as:

$$\text{BIOM} = 8.1 - 5.6 \cdot D + 1.2 \cdot D^2 \qquad (R^2 = 0.9) \tag{11}$$

with BIOM as biomass (t ha^{-1}) and $D = \text{dbh}$ (cm).

The calculation of the crown diameter of *R. mangle* (used for Fig. 4) derives from the approximation given by Cintrón and Schaeffer Novelli (1985):

$$r = 0.222 \cdot D^{0.654} \tag{12}$$

with crown diameter r (m) and $D = \text{dbh}$ (cm).

5. Results

5.1. Intra-specific competition

The explicit description of tree spacing by KiWi enables the process of self-thinning caused by competition among individuals to be studied. Our working hypothesis is that self-thinning occurs in natural mangrove forests in a similar way to that in terrestrial forest. We therefore studied self-thinning in order to test the FON approach, i.e. to see whether FON is able to reproduce self-thinning realistically.

We started with randomly distributed sapling cohorts of *A. germinans* and *R. mangle*. The size of the simulated area was 1 ha according to the ecological scale of the empirical studies being under focus. Initial density was 1000, 2000 and 3000 individuals per ha; initial age was 0, and dbh 1.37 cm. After initialisation no new sapling entered the plot. Fig. 3 shows self-thinning trajectories, i.e. how the number of individuals and the averaged biomass change in the course of time as a result of growth and mortality. The lines with a slope of -3/2 are the so-called 'self-thinning lines' (Begon et al., 1991). Regardless of initial density, all curves approach this line after a certain time period. The slope of $-3/2$ means that biomass increases faster than density decreases. This trend is not unlimited because the trees 'cannot grow to the sky'. Consequently, the self-thinning section of the trajectories is followed by a section there the loss of individuals is balanced by biomass increase of the remaining trees. The peak at the beginning of the trajectories of *A. germinans* (Fig. 3a) is caused by the different calculation of the biomass for trees with a dbh larger or smaller than 4 cm (Eqs. (9) and (10)). A comparison of Fig. 3a and b shows that the cohorts of *A. germinans* reach the self-thinning line at higher N than those of *R. mangle*.

Fig. 4 illustrates the self-thinning process described above. It presents the model output of an exemplary simulation run of an *R. mangle* cohort initialised at 1000 individuals per ha.

5.2. Inter-specific competition

Simulations were run with the same configuration as for the self-thinning process, except that now both *R. mangle* and *A. germinans* occur in the same plot. If both species enter the habitat at the same time, *R. mangle* dominates the forest at the beginning (Fig. 5a). This is caused by the faster initial growth of this species. However, because *A. germinans* has a longer mean lifetime, dominance is reversed after 200 years.

In Fig. 5b, saplings of *A. germinans* enter the plot 10 years after *R. mangle*. In this scenario, the initial advantage allows *R. mangle* to suppress the growth of *A. germinans* individuals, leading to a markedly smaller overall biomass of *A. germinans*. On the other hand, if *A. germinans* is the first species in the plot and *R. mangle* enters 10 years later, *A. germinans* dominates *R. mangle* all the time (Fig. 5c). Note that in all three scenarios in Fig. 5, the maximum overall biomass that 1 ha can produce is more or less the same (about 90 000 kg ha^{-1}).

6. Discussion

The main objective of this paper is to introduce the FON approach and to demonstrate its suitability for the analysis of tree spacing effects on forest dynamics. The suitability of the FON approach was tested by its implementation in the KiWi model. Here, we will first discuss whether KiWi provides new insights into mangrove forest dynamics, before assessing the potential of the FON approach in general.

6.1. The KiWi model

Compared with FORMAN (Chen and Twilley, 1998) KiWi uses one mortality function only. This 'memory function' considers parts of the tree's life history. Tree mortality is described as depending on this function only and, in turn, on the growth rate of the trees. The model results show that this description is sufficient to keep the maximum age within a reasonable range. Since there are doubts as to any direct relationship between tree age and mortality in the case of mangrove trees, and that the age of a mangrove tree cannot be determined as yet, this feature of KiWi is especially important.

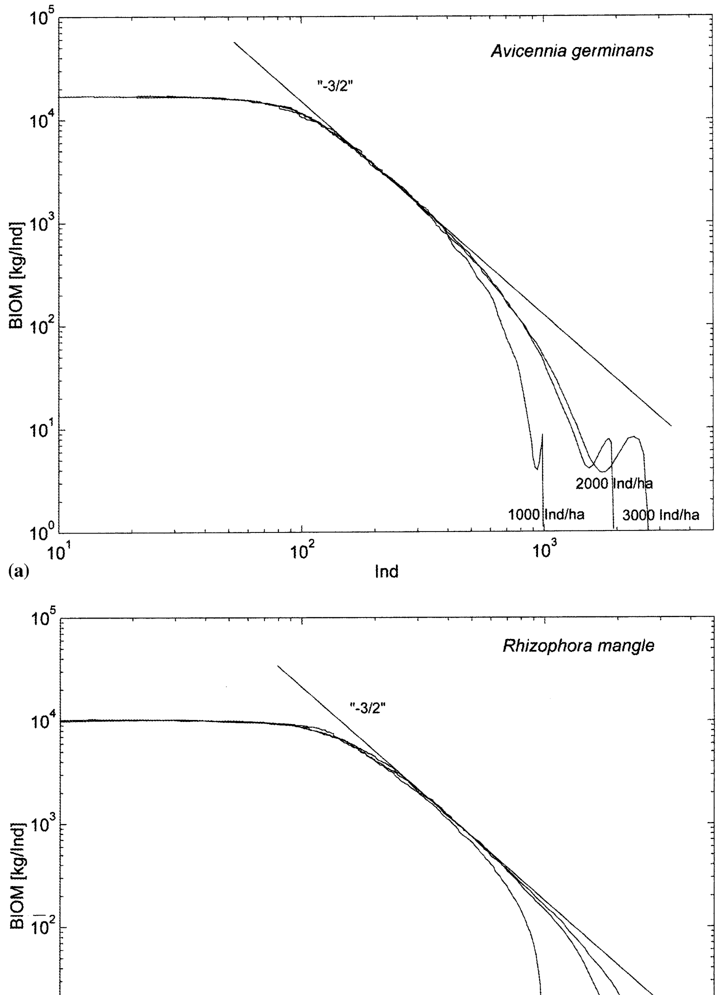

Fig. 3. Self-thinning trajectories of even-aged mangrove cohorts, i.e. development of density and averaged biomass in the course of time. Initial points of the trajectories are labelled with initial densities. (a) *A. germinans*; (b) *R. mangle*.

Another powerful feature of KiWi is its potential to give explicit consideration to tree spacing and, in turn, local competition. The resultant self-thinning trajectories match theoretical (Begon et al., 1991) and empirical trajectories (Londsdale and Watkinson, 1982; Cintrón and Schaeffer

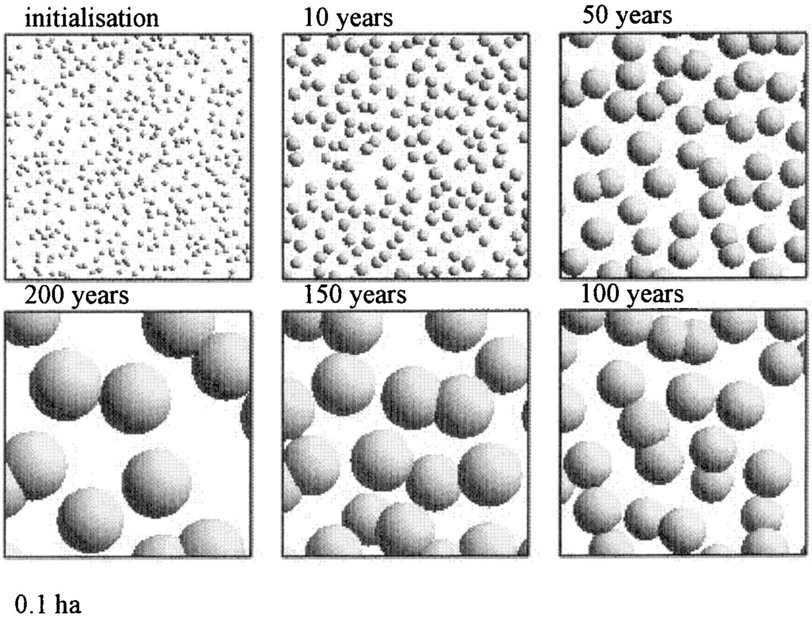

Fig. 4. Exemplary simulation run showing the development of a *R. mangle* cohort with an initial density of 1000 individuals per ha. The panels show the distribution of trees for consecutive time steps. The fate of selected individuals can thus be traced.

Novelli, 1985) astonishingly well. Thus, the self-thinning simulations show that the phenomenological description of local competition by ZOIs and FONs leads to realistic stand dynamics.

The self-thinning trajectories might suggest, erroneously, that the number of individuals is the independent variable and overall biomass the dependent one. Overall biomass increases due to the growth of the trees. Due to the constant and limited space available, an increase in overall biomass directly influences mortality and, in turn, the number of individuals. On the other hand, a high tree density may cause a depression of individual growth rates, which means there is a mutual relationship between biomass and density.

The overall maximum biomass which can be produced per ha is species-independent and limited to about 9×10^5 kg ha^{-1}. This result is confirmed by the results of the two-species system (Fig. 4). The specific values of the maximum overall biomass and of the density associated with it are dependent on the assumed relationship between FON and dbh, and on the calculation of the biomass as a function of dbh. Hence, they are suitable quantities for calibration and validation of KiWi against field data.

The self-thinning trajectories can also be used for validation. Although the specific slope of " − 3/2" cannot be expected for uneven-aged or mixed forests, a comparison of simulated forests with structural data for real forests of known age will help to prove the goodness-of-fit of the FON assumptions and to improve our understanding of the colonisation dynamics of existing habitats.

Despite the demonstration character of the simulations focusing on inter-specific competition, the results shown in Fig. 5 are interesting. Depending on the temporal sequence of establishment and on the delay between the date of emergence of the different species, the species dominating the forest may alternate.

The structure of the model is such that extensions can easily be made. Other heterogeneously distributed environmental parameters (e.g. flood

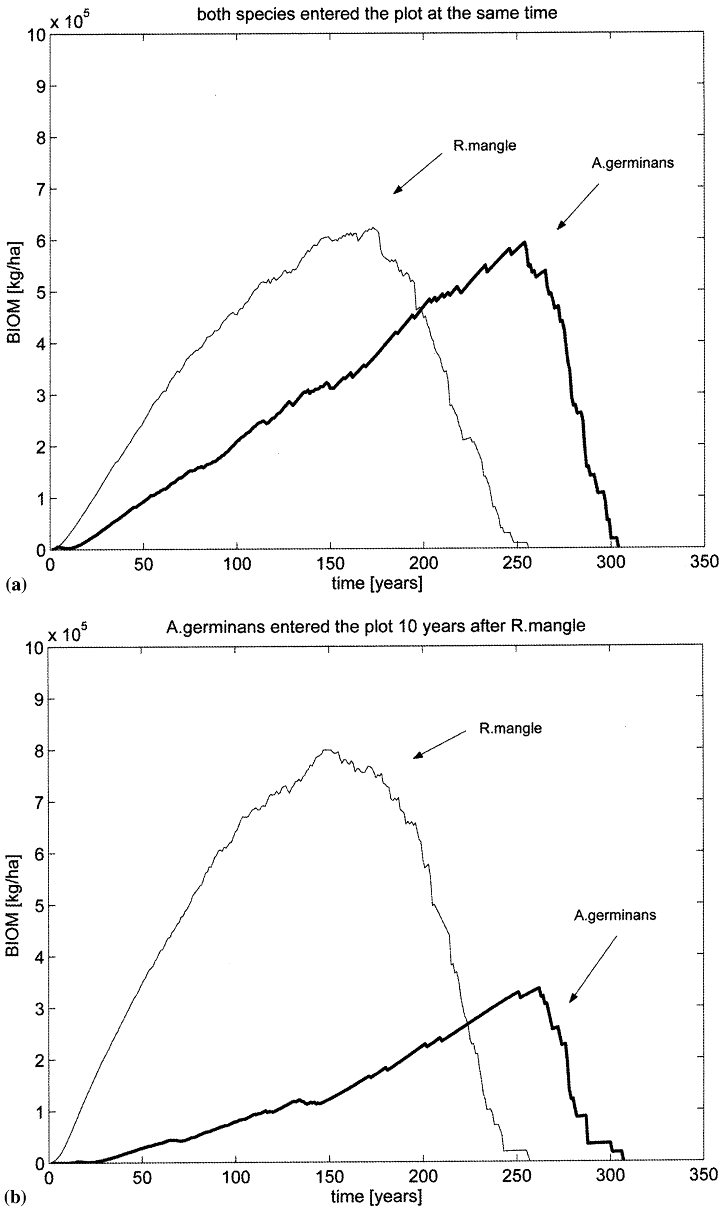

Fig. 5. Plot of overall biomass against time for two competing cohorts of *A. germinans* and *R. mangle*. The runs were performed as in Figs. 3 and 4: the habitat is initialised by a fixed numbers of individuals. After this initialisation, no more individuals enter the plot. (a) Saplings (1000) of both *A. germinans* and *R. mangle* enter the area at the same time. (b) The saplings of *R. mangle* enter the plot 10 years earlier than *A. germinans*. (c) The saplings of *A. germinans* enter the plot 10 years earlier than *R. mangle*.

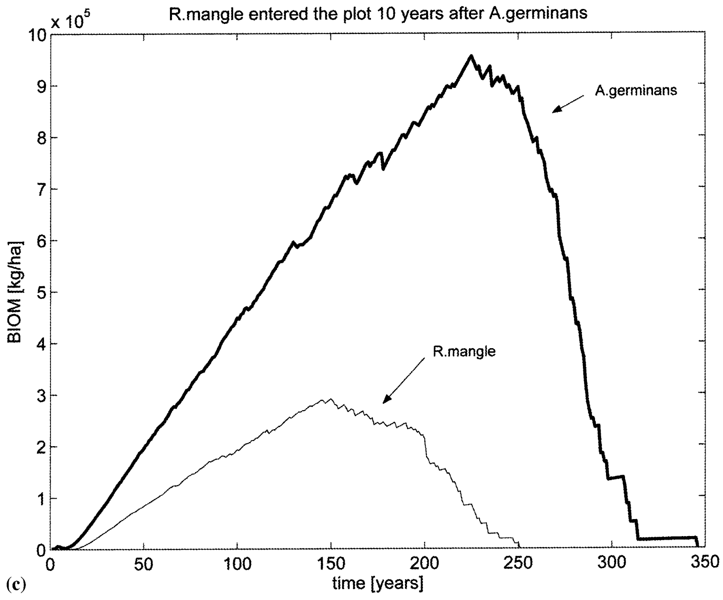

Fig. 5. (*Continued*)

ing, light and nutrient availability) can be described by additional maps (analogous to the salinity bitmap) and would then enter the growth equation as additional correction factors or logical rules. Likewise, differences in the environmental conditions for saplings, younger trees, or mature trees in different soil horizons can be considered by using further maps.

However, even the results obtained with the most simple version of a mangrove model based on the FON approach, i.e. the KiWi model, are promising and suggest further analyses using this and extended models. The KiWi model seems to be a step in the right direction towards the tool for theoretical synthesis needed by mangrove research.

6.2. The FON approach

FORMAN (Chen and Twilley, 1998), considers competition as well that is related to density of trees-using a mechanistic relationship with light. The FON approach is phenomenological in the same way as the Lotka–Volterra model of competition, but at the individual and neighbourhood level, not the population level. Competition is described by its results, not by its mechanism. Its consideration is not specifically linked to any resource. Although FON does not differentiate between the specific kinds of neighbourhood competition (e.g. canopy or root competition), the preliminary results of KiWi show that FON is a good metaphor for describing local competition. This may be due to the fact that the FON approach combines the advantages of grid-based and ZOI models, i.e. the emphasis on neighbourhood description with explicit consideration of the continuous space.

The function describing the FON, as well as the minimal field strength at the boundary of the ZOI of a tree, are not derived from field measurements. However, the analysis of aerial photographs could help to derive empirically motivated functions and parameters. Furthermore, the integration of photo imaging, field experiments and simulations would offer new opportunities for tree competition research. This could be especially important with regard to root spacing, considering the complicated and hence limited options for field experiments in most cases.

Finally, it should be noted that the FON approach is not limited to mangrove forest models. In our opinion, FON provides the basis for a great number of powerful models for explicit analysis of spatial heterogeneity and neighbourhood effects, not only of other forests and plant communities, but also of communities of other sessile organisms, e.g. benthic organisms. We do not view FON as an exclusive alternative to grid-based models, but as a tool for tackling problems which cannot be addressed with grid-based models. Often, a combination of FON at the local scale and grid cells at larger scales might be the most appropriate choice.

Acknowledgements

We thank Marie-Luise Schnetter who explained to us what mangroves 'feel'. Ernesto Medina and Robert Twilley found the time to read the first version of this paper and gave many helpful comments. Special thanks are extended to Rubén Lara, who sacrificed a great deal of time and energy during the preparation of the manuscript, and to Volker Grimm, who put some shine on the diamond. This study is a result of co-operation between the Center of Tropical Marine Ecology (ZMT), Bremen, Germany and the Universidade Federal do Pará e do Museum Paraense Emilío Goeldi (MPEG), both Belém, Brazil, under the Governmental Agreement on Co-operation in the Field of Scientific Research and Technological Development between Germany and Brazil financed by the German Ministry of Education, Science, Research and Technology (BMBF) (MADAM — Mangrove Dynamics and Management (Project number: 03F0154A)), and the Conselho Nacional de Pesquisa e Tecnologia (CNPq). This is MADAM contribution number #.

Appendix A. The calculation of F_A

As mentioned in Section 3, interpreting F_A as a mean value tremendously simplifies the calculation of the integrals in:

$$F_A^k = \frac{1}{A} \sum_{n \neq k} \int_{A'} \mathrm{FON}_n(x,y)\, \mathrm{d}a'. \tag{A1}$$

But still, depending on the complexity of the local FON, it could be hard to give an exact solution for Eq. (A1). This appendix gives a simple but effective generic algorithm to compute (Eq. (A1)) approximately.

In the given form the algorithm addresses only FONs that are rotationally symmetrically, i.e. the only independent variable is the distance r to the stem position. The idea of this algorithm is to divide the overlapping area of two ZOIs, into pitch circle rings (Graphic A1: dividing the overlapping area of two trees into pitch circle rings).

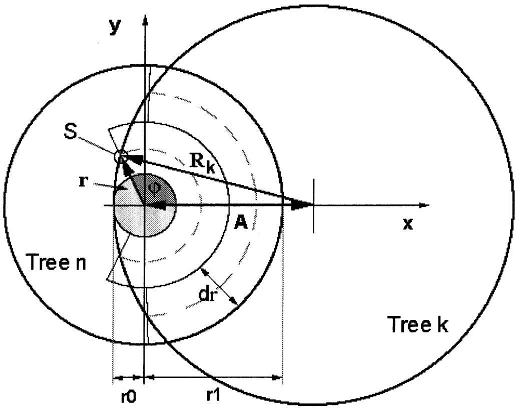

Hence you have to implement a function like this:

```
// Calculate the integral over the pitch circle ring with
// the half central angle phi and the thickness $(r1 - r0)$
double Tree.FON_PCR(double $\varphi$, double $r0$, double $r1$)
{
return $\int_{-\varphi}^{\varphi} \int_{r0}^{r1} \mathrm{FON}(r)\, \mathrm{d}r\, \mathrm{d}\varphi$;
}.
```

Due to the rotational symmetry the φ-integral collapses to the factor 2φ.

Now, if we focus on the kth tree, we have to integrate the FON of the nth tree over the overlapping area of the nth with the *k*th tree. We calculate this in the local system of coordinates of the *n*th tree with the origin at its stemming point and the *x*-axis pointing toward the stemming point of the *k*th tree (Graphic A1).

```
// Calculate the integral over the overlapping area of two trees.
// treeK is the focused, treeN the neighbour tree.
// treeN.R resp. treeK.R give the radius of the ZOI/FON.
double FA_kn(tree treeK, tree treeN)
{
  result = 0.0// suppose, they do not overlap
  A = distance between the steaming positions
  if (A > treeN.R + treeK.R)
  return result;  // no overlap
  // first we compute the max. diameter of the overlapping area
  r0 = A − treeK.R        // 'left' side of overlapping area
  if ( r0 < 0.0)
  {
    // a whole concentric circle (grayed in Fig. A1) is overlapped
    r0 = − r0;
    result = treeN.FON_PCR($\pi$, 0.0, r0);
    if (r0 > = treeN.R)
    {
      // treeN is completely overlapped by treeK
    return result;// return the (exact) result to the caller
  }
}
r1 = min( treeN.R, A + treeK.R); // 'right' side of overlapping area
// the (rest of the) overlapping area reaches from |r0| to r1
// and is now divided into nStrides pitch circle rings.
// (in Fig. A1 nStrides is only 2)
dr = (r1 − r0)/nStrides;  // s. Fig. A1
r = r0 + dr/2;  // centre radius of the first PCR, s. Fig A1
for (i = 0, i < nStrides, + + i )
{
// we have to calculate the angle $\varphi$ (□ in Fig. A1).
// with a little help from Pythagoras the coordinates of the
// intersection S (s. Fig. A1) are:
x = ($A^2 + r^2$ − treeK.$R^2$)/(2*A);
y = sqrt($r^2 - x^2$);
// and hence $\varphi$ is given by:
phi = arctan(y/x);
// add the integral over this pitch circle ring
result = result + treeN.FON_PCR($\varphi$,    r dr/2, r + dr/2);
r = r + dr;  // go to the next pitch circle ring
}
return result;  // return the result to the caller
}
```

Next, the summation in Eq. (A1) has to be performed, i.e. the summation of the overlapping FON of all trees:

```
// Calculate FA for all trees.
// N is the total number of trees.
// tree[k].FA holds the result for the kth tree
void CalculateFA( void)
{
// supposing you have an array [0...N − 1] of trees...
for (n = 0; n < N; + + n)
  tree[n].FA = 0.0;
for (k = 0; k < N; + + k)
{
  for (n = k + 1; n < N; + + n)
  {
    tree[k].FA = tree[k].FA + FA_kn( tree[k], tree[n]);
    tree[n].FA = tree[n].FA + FA_kn( tree[n], tree[k]);
  }
// get rid of the dimension: dividing by the ZOI
tree[k].FA = tree[k].FA/($\pi$*tree[k].$R^2$);
}
}
```

Although the code presented here has not been optimised at all, performance of this algorithm should not be worse then traversing a huge grid.

References

Adler, F.R., 1996. A model of self-thinning through local competition. Proc. Natl. Acad. Sci. 93, 9980–9984.

Baker, W.L., 1992. Effects of settlement and fire suppression on landscape structure. Ecology 73, 1879–1887.

Begon, M., Harper, J.L., Townsend, C.R., 1991. Ökologie Individuen, Populationen und Lebensgemeinschaften. Birkhäuser, Basel.

Berger, U., Wagner, G., Wolff, M., 1999. Virtual biologists observe virtual grasshoppers: an assessment of different mobility parameters for the analysis of movement patterns. Ecol. Model. 115, 119–127.

Berger, U., Glaser, M., Koch, B., et al., 1999. MADAM — the approach of an integrated project on mangrove dynamics and management. J. Coast. Conserv. 5, 125–134.

Chen, R., Twilley, R.R., 1998. A gap dynamic model of mangrove forest development along gradients of soil salinity and nutrient resources. J. Ecol. 86, 37–51.

Cintrón, G., Schaeffer Novelli, Y., 1985. Caracteristicas y desarrollo estructural de los manglares de norte y sur america. Cienc. Interam. 25, 4–15.

Czárán, T., 1998. Spatiotemporal Models of Population and Community Dynamics. Chapman and Hall, London Population And Community Biology Series 21.

Davie, T.J.A., 1999. A numerical model to quantify the growth of a canopy for a forest hydrology model. Appl. Geogr. 19, 45–67.

DeAngelis, D.L., Gross, L.J., 1992. Individual-Based Models and Approaches in Ecology. Chapman and Hall, London.

Fromard, F., Puig, H., Mougin, E., Marty, G., Bétoulle, J.L., Cadamuro, L., 1998. Structure, above-ground biomass and dynamics of mangrove ecosystems: new data from French Guiana. Oecologia 115, 39–53.

Galitsky, V.V., 1990. Dynamic 2D model of plant communities. Ecol. Model. 50, 95–105.

Gates, D.J., Westcott, M., 1978. Zone of influence models for competition in plantations. Adv. Appl. Prob. 10, 299–537.

Green, D.G., House, A.P.N., House, S.M., 1985. Simulating spatial patterns in forest ecosystems. Math. Comput. Simul. 27, 191–198.

Grimm, V., 1994. Mathematical models and understanding in ecology. Ecol. Model. 75/76, 641–651.

Grimm, V., 1999. Ten years of individual-based modelling in ecology: what have we learned, and what could we learn in the future? Ecol. Model. 115, 129–148.

Grimm, V., Frank, K., Jeltsch, F., Brandl, R., Uchmanski, J., Wissel, C., 1996. Pattern-oriented modelling in population ecology. Sci. Total Environ. 183, 151–166.

Hogeweg, P., 1988. Cellular automata as paradigm for ecological modelling. Appl. Math. Comput. 27, 81–100.

Huston, M., DeAngelis, D., Post, W., 1988. New computer models unify ecological theory. BioScience 38, 682–691.

Jeltsch, F., 1992. Modelle zu natürlichen Waldsterbephänomenen. Biologie, Shaker, Marburg/Lahn.

Jeltsch, F., Wissel, C., 1994. Modelling dieback phenomena in natural forests. Ecol.l Model. 75, 111–122.

Jeltsch, F., Milton, S.J., Dean, W.R.J., Rooyen, N.v., 1996. Tree spacing and coexistence in semiarid savannas. J. Ecol. 84, 2414–2427.

Jeltsch, F., Müller, M.S., Grimm, V., Wissel, C., Brandl, R., 1997. Pattern formation triggered by rare events: lessons from the spread of rabies. Proc. R. Soc. Lond. B 264, 495–503.

Jeltsch, F., Moloney, K., Milton, S.J., 1999. Detecting process from snapshot pattern: lessons from tree spacing in the southern Kalahari. OIKOS 85, 451–466.

Londsdale, W.M., Watkinson, A.R., 1982. Light and self-thinning. New Phytol. 90, 431–435.

Okabe, A., Boots, B., Sugihara, K., 1992. Spatial Tessellations; Concepts and Applications of Voronoi Diagrams. Wiley, Chichester.

Silvertown, J., Holtier, S., Johnson, J., Dale, P., 1992. Cellular automaton models of interspecific competition for space — the effect of pattern on process. J. Ecol. 80, 527–534.

Turner, M.G., 1987. Spatial simulation of landscape changes in Georgia: a comparison of three transition models. Landsc. Ecol. 1, 29–36.

Uchmanski, J., Grimm, V., 1996. Individual-based modelling in ecology: what makes the difference? Trends Ecol. Evol. 11, 437–441.

Wissel, C., 1992. Modelling the mosaic-cycle of a Middle European beech forest. Ecol. Model. 63, 29–43.

Wolfram, S., 1984. Cellular automata as models of complexity. Nature 311, 419–424.

Wyszomirski, T., 1983. A simulation model of the growth of competing individuals of a plant population. Ekol. Pol. 31, 73–92.

Wyszomirski, T., Wyszomirska, I., Jarzyna, I., 1999. Simple mechanisms of size distribution dynamics in crowded and uncrowded virtual monocultures. Ecol. Model. 115, 253–273.

Zeigler, B.P., 1977. Persistence and patchiness of predator–prey-systems induced by discrete event population exchance mechanisms. J. Theor. Biol. 67, 687–713.

Kapitel II,2

Nachbarschaftsfelder zur Untersuchung ökologischer Interferenz – vom Anfang und Ende der Selbstausdünnung

UTA BERGER[1], HANNO HILDENBRANDT[1]

[1] Center for Tropical Marine Ecology (ZMT), Bremen, Germany

In: F. Jopp & G. Wiegmann (eds.),
Rolle und Bedeutung von Modellen für den Erkenntnisprozeß in der Ökologie.
Theorie in der Ökologie Band 4, 19-30 (2001)

GfÖ-Arbeitskreis Theorie in der Ökologie, Jahrestreffen 2000, Seite 19-30

Nachbarschaftsfelder zur Untersuchung ökologischer Interferenzen – vom Anfang und Ende der Selbstausdünnung

Uta Berger[1], Hanno Hildenbrandt[1]

Zentrum für Marine Tropenökologie
Fahrenheitstr.1, 28359 Bremen

eMail: uberger@zmt.uni-bremen.de

Abstract

This paper focuses on the self-induced thinning process of tree cohorts. We analyse the emergence of a size hierarchy through local neighbourhood competition and its consequences on population's dynamics. We will show that the ongoing search for a fixed slope of the linear segment of the biomass-density-trajectory (*bdt*) can't be successful since it is species-specific and might be site dependent. Nevertheless, the concrete value of the slope is restricted in two directions: morphological constrains determine the lower limit; the strength of neighbourhood competition exerted by the individuals marks the upper one. The whole *bdt* can be divided into four segments which are related to characteristic stem diameter distributions of the cohort. During the first stage a minority of the individuals only are hindered in growing. During the second and the third stage, mortality induced by neighbourhood competition occurs. Then the skewness of the stem diameter distribution is positive indicating that the majority of the individuals is small and hindered in growth. The linear *bdt* segment starts with the maximum skewness of the stem diameter distribution and is linked to the homogenisation of this distribution. The investigations are based on the spatially explicit simulation model KiWi. This model is an application of the *field of neighbourhood* approach (FON). FON describes an individual tree by a function of competition defined on the *zone of influence* (ZOI) around the stem. The FON effects growth depression of the trees involved. Longer lasting growth depression results in dying trees. All simulations were carried out with growth parameters of the mangrove species (*Rhizophora mangle*), but the results are qualitatively valid in general.

Keywords: *self-thinning, forest dynamic, tree cohorts, simulation model, field of neighbourhood, zone of influence.*

Schlüsselwörter: *Selbstausdünnung, Walddynamik, Baumkohorten, Simulationsmodell, Nachbarschaftsfeld, Einflusszone.*

1. Einleitung

Die vorliegende Arbeit beschäftigt sich mit dem qualitativen und quantitativen Verlauf von Biomasse – Dichte – Trajektorien (*bdt*) während der Selbstausdünnung von Baumkohorten. Da diese Thematik bis heute zu den umstrittensten in der Ökologie zählt, sei hier eine kurze historische Einführung in die Problematik gegeben:

YODA et al. zeigten in einer Arbeit von 1963, dass während der Selbstausdünnungsphase von Kohorten höherer Pflanzen die Logarithmen der mittleren Biomasse in einem linearen

Zusammenhang mit den Logarithmen der Bestandsdichte stehen. Als Proportionalitätsfaktor zwischen beiden Größen wurde zu „-3/2" ermittelt. Dieser Zusammenhang wurde geometrisch begründet und als allgemein gültig postuliert. Seither wurden zahlreiche empirische und theoretische Untersuchungen vorgestellt, die zeigen, dass es tatsächlich weitere Pflanzenarten gibt, für die das „-3/2-Gesetz" gilt. Allerdings wurden noch häufiger Gegenbeispiele gefunden. Heute ist man sich weitestgehend darüber einig, dass ein fixer Wert nicht angegeben werden kann. Umstritten ist aber nach wie vor, ob es einen festen Grenzwert gibt, den die Anstiege aller Selbstausdünnungslinien nicht überschreiten können. Dafür sind „-3/2" bzw. „-4/3" in der Diskussion. Für letzteren wird dabei eine allometrische Begründung gegeben (siehe u.a. WHITE 1981). Interessant ist in diesem Zusammenhang auch eine Arbeit, die sich gar nicht direkt mit Selbstausdünnung beschäftigt. CINTRÓN & SCHAEFFER NOVELLI (1985) verwenden ein Biomasse-Dichte-Diagramm, in das Felddaten von 125 verschiedenen Mangrovenwäldern eingetragen wurden. Der Anstieg der Regressionslinie, die für diese Daten berechnet wurde, beträgt ebenfalls „-3/2". Interessant hieran ist, dass dieser „klassische" Wert ermittelt wurde, obwohl die Daten verschiedener Wälder gemischt verwendet wurden, die sich sowohl im individuellen Alter der Bäume als auch in der Artenzusammensetzung unterscheiden. Es scheint verwunderlich, dass der gefundene Proportionalitätsfaktor unabhängig von diesen Waldcharakteristika und von verschiedenen Standortbedingungen gelten soll. Dies führte uns zu folgenden Fragen:

Welche Entwicklungsstadien werden durch den Gesamtverlauf der Biomasse-Dichte-Trajektorie charakterisiert? Wird der Prozess der Selbstausdünnung in einem Biomasse-Dichte-Diagramm vollständig durch eine Gerade beschrieben? Inwieweit gibt es systemübergreifende Proportionalitätsfaktoren zwischen Biomasse und Dichte und was würde sie bestimmen?

Zur Untersuchung dieser Fragen simulierten wir mit Hilfe eines Computermodells die Entwicklung von Baumkohorten. Das verwendete Modell KiWi wurde ursprünglich entwickelt, um die Dynamik von Mangrovenwäldern zu untersuchen (BERGER & HILDENBRANDT 2000). Es basiert auf den Modellansatzes FON (*field of neighbourhood*), der die Nachbarschaftskonkurrenz zwischen einzelnen Pflanzen explizit beschreibt (BERGER & HILDENBRANDT 2000, BAUER et al. 2000). Er wurde speziell für die Beschreibung ökologischer Interferenzen innerhalb sessiler Artengemeinschaften entwickelt, deren Individuen variable morphologische Eigenschaften besitzen. Da sowohl KiWi als auch FON in BERGER & HILDENBRANDT (2000) ausführlich beschrieben wurden, beschränkt sich ihre Erläuterung im folgenden Abschnitt auf das Wesentliche. Im dritten Teil des Artikels werden Simulationsergebnisse zur Kohortenentwicklung der Mangrovenart *Rhizophora mangle* vorgestellt. Diese werden abschließend in generellem Kontext hinsichtlich der Selbstausdünnung von Pflanzengemeinschaften diskutiert.

2. Methodik

2.1 Der Modellansatz FON

FON ist das Kürzel für den englischen Begriff „field of neighbourhood". Der Ansatz basiert auf der Beschreibung von Individuen über eine sogenannten „zone of influence" (ZOI)

(CZÁRÁN 1998). Danach wird ein Individuum durch seine (Stamm-)Position charakterisiert. Eine kreisförmige Zone (ZOI), deren Durchmesser mit der Größe des Individuums wächst, umgibt diese Position. Sie definiert die Fläche, innerhalb der das Individuum seine Umgebung beeinflusst. Die Erweiterung des FON-Ansatzes besteht nun darin, dass innerhalb der ZOI eine Konkurrenzfunktion aufgeprägt wird. Das dadurch beschriebene, rotationssymmetrische Nachbarschaftsfeld (FON) stellt die ortsabhängige Konkurrenzstärke dar, die das Individuum auf seine Nachbarn bzw. seine Umgebung ausübt. Unter der Annahme, dass sich die Nachbarschaftsfelder aller Individuen überlagern, sind 2 Größen von Bedeutung (Abb.1): Das Gesamtfeld $F(x,y)$ gibt die Konkurrenzstärke an, die durch die etablierten Individuen an der Position (x,y) erzeugt wird. Für ein einzelnes Individuum wird F_A als ein Maß für die Konkurrenz, die es durch seine Nachbarn erfährt, eingeführt. F_A berechnet sich als Mittelwert des Gesamtfeldes (abzüglich des eigenen FONs) auf der ZOI, die von dem betrachtetem Individuum aufgespannt wird. $F(x,y)$ und F_A informieren somit über die konkrete Nachbarschaftssituation für einen Punkt bzw. für ein Individuum, die durch die Zahl der Nachbarn, deren Größe und lokaler Anordnung definiert wird.

2.2 Das Simulationsmodell KiWi

KiWi verwendet den FON-Ansatz zur Beschreibung von Mangroven. Der Radius der Einflusszone eines Baumes wird hier durch den Ausdruck $a \cdot rbh^b$ beschrieben (Abb. 1). *rbh* steht dabei für den Stammradius. Die Parameter a und b wurden zunächst fiktiv gewählt, orientieren sich aber grob an Kronendurchmesser bzw. Wurzelkreisdurchmesser für Mangroven, die FORMAD et al. (1998) anführt. Das Nachbarschaftsfeld wurde so definiert,

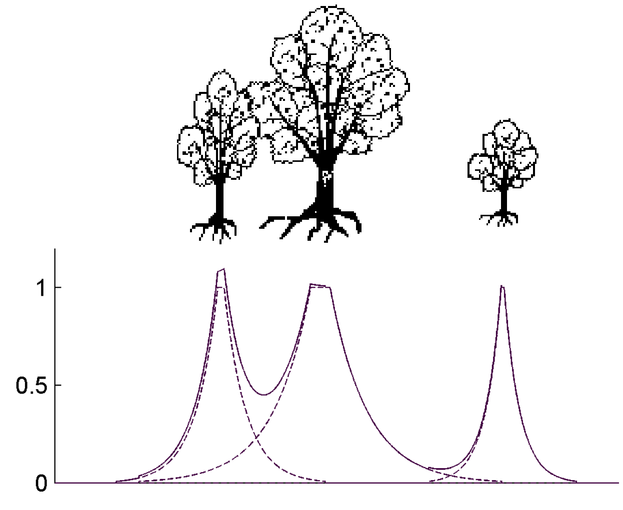

Radius der Einflusszone:

$$R = a \cdot rbh^b$$

Nachbarschaftsfeld eines Baumes:

$$FON(r) = e^{-c(r-rbh)}$$

Gesamtfeld:

$$F(x,y) = \underset{N}{\quad} FON_n(x,y)$$

Konkurrenzmaß für k-ten Baum:

$$F_A^k = \frac{1}{A} \sum_{A\, n \neq k} FON_n(x,y) \cdot da$$

Abb. 1: Der „*field of neighbourhood*“ – Ansatz (FON) beschreibt ein Individuum über seine Einflusszone (ZO auf die ein exponentiell abfallendes Nachbarschaftsfeld aufgeprägt ist (gestrichelte Linien). Die FONs al Individuen überlagern sich zu dem Gesamtfeld $F(x,y)$ (durchgezogene Linie). Der für das ein einzelr Individuum relevante Wert F_A ergibt sich aus dem Mittelwert des Gesamtfeldes aller anderen Individuen auf c Fläche der ZOI dieses Individuum.

dass es innerhalb des Baumstammes 1 beträgt. Außerhalb des Stammes fällt es exponentiell bis zu einem Minimalwert ab, den es am Rand der Einflusszone erreicht (Abb.1, BERGER & HILDENBRANDT 2000).

Das Wachstum der Bäume wird entsprechend CHEN & TWILLEY (1998) beschrieben. Danach wird der jährliche Stammzuwachs entsprechend einer sigmoiden Funktion berechnet, die unter optimalen Bedingungen gültig ist. Beeinträchtigende Umweltfaktoren werden durch Korrekturfaktoren berücksichtigt. CHEN & TWILLEY (1998) führten entsprechende Faktoren für die Salinität, Nährstoffe und Bodenfeuchte ein. Wir wollen uns aber in dieser Arbeit auf die Wirkprinzipien innerartlicher Konkurrenz konzentrieren. Deshalb nehmen wir die vorherrschenden Nährstoff- und Feuchtigkeitsgehalte des Sedimentes als optimal an und setzen voraus, dass die Porenwassersalinität mit ≤ 40 %o moderat ist. Unter diesen Annahmen benötigen wir nur einen Korrekturfaktor für die Nachbarschaftskonkurrenz (BERGER & HILDENBRANDT 2000). Für einen Baum beträgt er 1, wenn dieser keine konkurrierende Nachbarn hat. Andernfalls verringert er sich mit zunehmender Konkurrenzmaß F_A. Ist $F_A \geq 0.5$ ist der Konkurrenzkorrekturfaktor gleich 0 und somit kein Wachstum möglich (BAUER et al. (2000) untersuchen eine Modellvariante bei der erst für $F_A \geq 1$ das Wachstum Null wird).

Über das Alter von Mangrovenbäumen ist wenig bekannt. In der Literatur variieren die Angaben für das Maximalalter zwischen 70 und 350 Jahren (BURNS & OGDEN 1985, CHEN & TWILLEY 1998). In KiWi wird die Mortalität deshalb nicht direkt an das Baumalter gekoppelt. Stattdessen wird davon ausgegangen, dass die Sterbewahrscheinlichkeit mit verringertem Wachstum steigt. Um jedoch zu ermöglichen, dass sich ein Baum nach einer Periode schlechter Wuchsjahre „erholen“ kann, wird dieser Zusammenhang in einer „Memoryfunktion“ dargestellt (BERGER & HILDENBRANDT 2000). Danach stirbt ein Baum, falls seine mittlere Stammdurchmesserzunahme innerhalb der letzten 5 Jahre kleiner als die Hälfte derjenigen war, die er im Mittel unter optimalen Bedingungen erreicht hätte.

2.3 Durchgeführte Simulationen zur Untersuchung selbstinduzierter Ausdünnung

Mit den Wachstumsparametern von *Rizophora mangle* (CHEN & TWILLEY 1998) wurde die Entwicklungsdynamik einer Mangrovenkohorte auf einer 1 ha großen Fläche simuliert. Der Stammdurchmesser aller eingesetzten Bäume war einheitlich 1 cm. Die Bäume werden zufällig auf der Fläche verteilt. Untersucht wurde der Einfluss der individuellen Konkurrenzstärke auf die Dynamik der Population. Diese wurde durch die Form des Nachbarschaftsfeldes variiert. Dazu wurde in der Gleichung für den FON-Radius (s. Abb.1) bei $a = 10$ = konstant der Parameter b im Bereich von 0.4 ... 1.0 verändert. Das Diagramm in Abb.2 zeigt, wie mit kleinerem b der FON-Radius für einen bestimmtem Stammdurchmesser steigt. Dadurch wird das Nachbarschaftsfeld des Individuums vergrößert. Stellt man sich nun einen speziellen Punkt innerhalb des rotationssymmetrischen Feldes vor, so kann man erkennen, dass sich durch die Vergrößerung des Feldbereiches auch die Feldstärke im betrachteten Punkt erhöht. Allgemein vergrößert sich demnach die Konkurrenzstärke eines Individuums je kleiner b ist. Die gestrichelte Linie innerhalb des Diagramms markiert zum Vergleich den Kronenradius von *R. mangle* in Abhängigkeit vom Stammradius (FROMARD et al. 1998). Auf die Bedeutung dieser Funktion wird im Abschnitt *Diskussion* näher eingegangen.

Für jeden b -Wert wurden 50 Simulationen durchgeführt. Pro Simulationsjahr wurde die

Anzahl der Individuen und deren Stammdurchmesser registriert. Die Biomasse wurde aus diesen Angaben gemäß FROMARD (1998) berechnet. Da die am Rand der Fläche stehenden Bäume weniger konkurrierende Nachbarn haben als die, die in der Mitte stehen, wurden alle Individuen, die innerhalb eines zusätzlichen 10 m breiten Randstreifens stehen, von der Auswertung ausgeschlossen.

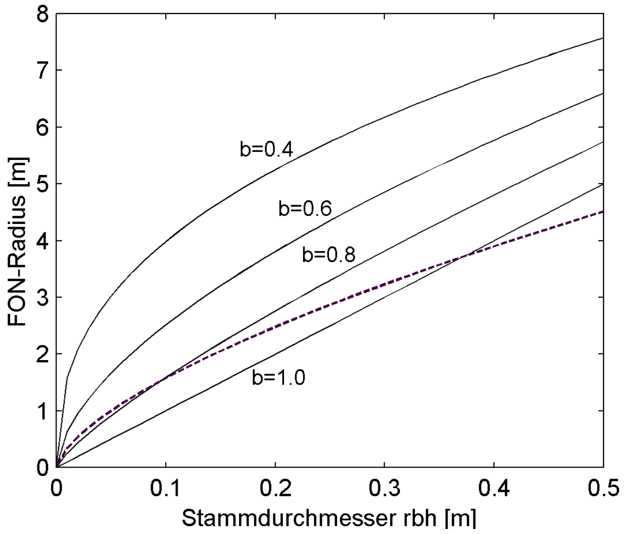

Abb. 2: FON-Radius in Abhängigkeit vom Stammdurchmesser *rbh* für verschiedene Parameterwerte von *b*. Zum Vergleich ist Kronenradius von *R. Mangle* nach FORMAT et al. (1998) eingezeichnet (gestrichelte Linie).

3. Ergebnisse

Abb. 3 zeigt die am Modell aufgenommenen Biomasse-Dichte-Trajektorien für verschiedene Werte von *b* und für zwei unterschiedliche Ansiedlungsdichten N_0. Sie informieren über die Zahl der überlebenden Individuen und deren mittlerer Biomasse während der Kohortenentwicklung. Die Leseweise ist entsprechend der zeitlichen Abfolge von rechts unten nach links oben.

Alle aufgenommenen Trajektorien lassen sich in vier distinkte Abschnitte einteilen. Der erste Abschnitt ist durch eine schnelle Biomassezunahme der Individuen gekennzeichnet. Mortalität tritt in den Anfangsjahren kaum auf. Später ist sie durch das „Abschwenken“ der Kurven nach links zu erkennen. Das geschieht um so eher, je stärker die individuelle Konkurrenzstärke ist (je kleiner *b* ist). Der sich anschließende, lineare Bereich ist mit der klassischen „Selbstausdünnungslinie“ identisch. Ausprägung und Steigung des linearen Bereiches ist wiederum von der individuellen Konkurrenzstärke abhängig. Ist die Konkurrenzstärke dagegen zu gering, kann ein linearer Abschnitt kaum oder gar nicht festgestellt werden. Der Vergleich der beiden Diagramme für $N_0 = 500$ und $N_0 = 1000$ Individuen zeigt, dass Lage und Steigung der hier angelegten Tangenten nahezu identisch sind. Für $b = 0.6$ wurde eine „-3/2“ Vergleichslinie eingezeichnet. Dieser, einst als

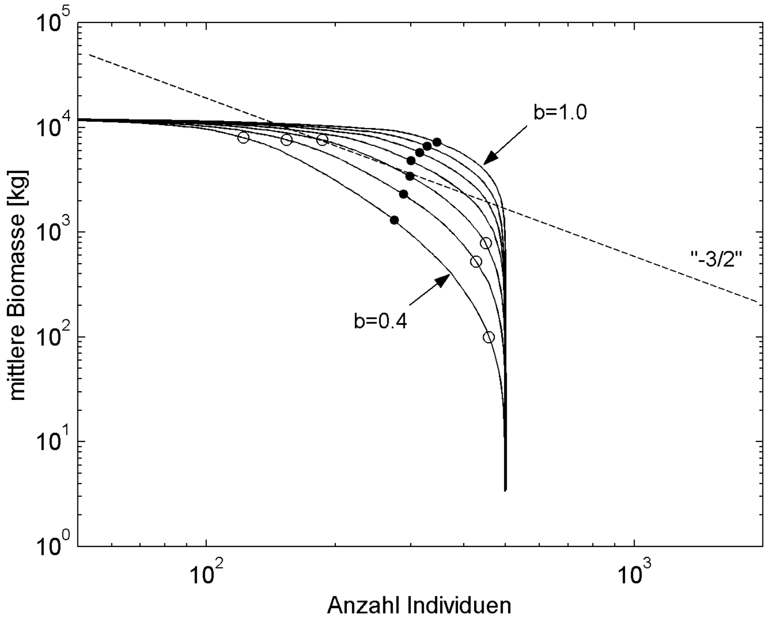

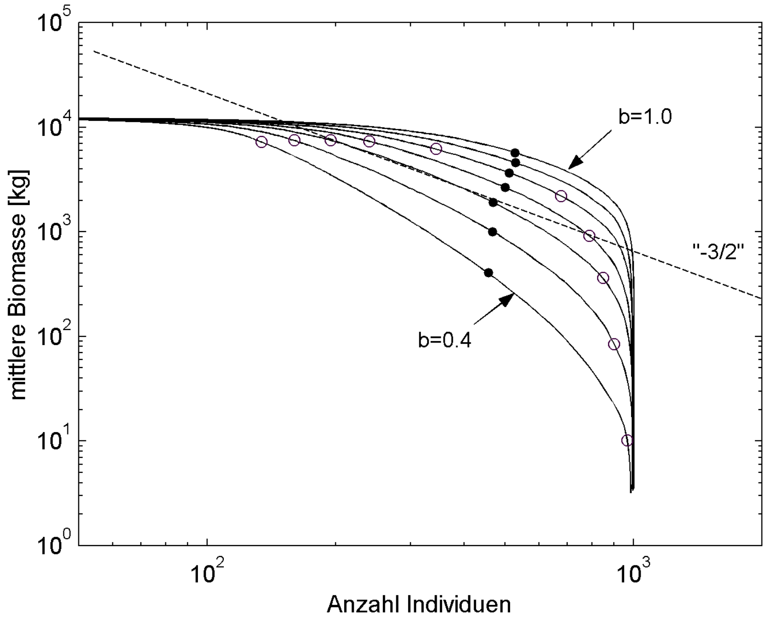

Abb. 3: Am Modell aufgenommene Biomasse - Dichte - Trajektorien für die Parameterwerte b=0.4 bis b=1.0 in 0.1-Schritten. Oben: Ansiedlungsdichte N_0=500 Individuen; Unten: Ansiedlungsdichte N_0=1000 Individuen. Geschlossene Kreise markieren die Maxima, offene Kreise die beiden Nulldurchgänge (soweit vorhanden) der Schiefe der Stammdurchmesser-Verteilung (vgl. Abb. 4). Gestrichelt ist jeweils eine Tangente der Steigung -3/2 an die Trajektorie für b=0.6 eingezeichnet. Sie wird als klassischer Fall des "Selbstausdünnungesetzes" in der Literatur diskutiert. Weitere Erläuterungen im Text.

„Selbstausdünnungs-Gesetz“ bezeichnete Anstieg wird von dem Model nur bei einer „zufällig passenden“ Konkurrenzstärke reproduziert.

In der verringerten Biomassezunahme der späteren Entwicklungsstadien wird die natürliche Limitierung des Wachstums der Individuen sichtbar. Der letzte Kurvenabschnitt, parallel zur x-Achse, zeigt die maximal erreichbare mittlere Biomasse an. Da sie von den Wachstumsparametern und nicht von der Konkurrenzstärke bestimmt wird, ist sie für alle *b*-Werte identisch. Jedoch steigt die Dichte, bei der die Individuen sie erreichen können mit *b*. Aus diesem Grund wächst die maximale absolute Biomasse mit kleiner werdender individueller Konkurrenzstärke. Diese definiert somit, unter der Voraussetzung, dass keine Ressourcenlimitierung auftritt, auch die optimale Bestandsdichte auf der Fläche.

Es wurde erwartet, dass sich infolge dieses Prozesses eine Größenhierarchie herausbildet, in der wenige große Bäume viele kleine dominieren. Diese Charakteristik asymmetrischer Konkurrenz gilt als typisch für selbstausdünnende Populationen (ADLER 1996, DAVIE 1999). Man kann sie an Hand der Schiefe (3.Moment) der Stammdurchmesserverteilung verfolgen. Ist dieser Verteilungsparameter negativ, stehen wenige kleine Bäume einer Mehrzahl größerer gegenüber. Eine positive Schiefe informiert darüber, dass in der Kohorte wenige große Bäume sehr vielen kleinen gegenüber stehen.

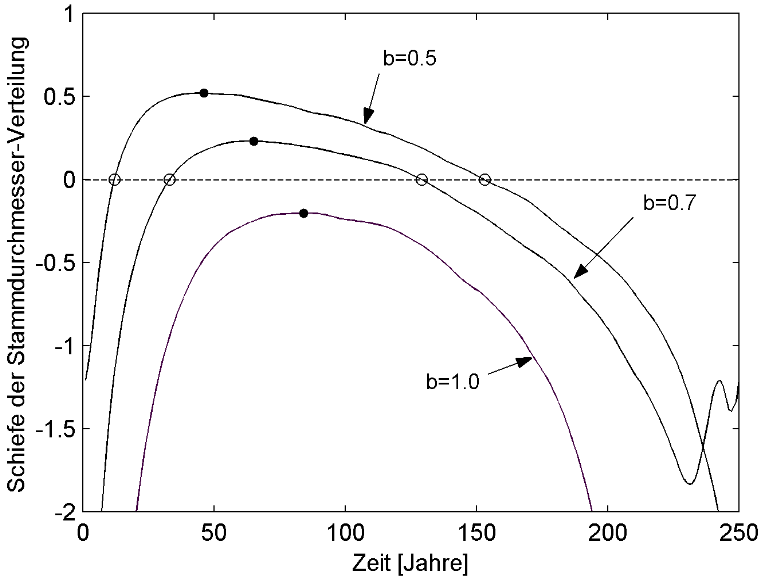

Abb. 4: Verlauf der Schiefe der Stammdurchmesser - Verteilung während der Kohortenentwicklung bei der Ansiedlungsdichte N_0=1000 Individuen. Geschlossene Kreise markieren die Maxima, offene Kreise die beiden Nulldurchgänge (soweit vorhanden).

Abb.4 zeigt die Symmetrieeigenschaften der Stammdurchmesser - Verteilung exemplarisch für *b* = 0.5, 0.7 und 1.0 während der Kohortenentwicklung. Der prinzipielle Verlauf ist jedoch für den gesamten untersuchten Bereich von *b* wie auch für die beiden Ansiedlungsdichten identisch. Anfangs ist die Schiefe der Verteilung stark negativ. Bedingt durch die zufällige Ansiedlung entstehen zufällige Klumpungen. Dadurch werden einige wenige Individuen besonders in ihrer Entwicklung behindert. Da dies jedoch die ersten Kandidaten sind, die „aussortiert“ werden, homogenisiert sich die Verteilung rasch. Bei genügender Konkurrenzstärke schließt sich eine Periode an, in der die Stammdurchmesser - Verteilung, so wie ursprünglich erwartet, positiv schief ist.

An den in Abb.3 und Abb.4 eingezeichneten Markern lässt sich erkennen, dass sich ein linearer Abschnitt in den Biomasse - Dichte - Trajektorien nur zwischen einem positiven Maximum und dem folgendem Nulldurchgang in der Schiefe der Stammdurchmesser - Verteilung ausbildet. Fehlt ein solches positives Maximum, prägt sich auch kein linearer Abschnitt aus. Ein positives Maximum in der Stammdurchmesser - Verteilung wird wiederum nur bei genügend hoher individueller Konkurrenzstärke erreicht.

4. Diskussion

Bis zu diesem Zeitpunkt wurden einzelne Abschnitte, die qualitativ für alle Trajektorien gleichermaßen gelten, diskutiert. Da der FON- Parameterbereich *b* in KiWi jedoch willkürlich festgelegt wurde, soll im Folgenden der Frage nachgegangen werden, welche der Trajektorien die Entwicklung von *R. mangle*- Kohorten unter optimalen Bedingungen beschreibt bzw. beschreiben. Da keine Feldmessungen dazu vorliegen, ist eine direkte Auswahl nicht möglich. Der Bereich der potentiell möglichen Kurven ist jedoch indirekt einschränkbar. Dazu wurde in Abb.2 der Kronenradius in Abhängigkeit vom Stammradius eingezeichnet. Wenn man annimmt, dass dieser Radius den Platz vorgibt, den ein Baum mindestens benötigt, dann sind *b*-Parameter, die zu kleineren FON Durchmessern führen, unrealistisch. Da sie einem Baum eine geringere FON – Fläche zuweisen, als er für seine Krone mindestens benötigt, führen sie zu Baumdichten pro Fläche, die unter natürlichen Bedingungen nicht auftreten können. Für die Biomasse - Dichte - Trajektorien in Abb.3 heißt das, dass alle Kurven für $b > 0.7$ nicht erlaubt sind. Daraus ergeben sich folgende allgemeine Hypothesen bezüglich des Anstieges von Selbstausdünnungslinien für Kohorten, die sich unter natürlichen, optimalen Bedingungen entwickeln: der Betrag des Anstieges der Selbstausdünnungskurve wird nach unten durch die Morphologie der Art begrenzt. Das begründet sich aus der Tatsache, dass der Anstieg der Trajektorien um so flacher ist, je größer *b* ist. Der maximale *b* – Wert wird aber durch Größenparameter, wie den Kronendachdurchmesser, vorgegeben. Die morphologischen Grenzen müssen dabei nicht immer offensichtlich sein. Ebenso könnte die unterirdische Wurzelfläche die Definition der FON – Fläche bestimmen. Nach oben wird der Betrag des Anstieges durch die individuelle Konkurrenzstärke bestimmt (der Anstieg ist um so steiler, je geringer *b* ist). In unserem konkreten Fall wird eine Erhöhung der Konkurrenzstärke durch eine Vergrößerung des FON – Fläche erreicht. Eine biologische Interpretation hierfür wäre das Ausscheiden toxischer Substanzen, die die Ansiedlung anderer Individuen in einem bestimmten Umkreis hemmt. Eine Erhöhung der Konkurrenzstärke kann aber auch durch eine Veränderung der Form des FON – Feldes erreicht werden. Dies könnte der veränderten Dichte des Kronendaches bzw. des Wurzelballens entsprechen.

Der gewählte Modellansatz gibt die Art der Ressource und somit die Form der individuellen

Konkurrenz nicht vor. Mit seiner Hilfe könnte aber eine systematische Analyse empirischer Daten zu einem weiteren Verständnis des Selbstausdünnungsprozesses höherer Pflanzen führen. Es sei an dieser Stelle vermerkt, dass die gefundenen Ergebnisse qualitativ nicht an das Ökosystem Mangrove gebunden sind und auch nicht von der gewählten Baumart *R. mangle* abhängen. Der prinzipielle Verlauf der Biomasse - Dichte - Trajektorien bleibt erhalten, auch wenn andere Wachstumsparameter angenommen werden (siehe auch BERGER & HILDENBRANDT 2000). Die durch die Variation von *b* gewonnene Kurvenschar in Abb.3 ist vielmehr wichtig für die Interpretation aller bisher erhobenen und scheinbar widersprüchlichen Aussagen, die durch Selbstausdünnungsexperimente verschiedener Arten erhoben wurden. Sie zeigen, dass es keinen allgemein gültigen, fixen Selbstausdünnungsfaktor gibt. Je nach Konkurrenzstärke sind für verschiedene Arten auch unterschiedliche Selbstausdünnungslinien zu erwarten.

Abschließend sollen die präsentierten Ergebnisse mit den eingangs gestellten Fragen verglichen werden: Es wurde gezeigt, dass einzelne Kurvenabschnitte der Biomasse - Dichte - Trajektorie charakteristischen Populationsstrukturen zuordenbar sind. Eine Gerade markiert nur den Abschnitt der Selbstausdünnung, bei dem die Größenasymmetrie der Kohorte abnimmt. Die Schiefe der Stammdurchmesserverteilung muss dabei positiv sein. Die durch CITRÓN & SCHAEFFER NOVELLI (1985) stimulierte Frage nach der Existenz eines für Mangrovenwälder gültigen, systemübergreifenden Selbstausdünnungsfaktors, kann mit dieser Arbeit nicht beantwortet werden. Es konnte aber gezeigt werden, dass sein Vorhandensein ähnliche Konkurrenzstärken der in den Untersuchungsgebieten auftretenden Mangrovenarten *Rhizophora mangle*, *Avicennia germinans* und *Laguncularia racemosa* voraussetzt.

Danksagung

This study is a result of co-operation between the Center of Tropical Marine Ecology (ZMT), Bremen, Germany and the Universidade Federal do Pará e do Museum Paraense Emilío Goeldi (MPEG), both Belém, Brazil, under the Governmental Agreement on Co-operation in the Field of Scientific Research and Technological Development between Germany and Brazil financed by the German Ministry of Education, Science, Research and Technology (BMBF) [MADAM – Mangrove Dynamics and Management (Project number: 03F0154A)], and the Conselho Nacional de Pesquisa e Tecnologia (CNPq). This is MADAM contribution number #.

Literatur

ADLER, F.R. 1996: A model of self-thinning through local competition. - Proceedings National Academy of Science USA 93: 9980-9984.

BAUER, S., BERGER, U., HILDENBRANDT, H., EISINGER, D. & V. GRIMM 2000: Modellierung von Nachbarschaftskonkurrenz in Pflanzenpopulationen: Test eines neuen Ansatzes -**BEITRAG IN DIESEM HEFT.**

BEGON, M., HARPER, J.L. & C.R. TOWNSEND 1991: Ökologie: Individuen, Populationen und Lebensgemeinschaften. Basel: Birkhäuser Verlag.

BERGER, U. & H. HILDENBRANDT 2000: A new approach to spatially explicit modelling of forest dynamics: spacing, ageing and neighbourhood competition of mangrove trees. - Ecological Modelling 132: 287 - 302.

BURNS, B.R. & J. OGDEN 1985: The Demography of the Temperate Mangrove Avicennia marina (Forsk.)

Vierh. at its Southern Limit in New Zealand. - Australian Journal of Ecology 10: 125-133.

CHEN, R. & R.R. TWILLEY 1998: A gap dynamic model of mangrove forest development along gradients of soil salinity and nutrient resources. Journal of Ecology 86: 37-51.

CINTRÓN, G. & Y. SCHAEFFER NOVELLI 1985: Caracteristicas y desarrollo estructural de los manglares de norte y sur america. Cienca Interamericana 25: 4-15.

CZÁRÁN, T. 1998: Spatiotemporal models of population and community dynamics. London . Weinheim . New York . Tokyo . Melbourne . Madras: Chapman & Hall.

DAVIE, T.J.A. 1999: A numerical model to quantify the growth of a canopy for a forest hydrology model. Applied Geography 19: 45-67.

FROMARD, F., PUIG, H., MOUGIN, E., MARTY, G., BÉTOULLE, J.L. & L. CADAMURO 1998: Structure, above-ground biomass and dynamics of mangrove ecosystems: new data from French Guiana. Oecologia: 115, 39-53.

WHITE, J. 1981: The allometric interpretation of the self-thinning rule. Journal of Theoretical Biology 89: 475-500.

YODA, K., KIRA, T., OGAWA, H. & K. HOZUMI 1963: Intraspecific competition among higher plants. XI: Self-thinning in overcrowded pure stands under cultivated and natural conditions. Journal of Osaka City University Institute of Polytechnics D 14: 107-129.

Kapitel II,3

About the competition strength of individual trees and its influence on the curvature of the biomass-density-trajectory of the whole cohort

UTA BERGER[1], HANNO HILDENBRANDT[1]

[1] Center for Tropical Marine Ecology (ZMT), Bremen, Germany

Plant Ecology, in press (2002)

TITLE PAGE

Full title

About the competition strength of individual trees and its influence on the curvature of the biomass-density-trajectory of the whole cohort

Authors

Uta Berger
Hanno Hildenbrandt

Affiliation and address for each author:

Uta Berger[1]

uberger@zmt.uni-bremen.de

Hanno Hildenbrandt[1]

hildenbr@zmt.uni-bremen.de

[1] Center for Tropical Marine Ecology, Fahrenheitstr.6, 28359 Bremen, Germany

Corresponding author

Uta Berger
Center for Tropical Marine Ecology, Fahrenheitstr.6, 28359 Bremen, Germany

Key words: self-thinning, forest dynamics, tree cohorts, simulation model, field of neighbourhood, zone of influence

Abstract

We simulated the self-thinning of *Rhizophora mangle* mangrove forests with the spatially explicit simulation model *KiWi.* This model is an application of the *field of neighbourhood* (*FON*) approach which describes an individual tree by a competition function defined on the *zone of influence* (*ZOI*) around the stem. The *FON* causes growth depression of the trees involved. Sustained growth depression results in tree death. We propose a subdivision of the biomass density trajectories (*bdt*), obtained during the thinning process, into four segments which are related to characteristic shapes of the stem diameter distribution of the cohort. A positive skewness of the stem diameter distribution, indicating that the majority of the individuals are small and hindered in growth, is necessary for the occurrence of a linear segment within the *bdt*, the so-called 'self-thinning line'. This segment is the third *bdt* segment according to our classification. It is reached when the positive skewness of the stem diameter distribution is maximal and ends when the skewness reaches its second zero transition. The thinning line is therefore linked to the homogenisation process which forces the symmetry of the stem distribution. We show that the ongoing search for an universal slope for the linear segment of the biomass-density trajectory *(bdt*) cannot succeed since it is species-specific and may also be site-dependent. The slope increases with increasing competition strength of the individuals. Nevertheless, the lower limit of the slope is pre-defined by geometrical constraints and modified by the actual strength of the neighbourhood competition. Although the simulations were all carried out with growth parameters of the mangrove species *(Rhizophora mangl*e), our results should be qualitatively valid and form a plausible theoretical framework to account for different biomass-density trajectories.

Introduction

For the self-thinning of cohorts of higher plants, Yoda et al. (1963) outlined a linear relationship between the logarithms of average biomass and plant density (Harper 1977, Westoby 1984, Silvertown 1992). The slope of this linear relationship was determined to be -3/2. Both the linearity and the slope were explained geometrically and were postulated to be generally valid. Since then, numerous empirical and theoretical cases have been found in which the '–3/2-rule' has been shown to be valid. However, counterexamples have been found even more frequently (Weller 1987). Today, most ecologists agree there is no universal value for the slope. However, whether there is an upper limit which the slopes of self-thinning lines cannot exceed is still disputed. Both '–3/2' and '–4/3' have been proposed as an upper limit. For the latter value, an allometric explanation is given (e.g., White 1981, Enquist et al. 1998). Given the diversity of values found for the slope of the self-thinning line, whether the 'self-thinning rule' deserves its name has been the subject of controversial discussion (Lonsdale 1990, Weller 1991, Sackville Hamilton 1995). We do not want to enter this discussion here. Instead, we simply assume that all different empirical findings regarding self-thinning are significant; our aim is to find a theoretical framework which can account for these different biomass-density trajectories (*bdt*). This concept should include both the emergence of the different segments of the *bdt's* and the different slopes of the self-thinning line. To provide the basis for the development of this framework, the three classic segments of the *bdt* suggested by Begon et al. (1991), and Silvertown and Doust (1993) will be analysed while considering variations in the population structure during the development of a simulated mangrove forest.

Methods

The FON approach: The mangrove forest model *KiWi* used for the simulations is based on the individual-based approach of modelling local plant interactions: the 'field of neighbourhood' or *FON* approach (Berger & Hildenbrandt 2000). In this approach individuals are characterized at first by their stem position which is surrounded by a circular 'zone of influence' (*ZOI*) whose diameter increases with the individual's size. This zone defines the area within which the individual influences its surroundings (neighbours and abiotic factors). Within the *ZOI*, a competition function is defined: the 'field of neighbourhood' (*FON*). This competition function is a scalar field representing the local competition strength at any point within the individual's *ZOI*. Assuming that the fields of neighbouring individuals overlap, two parameters are of importance (Fig. 1): the total field *F(x,y)* defines the competition strength exerted by all the individuals, which influences the position *(x,y)*. For one single individual, F_A quantifies the competition that the individual suffers from its neighbours. F_A is calculated as the integral of the total field (minus the *FON* of the focal individual) on the individual's *ZOI* divided by the area of the *ZOI* of the focal individual. *F(x,y)* and F_A quantify the neighbourhood situation for a point and an individual, respectively. This neighbourhood situation is consequently defined by the number of neighbours, their size and local constellation.

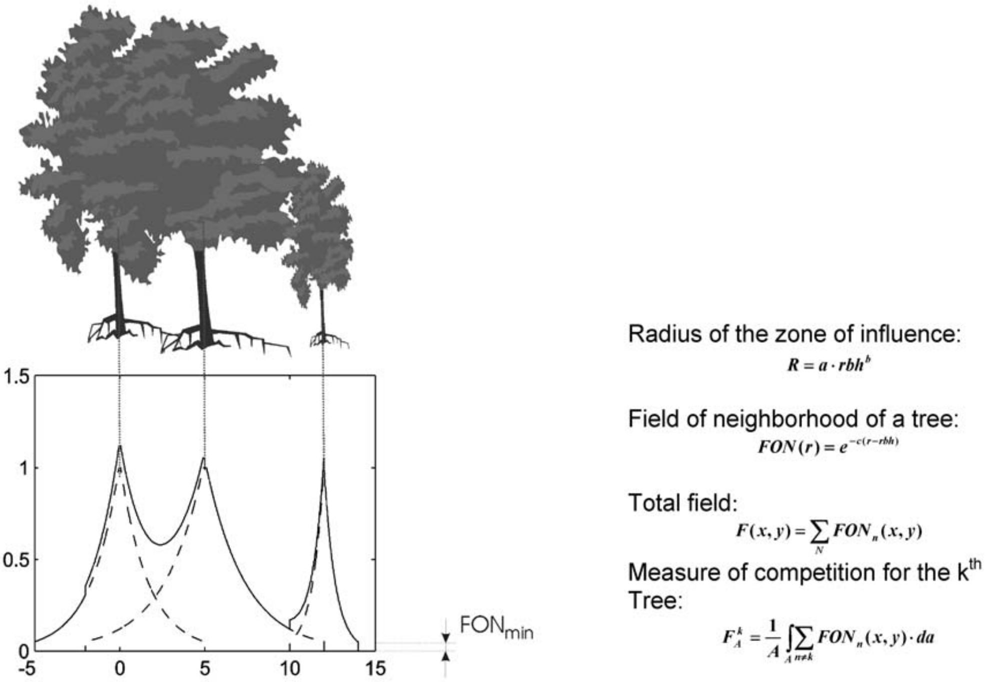

Fig. 1: The 'field of neighbourhood' (*FON*) approach describes an individual by means of its 'zone of influence' (*ZOI*), on which an exponentially decreasing neighbourhood field (dashed lines) is defined. The *FON*s of all individuals are superimposed on the total field F(x,y) (solid line). The value F_A which is relevant for a single individual results from the mean value of the total field of all other individuals exposed on the *ZOI* of the focused individual.

The mangrove model KiWi: KiWi uses the *FON* approach for the description of mangroves. The *ZOI* radius of a tree is described by the expression $a*rbh^b$ (Fig. 1), where *rbh* is the stem radius. The formula used provides an approximation of ZOI dimensions based on the allometric relations of the trees measured in the field (e.g., *rbh* versus projected root area or *rbh* versus projected canopy area). The parameters *a* and *b* were at first assumed arbitrarily but then roughly determined based on the relationship between *rbh* and crown diameters of *Rhizophora mangle*: $r_{crown} = 7.113 \cdot rbh^{0.654}$ (Cintrón & Schaeffer Novelli, 1985) with r_{crown} and *rbh* given in meter. The field of neighbourhood used in *KiWi* is similar to the competition function used by Adler (1996). It is defined as:

$$
\begin{array}{ll}
FON(r) = 1 & ; \text{for } 0 \le r < rbh \\
FON(r) = e^{-c(r-rbh)}, \quad c = \dfrac{|\ln(F_{\min})|}{R - rbh}, \text{ R from (1)} & ; \text{for } rbh \le r \le R \\
FON(r) = 0 & ; \text{otherwise}
\end{array}
\qquad (1)
$$

In contrast to Adler's competition function, the maximum *FON* value of 1 is assumed for the whole stem of the tree. This ensures that neighbouring trees do not overlap with their stems. From the perimeter of the stem, the *FON* decreases exponentially. A second difference to Adler's competition function is the limitation of *FON* to the minimum value FON_{min} at the edge of the *ZOI* (Fig. 1, Berger & Hildenbrandt 2000). Thus *FON* is directly assigned to the physical dimension of the tree as described by the *ZOI.* Adler considers furthermore only distances between the individuals by the competition function, whereas *KiWi* works with overlapping areas and fields, describing individual dimensions and competition strengths. The growth of the trees is described according to Chen & Twilley (1998):

$$\frac{\Delta dbh}{\Delta t} = \left[\frac{G \cdot dbh \cdot (1 - dbh \cdot H / dbh_{\max} \cdot H_{\max})}{274 + 3b_2 \cdot dbh - 4b_3 \cdot dbh^2} \right] \cdot C \qquad (2)$$

with $$H = 137 + b_2 \cdot dbh - b_3 \cdot dbh^2 \qquad \text{(height of the tree)} \tag{3}$$

Thus, the annual stem increase is calculated after a sigmoid function that is valid under optimum conditions (first right part of equation (1)). The parameters are given in Table 1. Impairing environmental factors are taken into account by the correction factor *C*. Chen & Twilley (1998) introduced corresponding factors for pore water salinity, nutrients, and sediment humidity. However, here we concentrate on mechanisms of intra-specific competition and assume optimal conditions regarding nutrients, sediment humidity and pore water salinity (i.e. ≤ 40 PSU). Therefore, we only consider the correction factor $C(F_A)$ which describes neighbourhood competition (Berger & Hildenbrandt 2000). Thus,

$$C = C(F_A) = (1 - 2 \cdot F_A)\ . \tag{4}$$

$C(F_A)$ is 1 if the tree does not have any competing neighbours. Alternatively, the factor decreases with increasing competition strength F_A. For $F_A \geq 0.5$, the competition correction factor is equal to 0 and therefore no growth is possible (Bauer et al. 2001 examine a model variation where the growth only stops if $F_A \geq 1$).

Parameters	Description	*R.mangle*	References
F_{min}	min. value of the FON (2)	0.1	assumed
G	Grow constant	267	Chen & Twilley 1998
D_{max}	Maximum *dbh* [cm]	100	Chen & Twilley 1998
H_{max}	Maximum height [cm]	3000	Chen & Twilley 1998
b_2	Constant in height to *dbh* relationship	77.26	Chen & Twilley 1998
b_3	Constant in height to *dbh* relationship	0.396	Chen & Twilley 1998

Table 1: Species-specific parameters for *R. mangle* used in the *KiWi* model

Little information exists about the age of mangrove trees. In the literature, descriptions of the maximum age vary between 70 and 350 years (Burns & Ogden 1985, Chen & Twilley 1998). In *KiWi*, mortality is therefore not directly linked to tree age but to growth. The likelihood of death increases with reduced growth. However, in order to enable a tree to 'recover' after a period of bad years when growth has been suppressed, a 'memory function' is introduced (Berger & Hildenbrandt 2000): according to this function, each tree "remembers" the growth increment Δdbh over a specified time range (5 years in *KiWi*). A tree dies only if its mean stem diameter increase in the last 5 years is less than half the increase it would on average have achieved under optimum conditions during these 5 years.

Simulation experiments to examine self-thinning: Using the growth parameters of *Rhizophora mangle* (Chen & Twilley 1998), the development of a mangrove cohort was simulated on 1 ha. The stem diameters of all trees were initially 1 cm. The trees were randomly distributed in the area. The influence of the individual competition strength on the population dynamic was examined. For this purpose, the shape of the individual neighbourhood fields was varied. This was done by varying the parameter *b* between 0.4 and 1.0, whereas *a* was kept constant at 10 (see equation for the *FON* radius, Fig. 1). Fig. 2 shows that for a given stem diameter the *FON* radius is larger for smaller values of *b* and, in turn, the individual's *ZOI* is larger. Hence, if a particular point within the *ZOI* is considered, it is clear that a larger *FON* radius implies a higher value of the *FON* at this point. Thus, *b* is a parameter which largely determines – inversely – competition intensity. The shaded line within the diagram marks the relationship between the stem and crown radius of *R. mangle* (Fromard et al. 1998) and is discussed below.

For each value of *b*, 50 simulations were executed. In each simulated year, the number of individuals and their stem diameter were registered. The biomass was calculated based on these values in accordance with Fromard et al. (1998):

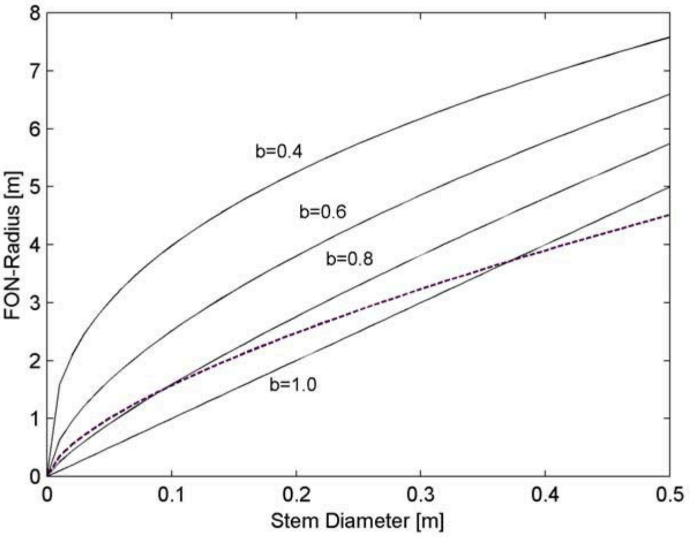

Fig. 2: *FON* radius depending on the stem diameter for different values of the parameter *b*. To the comparison, the crown radius of *R. mangle* was drawn according to Fromard et al. (1998) (dashed line).

$$BIOMASS = 8.1 - 5.6 \cdot dbh + 1.2 \cdot dbh^2 \qquad (5)$$

with *dbh* as stem diameter given in cm. Since the trees standing at the edge of the area have fewer competing neighbours than those standing in the middle, all individuals growing within the 10 m wide zone at the forest's border were excluded from the evaluation.

Results

Fig. 3 shows the biomass-density trajectories (*bdt*s) produced by the model for different values of *b* and for two different initial densities N_0. All trajectories show the three distinct, classic segments introduced and discussed by Begon et al. 1991, and Silvertown 1992: the fast growing segment, the intrinsic self-thinning line, and the post-thinning segment indicating the maximum mean biomass of the individuals. The first segment starts from N_0 with a rapid increase in biomass of the individuals. At the end of this segment, mortality occurs caused by the beginning interaction of the individuals. The mortality is higher for higher competition strength of the individuals as described by smaller values of *b*. The 'self-thinning line' is the second segment of the *bdt*. Its shape and its slope depend on the individual's competition strength. For comparison, a '–3/2'-line was drawn for $b = 0.6$. Comparison of the *bdt*s for $N_0 = 500$ and $N_0 = 1000$ individuals reveals that the location and slope of the self-thinning line are almost identical for each *b*-value independent of the initial population size. If the competition strength is too low, the self-thinning line can be determined only with difficulty, if at all. The third, 'post-thinning' segment of the *bdt,* being parallel to the x-axis, points to the natural growth limit of the individuals. Since maximum mean biomass depends on the growth parameters and not on the competition strength, it is ultimately identical for all *b*-values. However, the density where this segment is reached by the individuals increases with b. Since the absolute biomass can be approximated by the product of the mean biomass and the number of individuals for each time step, the maximum absolute biomass increases with *b* as well. This is not surprising since it means that the optimum stand density of the forest depends on the individual competition strength of the trees.

Fig. 4 shows the skewness of the stem-diameter distribution during the development of the cohort (N_0=1000) for b = 0.5, 0.7 and 1.0. The principal course is identical for the entire range of *b* examined and also for the initial density N_0=500. Initially, the skewness of the distribution is strongly negative revealing that a few small trees and a majority of bigger ones occur in the cohort. Owing to the randomly scattered initial positions of the trees, random clumps of trees are generated. A few individuals are therefore particularly impeded in their development. These are the first candidates for 'thinning', and the distribution quickly homogenizes in the course of time. Given sufficient competition strength, a period follows in which the skewness of the stem-diameter distribution becomes positive. A few big trees and many smaller ones form the forest now. By means of the markers (points and circles) drawn in Figs. 3 and 4, it can be seen that the linear section of the *bdt* can only develop between a positive maximum of the skewness and its second zero transition. Without a positive maximum of the skewness, no linear section of the self-thinning trajectory is observed. On the other hand, a positive maximum in the stem-diameter distribution is only reached if the competition strength of the individuals is sufficiently high.

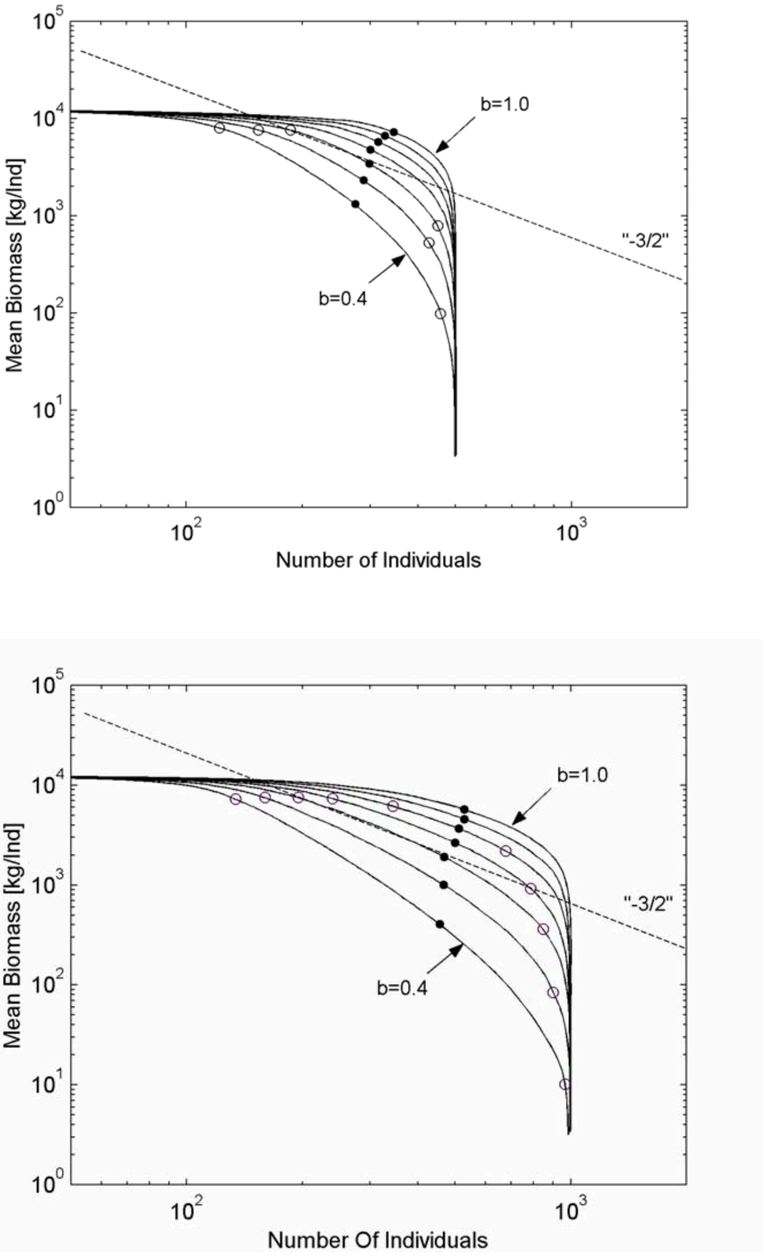

Fig. 3: Biomass-density trajectories produced by the *KiWi* model for the values of the parameter b between 0.4 and 1.0. Upper panel: N_0=500 individuals; lower panel: N_0=1000 ndividuals. Closed circles mark the maxima, open circles mark the two zero crossings (if they exist) of the skewness of the stem diameter distribution (see Fig. 4). In each case, a tangent of the slope –3/2 is drawn (dashed line) at the trajectory for *b*=0.6. It is discussed as a classic case of the 'self-thinning rule' in the literature. Further explanations are contained within the text.

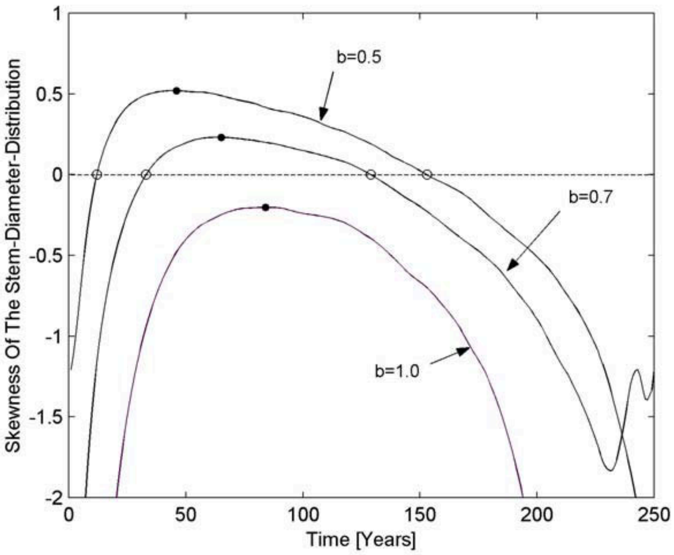

Fig. 4: The skewness of the stem diameter - distribution during cohort's development. The initial density was N_0=1000 individuals. Closed circles mark the maxima, open circles the two zero crossings as far as existing.

Discussion

Our first intention in this work was the analysis of the association between characteristic population structures and the shape of *bdt*s describing the self-thinning of tree cohorts. *Bdt*s were obtained by simulation experiments using the *KiWi* model. The simulations differed in the competition strengths of the individuals and initial densities. Independent of these variations, all *bdt*s showed the three characteristic segments discussed in detail by Begon et al. (1991), Silvertown (1992), and Silvertown & Doust (1993): the fast growing segment, the intrinsic self-thinning segment, and the post-thinning segment indicating the maximum mean biomass of the individuals. As Begon et al. (1991) mentioned, the final segment is difficult (if not impossible) to discern in natural forests. However, its existence is logical as long as the environmental conditions are constant and recruitment does not occur in the plot. Asymmetric competition among the plants differing in size causes the emergence of size hierarchies during the development of plant stands (see, e.g., Weiner & Thomas 1986, Hara 1988, Weiner 1990, Bauer et al. 2002, Berger et al. 2002). This process produces size inequalities but is accompanied by an opposing process of homogenisation if thinning occurs. The resulting changes in the homogeneity of the population can be demonstrated by sequential calculations of the Gini-index (De Camino 1976, Weiner & Solbrig 1984, Weiner & Thomas 1986, Hara 1986, Hara 1988, Kramer 1988, Weiner 1990). Although this index is clear in the interpretation of inequalities, it does not provide markers which associate different stages in the population structure to the different *bdt* segments. The search for such markers leads to the classical shape analysis of size distributions. Gates et al. (1983) studied the distribution of tree sizes in plantations of *Pinus radiata* and found that the height distribution was negatively skewed for a young forest, normally distributed for a mature forest and positively skewed for a senescent forest. Kramer (1988) confirmed the first phase found by Gates et al. (1983) and provided an explanation: in densely wooded, young forests, the weakest trees die. For the surviving trees, the height increment will be favoured at the expense of the diameter increment. This leads often to a week negative skewness of the height distribution. On the other hand, the diameter distribution is often positively skewed during this phase of development since the surviving mid-range trees are strongly hindered in their stem increment and only the dominating trees can achieve a sufficient stem growth. Wenk et al. (1990) added that the size distributions become more flat, broaden, and more symmetrical with aging of a forest.

The work presented here has considered the skewness of the stem diameter distribution during the development of simulated forests. Stem diameter distribution was preferred to height distribution as this is recommended for natural forests by Wenk et al., (1990); whereas the use of the height distribution is favoured in plantations. Furthermore, we used the Fisher skewness instead of the Pearson mode skewness used by Gates et al. (1983) since the model provides the stem diameters of all simulated trees and the loss of that precision through classification and consideration of the mode was undesirable. For a sufficiently high individual competition strength ($b \leq 0.7$), the skewness showed three prominent points: two zero transitions and a positive maximum (see markers in Fig. 4). The locations of the first zero transition and the maximum divide the first section of the *bdt* (Begon et al., 1991 and Silvertown & Doust, 1993) into two subsections (see markers Fig.3). Within both subsections, mortality occurs in the approach to the thinning line, before it is actually reached (Osawa & Sugita, 1989). However, the population structure shifts from a few smaller trees and a majority of bigger ones to a symmetric distribution within segment one. Within segment two, the actual approach to the thinning line occurs accompanied by a stem distribution shift from symmetrical to positive skewed. When the thinning line is reached, the difference between a few big trees and the majority of smaller ones is maximal. The subsequent thinning line starts with the positive maximum of the skewness and ends with its second zero transition. In other words:; a straight line of the *bdt* marks this section of self-thinning during which the positive skewness of the cohort decreases until the distribution is again symmetric.

During the simulations, the skewness of the stem diameter distribution shifts initially from negative skewed, to symmetric and further to positive skewed. This corresponds qualitatively with the findings on height distributions as measured by Gates et al. (1983). The first skewness inversion to positive values which was announced as typical for stem distributions (Kramer, 1988) was not observed. This finding is logical since the growth function of the *KiWi* model enforces a synchronous increase of tree height with stem diameter. Thus, a favoured height increment at the expense of the diameter increment cannot occur in the model but was announced to be the reason for the initial difference in the skewness of the height distribution and the diameter distribution in nature (Kramer, 1988). In difference to Gates et al. (1983), a second negative skewness section was observed in the simulations. This difference can be explained as long as we can assume that the plantations studied by Gates were always under a closed canopy. In this case, the investigated plantations cannot be assigned to the last *bdt* segment and the associated negative period of the skewness (Fig. 3). Considering, furthermore, that the last *bdt* segment is extremely difficult to discern in general (Begon et al. 1991), the skewness analysis of the simulated distributions has to stop at the second zero transition. By this, the simulations also demonstrate the trend that the size distribution becomes more symmetric in older natural forests (Wenk et al., 1990).

The second purpose of the paper was the evaluation and explanation of slope variations of the self- thinning line to find a general framework for the interpretation of all the seemingly contradictory findings achieved from self-thinning experiments to date. The set of curves produced by varying *b* (Fig. 3) demonstrate in fact that different self-thinning slopes are to be expected if the individuals differ in the strength of competition. This general statement corresponds to the finding of Adler (1996). However, Adler concluded that the slope becomes less steep with more rapid development of the size hierarchy corresponding to a more asymmetric competition. The results presented in this work show conversely that the slope becomes steeper with an increased competition strength of the individuals. This increase in individual competition strength is described by smaller *b* values. They effect an *ZOI* enlargement of an individual characterized by a certain stem diameter and/or a higher *FON* intensity at a certain position within the original *ZOI*. This leads finally to a more asymmetric competition and to a more pronounced size hierarchy (Bauer et al., 2002). An explanation of the discrepancy between Adler's and this work is as follows: the natural growth of an individual is limited to a maximum stem diameter and/or maximum height. Due to this fact, all *bdt*s must converge in their last segment since the mean weight or the mean biomass of an individual cannot be surpassed. Considering that the *bdt*s produced with higher competition strength of the individuals are more closely situated to the x axis, it is clear that they must show the steeper slope (see for comparison Figure 3 in this paper and Figure 4.3 at page 54 in Silvertown & Doust, 1993). The curve set produced by Adler's model (Figure 3 in Adler, 1996) cannot meet this criteria. This is due to the exponential growth as assumed by Adler, which is only limited by neighbourhood competition and not by maximum size parameter(s). Therefore, the maximum mean size which can be reached at the end of the self-thinning process differs with the assumed competition strength of the individuals. Thus, the assumption of exponential growth leads to wrong conclusions about the dependency of the self-thinning slope on the competition strength of the individuals.

Another difference between Adler's model and the *KiWi* model is the limitation of the *FON* to the *ZOI* of a tree. This provides a biological interpretation of the neighbourhood field since the *ZOI* can be interpreted as the physical area which is the minimum required by a tree. This area can be thought of, e.g., as a canopy projection on the ground or as the projected root area. If such empirical parameters are known, the slope of the self-thinning line can be pre-defined. In the case of *R. mangle,* the crown radius depending on the stem radius is available and useful for this purpose: *b* and *a* -parameters leading to smaller *ZOI*s than the projected crown area would lead to tree densities per area which cannot appear under natural conditions, and are, therefore, unrealistic. Fig. 2 shows that, for the given example of *R. mangle* cohorts, all *bdt*s with $b > 0.7$ are unlikely. Since all other *bdt*s show less steeper thinning segments than the *bdt*s with $b > 0.7$ (Figure 3), the potential minimum value of the thinning slope is thus restricted. In other words:; empirical, geometric parameter(s) which define the physical space required by an individual imposes the lower limit to the slope of the linear *bdt* segment (see Fig. 3). It should be mentioned that we used *b* in this work universally. It defined here the *FON*s geometric dimension as well as the concrete competition strength of the individual since the *ZOI* parameter *a* and the *FON* parameter *FONmin* were kept constant. However, the competition strength predefined by *a* and *b* can be modified in addition by a variation of *FONmin* depending, e.g., on the compactness of the roots and the density and architecture of the crown.

In conclusion, the different curve segments of the *bdt* are associated with characteristic population structures which can be characterized by the Fisher skewness of the stem distribution. Considering the variation of this distribution, the classical three segment division of the *bdt* should be extended to a four segment division through a subdividing of the first *bdt* segment. The occurrence and duration of a straight thinning line depend on a positive skewness and, therefore, on individuals' competition strength. A possible concept to interpret thinning slope variations might be postulated as follows; the area physically required by an individual defines the lowest possible slope of the self-thinning line of the cohort. This slope is made steeper by the competition strength of the trees within a cohort.

Acknowledgements

The authors are indebted to Volker Grimm, whose comments and suggestions greatly improved this paper. This study is a result of co-operation between the Center of Tropical Marine Ecology (ZMT), Bremen, Germany and the Universidade Federal do Pará e do Museum Paraense Emilío Goeldi (MPEG), both Belém, Brazil, under the Governmental Agreement on Co-operation in the Field of Scientific Research and Technological Development between Germany and Brazil financed by the German Ministry of Education, Science, Research and Technology (BMBF) [MADAM – Mangrove Dynamics and Management (Project number: 03F0154A)], and the Conselho Nacional de Pesquisa e Tecnologia (CNPq). This is MADAM contribution number 46.

References

Adler, F.R. 1996. A model of self-thinning through local competition. Proceedings National Academy of Science USA 93: 9980-9984.

Bauer, S., Berger, U., Hildenbrandt, H., Eisinger, D. & Grimm, V. 2001. Modellierung von Nachbarschaftskonkurrenz in Pflanzenpopulationen: Test eines neuen Ansatzes. pp. 31-42. In: Jopp F, Weigmann G. (eds.) Theorie in der Ökologie - Band 3. Peter Lang, Frankfurt/M.

Bauer, S., Wyszomirski, T., Berger, U., Hildenbrandt, H. & Grimm, V. 2002. Asymmetric competition as natural outcome of neighbour interactions among plants: results from the field-of-neighbourhood modelling approach . Plant Ecology (in press).

Begon, M., Harper, J.L. & Townsend, C.R. 1991. Ökologie: Individuen, Populationen und Lebensgemeinschaften. Basel: Birkhäuser Verlag.

Berger, U. & Hildenbrandt H. 2000. A new approach to spatially explicit modelling of forest dynamics: spacing, ageing and neighbourhood competition of mangrove trees. - Ecological Modelling 132: 287 - 302.

Berger, U., Hildenbrandt, H. & Grimm V. 2002. Towards a standard for the individual-based modeling of plant populations: self-thinning and the field-of-neighborhood approach. Natural Resource Modeling 15(1) (in press).

Burns, B.R. & Ogden J. 1985. The Demography of the Temperate Mangrove Avicennia marina (Forsk.) Vierh. at its Southern Limit in New Zealand. - Australian Journal of Ecology 10: 125-133.

Camino, R. de. 1976. Zur Bestimmung der Bestandeshomogenität. Allgemeine Forst und Jagdzeitung, Frankfurt/M. 147: 54-58.

Chen, R. & Twilley R.R. 1998. A gap dynamic model of mangrove forest development along gradients of soil salinity and nutrient resources. Journal of Ecology 86: 37-51.

Cintrón, G. & Schaeffer Novelli Y. 1985. Caracteristicas y desarrollo estructural de los manglares de norte y sur america. Cienca Interamericana 25: 4-15.

Enquist, B.J., Brown, J.H. & West, G.B. 1998. Allometric scaling of plant energetics. Nature 395: 163.

Fromard, F., Puig, H., Mougin, E., Marty, G., Bétoulle, J.L. & Cadamuro L. 1998. Structure, above-ground biomass and dynamics of mangrove ecosystems: new data from French Guiana. Oecologia 115: 39-53.

Gates, D. J., McMurtrie, R. & Borough, C.J. 1983. Skewness reversal of distribution of stem diameter in plantations of *Pinus radiata*. Australian Forest Research 13: 267-270.

Hara, T. 1986. Effects of density and extinction coefficient on size variability in plant populations. Annals of Botany 57:885-892.

Hara T. 1988. Dynamics of size structure in plant populations. Trends in Ecology and Evolution 3:129-133.

Harper, J.L. 1977. The population biology of plants. Academic Press, London.

Kramer, H. 1988. Waldwachstumslehre. Verlag Paul Parey, Hamburg und Berlin.

Lonsdale, W.M. 1990. The self-thinning rule: dead or alive? Ecology 71: 1373-1388.

Osawa, A. & Sugita, S. 1989. The self-thinning rule: another interpretation of Weller's results. Ecology 70:279-283.

Sackville Hamilton,N.R.; Matthew,C.; Lemaire,G. 1995. In defence of the -3/2 boundary rule: a re-evaluation of self-thinning concepts and status. Annals of Botany 76: 569-577.

Silvertown, J.W. 1992. Introduction to plant population ecology. Longman Scientific & Technical, Essex, England.

Silvertown, J.W. & Lovett Doust, J. 1993. Introduction to plant population biology. 3rd edn. Blackwell, London.

Weiner, J. 1990. Asymmetric competition in plant populations. Trends in Ecology and Evolution 5: 360-364.

Weiner, J. & Solbrig, O. T. 1984. The meaning and measurement of size hierarchies in plant populations. Oecologia 61: 334-336.

Weiner, J. & Thomas, S. C. 1986. Size variability and competition in plant monocultures. Oikos 47: 211-222.

Weller, D.E. 1987. A reevaluation of the -3/2 power rule of plant self-thinning. Ecological Monographs 57: 23-43.

Weller, D.E. 1991. The self-thinning rule: dead or unsupported? A reply to Londsdale. Ecology 72: 747-750.

Wenk, G., Antanaitis, V. & Smelko, S. 1990. Waldertragslehre. Deutscher Landwirtschaftsverlag. Berlin.

Westoby, M. 1984. The self-thinning rule. Adv Ecol Res, 14: 167-225.

White, J. 1981: The allometric interpretation of the self-thinning rule. Journal of Theoretical Biology 89: 475- 500.

Yoda, K., Kira, T., Ogawa, H. & Hozumi K. 1963: Intraspecific competition among higher plants. XI: Self-thinning in overcrowded pure stands under cultivated and natural conditions. Journal of Osaka City University Institute of Polytechnics D 14: 107-129.

Kapitel II,4

Asymmetric competition as a natural outcome of neighbour interactions among plants: results from the field-of-neighbourhood modelling approach

Silke Bauer[1], Tomasz Wyszomirski[2] , Uta Berger[3],
Hanno Hildenbrandt[3] and Volker Grimm[1]

[1] Centre for Environmental Research (UFZ), Leipzig-Halle, Germany
[2] Institute of Botany, Warsaw University, Warsaw, Poland
[3] Centre for Marine Tropical Ecology (ZMT), Bremen, Germany

Plant Ecology, in press (2002)

Asymmetric competition as a natural outcome of neighbour interactions among plants: results from the field-of-neighbourhood modelling approach

Silke Bauer[1*], Tomasz Wyszomirski[2] , Uta Berger[3], Hanno Hildenbrandt[3] and Volker Grimm[1]

[1] Dept. of Ecological Modelling, UFZ Centre for Environmental Research Leipzig-Halle, P.O. Box 500 136, D-04301 Leipzig, Germany

[2] Institute of Botany, Warsaw University, Al. Ujazdowskie 4, PL - 00 - 478 – Warsaw, Poland

[3] ZMT Centre for Marine Tropical Ecology, Fahrenheitsstr. 6, D-28359 Bremen, Germany

* Correspondence author:
e-mail: silke@oesa.ufz.de
tel. ++49-341-235 2478
fax ++49-341-235 3500

electronic copy:
operating system Windows NT disc, word processor MS Word 97, file „AsymComp.doc“

Key words

asymmetric competition, field-of-neighbourhood, individual-based model, plant, size distribution

Abstract

Numerous attempts have been made to infer the mode of competition from size or biomass distributions of plant cohorts. However, since the relationship between mode of competition and size distributions may be obscured by a variety of factors such as spatial configuration, density or resource level, empirical investigations often produce ambiguous results. Likewise, the findings of theoretical analyses of asymmetric competition are equivocal. In this paper, we analyse the mode of competition in an individual-based model which is based on the new field-of-neighbourhood approach. In this approach, plants have a zone of influence that determines the distance up to which neighbours are influenced. Additionally, a superimposed field within the zone of influence defines phenomenologically the strength of influence on neighbouring plants. We investigated competition at both individual and population level and characterised the influence of density and of the shape of the field-of-neighbourhood. After finding asymmetric competition emerging in all scenarios, we argue that asymmetric competition is a natural consequence of local competition among neighbouring plants. The failure to find asymmetric competition is thus not necessarily an indicator for symmetric competition.

Introduction

Asymmetric competition among individuals is defined as competition in which larger individuals have a disproportionate advantage (relative to their size) over smaller individuals. This asymmetry leads to the growth suppression of smaller individuals (Weiner 1990; Stoll & Weiner 2000), and increasing relative size differences between competitors. By contrast, symmetric competition refers to cases where resources are shared equally or proportionally to the size of the competing individuals. Knowing the mode of competition in which plants are involved (i.e. symmetric or asymmetric) is important since it has a major impact on population and community dynamics (Lomnicki 1980; Pacala & Weiner 1991; Schwinning & Fox 1995; Yastrebov 1996). For example, it is known from theoretical models of animal populations that symmetric (scramble) and asymmetric (contest) competition leads to completely different types of population dynamics (e.g. Uchmanski 2000).

However, the mode of competition among plants is still uncertain. Empirical investigations are difficult because they require knowledge of how plants acquire resources, how these resources are used for growth, survival and reproduction, and how the uptake of resources affects the performance of neighbours (Berntson & Wayne 2000). Moreover, empirical investigations have been hampered by the difficulty of simultaneously measuring the effects of competition for more than one resource. Therefore, numerous attempts have been made to infer the mode of competition from patterns at the population level, i.e. size or weight distributions of cohorts of certain species (Wyszomirski 1983; Uchmanski 1985; Hara & Wyszomirski 1994; Schwinning & Fox 1995; Wyszomirski *et al.* 1999; Stoll & Weiner 2000). It was hoped, for example, that positively skewed size distributions would indicate a size hierarchy in which a few large individuals suppress many small individuals, i.e. asymmetric competition.

Unfortunately, however, there are many factors which may obscure the relationship between the mode of competition and patterns in size distributions, e.g. spatial configuration, density, abiotic heterogeneity, overall resource level, and overall strength of competition. Consequently, despite the numerous empirical findings regarding the existence of size-hierarchies, the underlying mechanisms remain unclear. Furthermore, theoretical analyses are still equivocal (Bonan 1991; Hara & Wyszomirski 1994; Weiner *et al.* 2001).

Theoretically, the relationship between mode of competition and population level pattern has to be addressed with individual-based models because competition in plants is necessarily local (Houston *et al.* 1988; DeAngelis & Gross 1992). In a recent review, Stoll & Weiner (2000) listed the key elements of realistic individual-based plant population models: each model plant should have an explicit location, a basal extension where no other plant can exist and a zone of influence in which interactions with neighbour plants occur. Furthermore, the number, size and location of neighbours should be taken into account in the description of competition among neighbours. Until recently, only two modelling approaches existed which contained most of these key elements: zone-of-influence (ZOI) (Wyszomirski 1986) and ecological field (EF) models (Wu *et al.* 1985; Walker *et al.* 1989; cf. also a similar approach used by Adler 1996). EF models have not yet been widely used, and never to analyse the mode of competition. In contrast, ZOI models have been used to model the emergence of size-hierarchies in plant cohorts (e.g. Wyszomirski 1983; Wyszomirski 1986; Wyszomirski 1992; Firbank & Watkinson 1987; Bonan 1991; Bonan 1993; Hara & Wyszomirski 1994; Yastrebov 1996; Wyszomirski *et al.* 1999; Weiner *et al.* 2001). However, in these studies the mode of competition had to be specified by the modeller, e.g. whether resources in overlapping areas of ZOIs are shared equally, proportionally to the size of the competitors, or monopolised by the largest competitor (Weiner *et al.* 2001). But the modeller's decision on how to share resources is an example of what Railsback (2001) refers to as "imposed behaviour": the mode of competition does not emerge from the properties of the individuals but is imposed by the modeller. Assuming "imposed behaviour" largely restricts the insights that can be gained from an individual-based model (Railsback 2001). Given the limitations of the ZOI approach, Schwinning & Weiner (1998) conclude that it should be developed and that: "Alternative individually based, spatially explicit models are also needed, since the zone-of-influence approach is only one of several possible ways to model competition for space." (p. 451).

Here, we use a recently developed approach of individual-based modelling, the "field-of-neighbourhood" (FON) approach, to analyse the mode of competition among plants. Although the FON approach was originally developed to model spatio-temporal dynamics of mangrove forests (Berger & Hildenbrandt 2000), it also proved suitable for theoretical studies, e.g. for gaining new insights into self-thinning among plants (Berger *et al*. 2001) and reproducing empirical findings on self-thinning in mangroves (Berger and Hildenbrandt, *unpublished manuscript*). The advantage of the FON approach for analysing the mode of competition is that this mode was not at all in the focus of attention when the approach was developed. Instead, in FON models the influence on neighbour plants is described phenomenologically and the mode of competition emerges from neighbour interactions. Therefore in the following we analyse the mode of competition in simulation experiments with two plants and with populations at different densities. We show that in the FON approach, asymmetric competition is a natural consequence of neighbour interactions. Based on this result, we will argue that in real plants, too, competition among plants ought naturally to be asymmetric.

Model and methods

FON approach

In the field-of-neighbourhood approach (Berger & Hildenbrandt 2000), individuals have a circular zone of influence (ZOI) whose radius determines the distance up to which the individual interacts with neighbouring individuals. Within the zone of influence, a scalar field is defined which quantifies the strength of influence on potential neighbours (Fig. 1). This field of neighbourhood (FON) describes for every point within the ZOI the influence on neighbours.

As soon as the FONs of two or more individuals overlap, competition occurs. To quantify competition, the FON of the neighbour plant within the overlapping area is integrated. The resulting value *F* thus quantifies the influence of the neighbour on the focal plant. If, for example, the overlap is small, this influence may – depending on the shape of the field (Fig. 1) – be small as well. If more neighbours interact with the focal plant, it is assumed that their FONs superimpose independently, i.e. all neighbour fields are summed up in the overlapping areas. The resulting value *F* is divided by the area *A* of the ZOI of the focal plant *k*, which yields:

$$(1) \qquad F_A^k = \frac{1}{A} \sum_{n \neq k} \int_{A'} FON_n(x,y)\,da$$

An efficient algorithm for calculating F_A for each individual of a plant population is described in detail in Berger and Hildenbrandt (2000). F_A is used to calculate a competition factor *C*

$$(2) \qquad C = \begin{cases} 1-2F_A & \text{for } F_A \le 0.5 \\ 0 & \text{for } F_A > 0.5 \end{cases}$$

which determines how much the growth of the focal individual is reduced due to competition. If there is no interaction with neighbours, F_A is zero and, in turn, C=1, i.e. the individual grows at its maximum current growth rate. The more neighbours a plant has, and the closer and larger these neighbours are, the more the growth of the focal plant will be reduced or even completely suppressed. This whole approach describes local competition among individuals by its effects and not by its mechanisms (e.g. resource partitioning) and is thus phenomenological in the same way as, for example, Lotka-Volterra competition models at the population level (Berger *et al*. 2001).

For the shape of the field of neighbourhood, we assume a basal area where the field has the value 1. This means in particular that no recruitment can occur in this area. In real plants, the basal area may, for example, refer to stems in trees, tussocks in grasses, or simply zones of complete resource monopolisation of the focal plant. The basal radius, R_{Basal}, is the basic state variable in the FON approach and represents the individual's size. It may – if the model using the FON approach is designed for real species – be used to calculate individual biomass (for example, for mangrove trees, Berger & Hildenbrandt 2000). We assume that the size of an individual, i.e. its basal radius R_{Basal}, determines the radius of its zone of influence, R_{FON}:

$$(3) \qquad R_{FON} = a \cdot R_{Basal}{}^{b}$$

For the scaling parameters a and b we here choose a = 10.0 and b = 0.9 and 0.6 (Fig. 1). Note that since R_{Basal} is smaller than one (metre), larger values of b correspond to smaller radii of the zone of influence, R_{FON}.

From the basal area to the border of the FON, we assume an exponential decrease in the field of neighbourhood leading to a smaller influence on neighbours in the border ranges of the field:

$$I(r) = \exp\left[-\frac{|\ln(I_{Min})|}{R_{FON} - R_{Basal}} (r - R_{Basal}) \right]$$

where r is the distance from the centre of the field and I_{Min} the minimum field value at the border of the FON.

For the size-dependent, potential growth GR rate of the individuals, i.e. of the basal radius R_{Basal}, we assume a quadratic function:

$$GR = \left(\frac{4}{R_{\max}} * R_{Basal} - \frac{4}{R_{\max}^2} * R_{Basal}{}^2 \right) \cdot MGR$$

where MGR is the maximum growth and $R_{\max}$ the maximum basal radius. This growth model would yield a logistic growth curve for isolated individuals. The real growth rate ΔR_{Basal} takes into account the interaction with the neighbours, i.e. the competition factor C:

$$\Delta R_{Basal} = GR \cdot C$$

Simulation experiments

We varied the field of neighbourhood with respect to its range, i.e. radius, and its strength at the border of the FON. The radius is determined by parameter b (Eq. 3). We will in the following refer to the field with b=0.9 as the ‘compressed’ field and b=0.6 as the ‘extended’ field (Fig. 1). The strength of the field at the border of the FON is determined by I_{Min}. We used I_{Min}= 0.01, 0.2 and 0.6. Note that I_{Min} determines whether the onset of competition between neighbouring individuals, i.e. when the FONs start to overlap, is gradual (small I_{Min}) or abrupt (large I_{Min}). The reference parameters used in Berger and Hildenbrandt (2000) and Berger et al. (2001) were b=0.5 and I_{Min}= 0.01.

For all six scenarios (parameter combinations) of b and I_{Min} we performed experiments with two interacting individuals and with populations of 200 individuals. The two individuals were placed at a distance such that the zones of influence start to overlap at the 3rd time-step. For b=0.9 this meant that the distance between the centres of the plants was 0.7 while for b=0.6 it was 2.3 (all spatial dimensions are give in m). Except for initial size (R_{Basal} = 0.015 and R_{Basal} = 0.02) the model parameters were identical for both individuals: MGR = 0.02 and R_{Max} = 0.3. Growth was followed for 20 time-steps. To assign biomasses to the plants, we assumed the relationship $B = (\pi R_{\mathrm{Basal}}^2)^{3/2}$ between biomass B and basal radius.

In the population study, 200 individuals were randomly distributed over the sample area. The population density was varied from 0.125, 0.25, 0.5, 1 and 2 plants/m². To avoid changing sample sizes, we varied area size to change density. Individual variability was introduced in the maximum growth MGR (normal distribution with $\bar{x}$ = 0.02; σ = 0.005) and initial basal radius ($\bar{x}$ = 0.015, σ = 0.01). The maximum basal radius was equal for all individuals (R_{Max} = 0.3). To avoid edge effects, we used a toroidal sample area, i.e. periodic boundary conditions.

We analysed asymmetric competition at the population level by calculating a recently developed indicator of asymmetric competition, C_α (Wyszomirski *in prep.*). The advantage of this indicators is that it takes into account the spatial configuration of the individuals. The well-known effect that conventional measures of asymmetric competition (e.g. skewness) may be biased by spatial effects (Wyszomirski 1986; Miller & Weiner 1989; Bonan 1991) is thus reduced.

To calculate C_α, the degree of competitive asymmetry, three steps are required. First, for all plants their Voronoi-polygon is calculated (Fig. 2). Individuals at the border, and individuals which have a border individual as neighbour, are ignored. Then, a linear regression is performed between the log-transformed biomasses and Voronoi-areas of the plants:

$$log\ (biomass) = a\ \ log\ (Voronoi\text{-}area) + b.$$

This regression largely reflects differences in biomass caused by the spatial arrangements of the plants. Consequently, the residuals, i.e. the differences between predicted (regression) and observed (simulation) biomass, contain information about differences in biomass which are due to asymmetric competition. Therefore, in the third step, for each plant its neighbours' residuals are summarised and correlated with the residual of the target plant. This final correlation yields the indicator of asymmetric competition, C_α.

The rationale behind the indicator C_α is that if a target plant has a greater biomass than predicted by the regression, and its neighbours have lower biomasses than predicted, the residual of the target plant will be positive and the sum of the neighbour residuals will be negative. Hence, a correlation between these residuals will result in a negative value. Asymmetric competition leads to such situations. Therefore, negative values of C_α are indicative of asymmetric competition. Positive values may arise only in very exceptional situations (Wyszomirski *in prep.*), not encountered in the present study.

Results

Population experiments

The population average of F_A (Eq.1) is an indicator of overall competition strength at the population level. Parameter *b* (Eq. 3) determines the extension of the field of neighbourhood and, in turn, determines how soon competition starts because the FONs start to overlap. Thus, although competition is initially higher for extended fields (Fig. 3a), these differences cease over time. At the end of the growth period studied, average competition strength is determined more by I_{Min} than by *b*. Note that for individuals differences of F_A larger than 0.5 are irrelevant because for F_A>0.5 growth is completely suppressed (Eq. 2).

Populations with compressed fields and low values of I_{Min} reached the largest average basal radius (Fig. 3b). On the other hand, in populations with extended fields and high I_{Min}, individual growth was already almost completely suppressed in early time-steps. Individuals with extended fields of neighbourhood were generally smaller than their counterparts with the same I_{Min} and compressed fields (Fig. 3b).

Asymmetric competition as quantified by C_α was detected in all scenarios (Fig. 3d). C_α increases with increasing I_{Min} and reaches a maximum for I_{Min}=0.2 in extended fields (b=0.6) (Fig. 3c). Larger I_{Min} values (I_{Min}=0.6) did not lead to a higher degree of asymmetric competition because individuals stopped growing at early time-steps and therefore developed only slight differences in their sizes. For the same I_{Min}, asymmetry was generally higher in extended fields than in compressed fields (except for I_{Min}=0.6).

With increasing density, the average size decreased (Fig. 4a), but for all densities individuals grew larger when their field of neighbourhood had a border value of I_{Min} = 0.01 and for the same value of I_{Min} individuals were larger when their field was compressed.

Density changed the degree of asymmetric competition (Fig. 4b and c). In all scenarios with extended fields, competitive asymmetry reached a maximum at a certain density and decreased thereafter whereas in scenarios with compressed fields competitive asymmetry monotonically increased with density. The density at which maximum competitive asymmetry was observed for extended fields shifted from 0.5 plants/m² for I_{Min}=0.01 to 0.25 plants/m² for I_{Min}=0.2 and 0.6. The highest competitive asymmetry was found for I_{Min}=0.2 at density 0.25 plants/m² for extended fields and at 2 plants/m² for compressed fields.

Experiments with two individuals

Differences in F_A -values between the two individuals rose as I_{Min} values increased (Fig. 5, upper row) and were larger for compressed fields. Note that F_A quantifies the influence of the neighbour plant on the focal plant. Consequently, a large F_A means that the growth of the focal plant is strongly suppressed; if F_A>0.5, the focal plant even stops growing altogether (Fig.5, second row). Thus, for I_{Min}=0.6 and b=0.9, the individual with a slight initial advantage in size (individual 2) almost completely suppresses individual 1, whereas for I_{Min}=0.01, only weak growth suppression and, in turn, asymmetric competition occurs (Fig. 5, lower two rows). However, competition is still not symmetric for I_{Min}=0.01: the difference between the relative growth rates of the two plants, $D=|S_1-S_2|$, with $S=(GR-\Delta R_{\mathrm{Basal}})/GR=(1-C)$, would be zero if both plants were symmetrically suppressed to the same degree, but at the 20th time-step is 0.079 for b=0.9 and 0.076 for b=0.6.

To understand how asymmetric competition emerges from slight differences in initial size, in Fig. 6 not only F_A but also the area A of the zone of influence and $F = F_A \cdot A$ are shown for I_{Min}=0.2 and b=0.6. F is the integral over the FON of the neighbour in the overlapping zone (Eq. 1). Due to the almost symmetric configuration of the two individuals (Fig. 5), F is almost identical for both individuals for a long time. However, the area A by which F is scaled differs right from the beginning and leads to differences in F_{A}. Increasing differences in F_{A}, however, magnify differences in the individuals' size and, in turn, of the areas of their zones of influence. Asymmetric competition thus reinforces itself due to the area scaling of the FON approach.

Discussion

We used the new field-of-neighbourhood (FON) modelling approach to investigate the mode of competition of hypothetical plants. Two parameters of the FON approach which determine the shape of the FON were varied such that extended, gradually decreasing fields could be compared to compressed and abruptly decreasing fields.

In the population simulations, asymmetry was found in all scenarios, albeit to different degrees. Generally, higher I_{Min} values cause a stronger onset of competition as soon as plants interact and therefore lead to higher competitive asymmetry. However, this trend was not observed for the highest value of I_{Min} (=0.6). This is an effect of very strong overall competition which is described by Wyszomirski *et al.* (1999): asymmetric competition has two components, competition and asymmetry. For strong overall competition, growth is reduced so much that size differences hardly emerge and therefore competitive asymmetry is hard to detect.

The same effect is responsible for the effect of density on competitive asymmetry in the case of extended fields. Beyond a certain density the individuals interact with so many neighbours (because the field is extended and the plants are close to each other) that overall competition intensifies to the point where no further increase of competitive asymmetry with density can be observed.

The effects of the shape of the FON and of density on competitive asymmetry are thus easy to understand at the population level. However, to understand the mechanisms underlying asymmetric competition, the local interactions between pairs of individual had to be studied. The simulation experiments with two individuals which were of slightly different size at the beginning revealed that in the FON approach asymmetry, i.e. the suppression of the smaller individual, is not necessarily driven by asymmetric resource use in the overlapping zone which is affected by both plants. In contrast, the integral over the neighbours' FON in the overlapping zone is almost identical for both plants. Asymmetry comes into play by the scaling of the neighbours' effect by the area of the ZOI of the focal plant (Fig. 6).

This scaling was introduced for three reasons: (1) To turn F, which has the unit of m², into a dimensionless quantity, F_A; (2) The calculation of F_A is easy (Berger and Hildenbrandt 2000) because only pairwise interactions have to be quantified. The influence of more than two neighbours is independent of each other; (3) Consider a situation where the ZOI of a small plant is completely overlapped by the periphery of the ZOI of a larger plant. Without scaling, only the integrals over the FON in the overlapping zone, F, would be considered. However, on the one hand the F-value which describes the influence of the small plant on the large plant would be rather high, because F is the integral over the entire FON of the smaller plant. On the other hand, the F-value describing the influence of the larger plant on the smaller one would be rather small, because only the periphery of the larger plants' FON overlaps the smaller plant. As a result, without scaling the mutual effects of the plants on each others growth would be described with the wrong sign: the smaller plant would strongly reduce the growth of the larger one, but the larger one would only slightly affect the smaller one. This would be absurd because the larger plant is only affected by competition in a small part of its zone of influence, whereas the small plant 'feels' the larger one on its entire ZOI. There thus has to be a scaling by the area of the ZOIs of the plants involved.

Asymmetric competition emerges from this scaling by the positive feedback demonstrated in Fig. 6: even if F_A is virtually the same for both plants, a larger ZOI means that growth will be less reduced and thus, in the next time step, the size difference increases, and so on. Thus, in the FON approach, asymmetric competition results not from rules imposed on for instance resource partitioning, but mainly from the very simple fact that in plant-plant interactions, for larger individuals the proportion of the ZOI unaffected by the neighbour interaction is larger (a point also made by Schwinning and Weiner, 1998, Fig. 1). Hence, a larger plant does not 'feel' much of the influence of a smaller neighbour and its growth is mainly independent of the interaction. Additionally, size differences may be reinforced because growth is non-linear, which may contribute to the positive feedback between size differences and increase in size differences.

To summarise the results of our study: within the FON approach, asymmetric competition appears to be a natural outcome of local competition among individuals. Consequently, the failure to detect competitive asymmetry at the population level is not necessarily an indicator of symmetric competition at the individual level, but of mechanisms which conceal or prevent the asymmetric competition from unfurling. An important concealing mechanism is spatial configuration, which however can be controlled by using appropriate indicators of competitive asymmetry such as C_α. Moreover, the asymmetry of competition is not markedly expressed if competition is so strong that growth is strongly reduced and therefore the positive feedback described above only weak.

What do these theoretical results tell us about plant competition in the real world? Of course, a modelling study cannot 'prove' the prevalence of asymmetric competition in real plants, but it can provide a logical argument that has the potential to guide future empirical studies. The argument is: if the FON approach and its assumptions are considered realistic, then the consequences of this approach - i.e. that asymmetric competition is a natural outcome of local competition – must be accepted. In this context, the formal details of the FON approach are less important than the underlying idea: plants have a zone of influence in which they influence potential neighbours. We would like to emphasise that the FON approach is not – as the ZOI approach – based on the mechanistic notion of resource use within the zones-of-influence, but is purely phenomenological: the field-of-neighbourhood describes the influence on potential neighbours. If the zones of two plants overlap, they interact, which means that the mutually reduce each others growth. A larger plant is assumed to be less affected by the interaction with its smaller neighbour because a larger proportion of its ZOI is unaffected by neighbour interactions. On this ‘free’ part of the ZOI, the plant can still acquire resources undisturbed by any interaction. Since the particular form of the FON, which we varied by varying the border value I_{Min}, to some degree reflects the architecture of the plant and of its interaction with neighbour plants, our results also seem to be robust to changes in this architecture.

Acknowledgements

We thank Dirk Eisinger for his valuable assistance in mastering C++.

References

Adler, F. R. 1996. A model of self-thinning through local competition. Proceedings of the National Academy of Sciences of the United States of America 93:9980-9984.

Berger, U. & Hildenbrandt, H. 2000. A new approach to spatially explicit modelling of forest dynamics: Spacing, ageing and neighbourhood competition of mangrove trees. Ecological Modelling 132:287-302.

Berger, U., Hildenbrandt, H. & Grimm, V. 2001. Towards a standard for the individual-based modeling of plant populations: self-thinning and the field of neighbourhood approach. Natural Resource Modeling in press.

Berntson, G. M. & Wayne, P. M. 2000. Characterizing the size dependence of resource acquisition within crowded plant populations. Ecology 81:1072-1085.

Bonan, G. B. 1991. Density effects on the size structure of annual plant populations: an indication of neighbourhood competition. Annals of Botany 68:341-347.

Bonan, G. B. 1993. Analysis of neighborhood competition among annual plants: implications of a plant growth model. Ecological Modelling 65:123-136.

DeAngelis, D. L. & Gross, L. J. 1992. Individual-based models and approaches in ecology: populations, communities and ecosystems. Chapman & Hall, New York, London.

Firbank, L. G. & Watkinson, A. R. 1987. On the analysis of competition at the level of the individual plant. Oecologia 71:308-317.

Hara, T. & Wyszomirski, T. 1994. Competitive asymmetry reduces spatial effects on size-structure dynamics in plant populations. Annals of Botany 73:285-297.

Houston, A., Clark, J. C., McNamara, J. & Mangel, M. 1988. Dynamic models in behavioral and evolutionary ecology. Nature 332:29-34.

Lomnicki, A. 1980. Regulation of population density due to individual differences and patchy environment. OIKOS 35:185-193.

Miller, T. E. & Weiner, J. 1989. Local density variation may mimic effects of asymmetric competition on plant size variability. Ecology 70:1188-1191.

Pacala, S. W. & Weiner, J. 1991. Effect of competitive asymmetry on a local density model of plant interference. Journal of Theoretical Biology 149:165-179.

Railsback, S. F. 2001. Concepts from complex adaptive systems as a framework for individual-based modelling. Ecological Modelling 139:47-62.

Schwinning, S. & Fox, G. A. 1995. Population dynamic consequences of competitive symmetry in annual plants. OIKOS 72:422-432.

Schwinning, S. & Weiner, J. 1998. Mechanisms determining the degree of size asymmetry in competition among plants. Oecologia 113:447-455.

Stoll, P. & Weiner, J. 2000. A neighborhood view of interactions among individual plants. pp. 11-27. In: Dieckmann, U., Law, R., and Metz, J. A. J. (eds.), The Geometry of Ecological Interactions - Simplifying spatial complexity. Cambridge University Press, Cambridge.

Uchmanski, J. 1985. Differentiation and frequency distributions of body weights in plants and animals. Philosophical Transactions of the Royal Society London B. 310:1-75.

Uchmanski, J. 2000. Resource partitioning among competing individuals and population persistence: an individual-based model. Ecological Modelling 131:21-32.

Walker, J., Sharpe, P. J. H., Penridge, L. K. & Wu, H. 1989. Ecological field theory: the concept and field tests. Vegetatio 83:81-95.

Weiner, J. 1990. Asymmetric competition in plant populations. Trends in Ecology and Evolution 5:360-364.

Weiner, J., Stoll, P., Muller-Landau, H. & Jasentuliyana, A. 2001. Spatial pattern, competitive symmetry and size variability in a spatially-explcit, individual-based plant competition model. The American Naturalist 158:438-450.

Wu, H., Sharpe, P. J. H., Walker, J. & Penridge, L. K. 1985. Ecological field theory: a spatial analysis of resource interference among plants. Ecological Modelling 29:215-243.

Wyszomirski, T. 1983. A simulation model of the growth of competing individuals of a plant population. Ekologia Polska 31:73-92.

Wyszomirski, T. 1986. Growth, competition and skewness in a population of one-dimensional individuals. Ekologia Polska 43:615-641.

Wyszomirski, T. 1992. Detecting and displaying size bimodality: kurtosis, skewness and bimodalizable distributions. Journal of Theoretical Biology 158:109-128.

Wyszomirski, T., Wyszomirski, I. & Jarzyna, I. 1999. Simple mechanisms of size distribution dynamics in crowded and uncrowded virtual monocultures. Ecological Modelling 115:253-273.

Yastrebov, A. B. 1996. Different types of heterogeneity and plant competition in monospecific stands. OIKOS 75:89-97.

Figure legends

Fig. 1. Diagram of the different fields-of-neighbourhood used in our experiments. The differences in field extension and minimum values are shown for the same basal radius. Extended fields result from large b-values in the basal to FON-radius relation whereas compressed fields are typical for smaller b-values. Depending on the field minimum value, the fields-of-neighbourhood either decrease rapidly to a low I_{Min} value or gradually to a higher I_{Min}.

Fig. 2. Representation of individual plants in Voronoi-diagrams. The perpendicular bisections of plants are connected and yield individual Voronoi-polygons. We use the area of this polygon to predict the biomass of individual plants. Neighbouring individuals are herein defined as individuals that share at least one polygon intersection.

Fig.3. At medium density (0.5 plants/ m^2) the temporal development of F_A-values, basal radius, and C_α are shown for all scenarios.

Fig. 4. Changing density affects the outcome of competitive interaction as characterised by C_α. While competitive asymmetry reaches a maximum at a particular density in extended fields (striped bars), competitive asymmetry monotonically increases in compressed fields (single-coloured bars).

Fig. 5. In the 2-individual study, we tested the outcome of different field shapes on individual performance. Here, the F_A-values characterise the intensity of competition between both individuals. Higher I_{min} values lead to greater differences in performance. When using

extended fields (empty symbols) the onset of competition is delayed compared to extended fields (filled symbols).

Fig. 6. F_A, F (un-scaled), and A for the two-individual study I_{min}=0.2 and *b*=0.6.

fig. 1

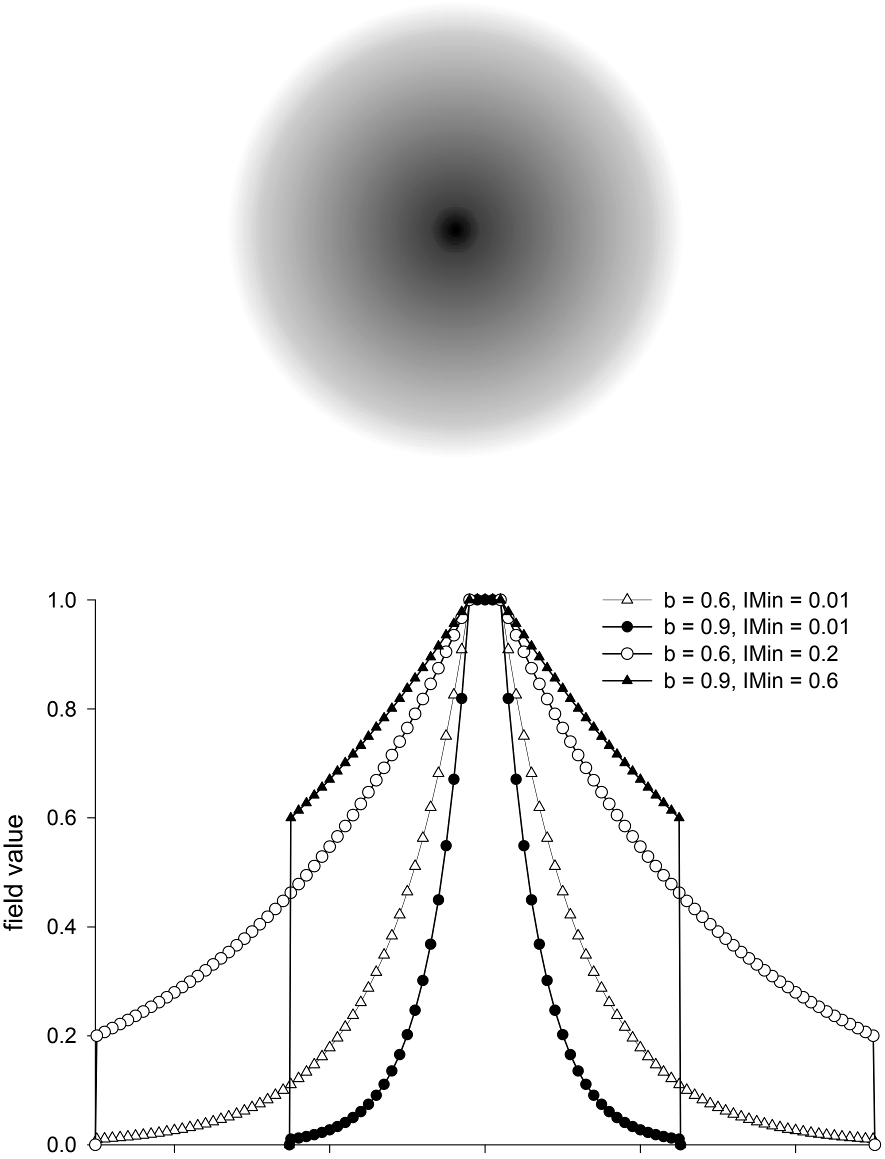
1.0
0.8
0.6
0.4
0.2
0.0
field value
b = 0.6, IMin = 0.01
b = 0.9, IMin = 0.01
b = 0.6, IMin = 0.2
b = 0.9, IMin = 0.6

fig. 2

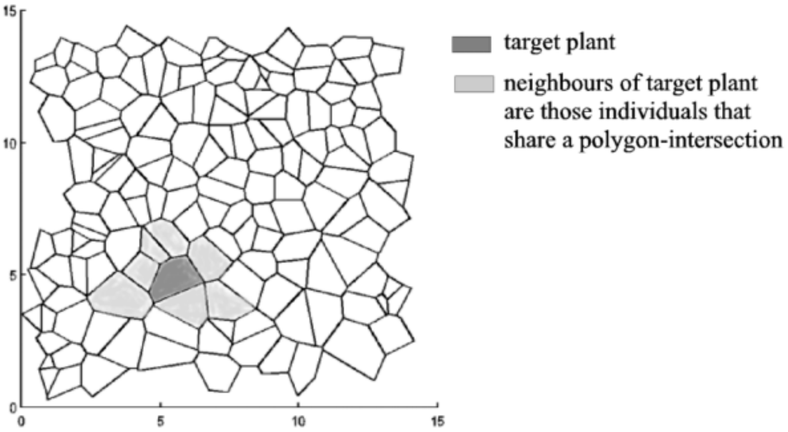
Calculation of C_α

fig. 3

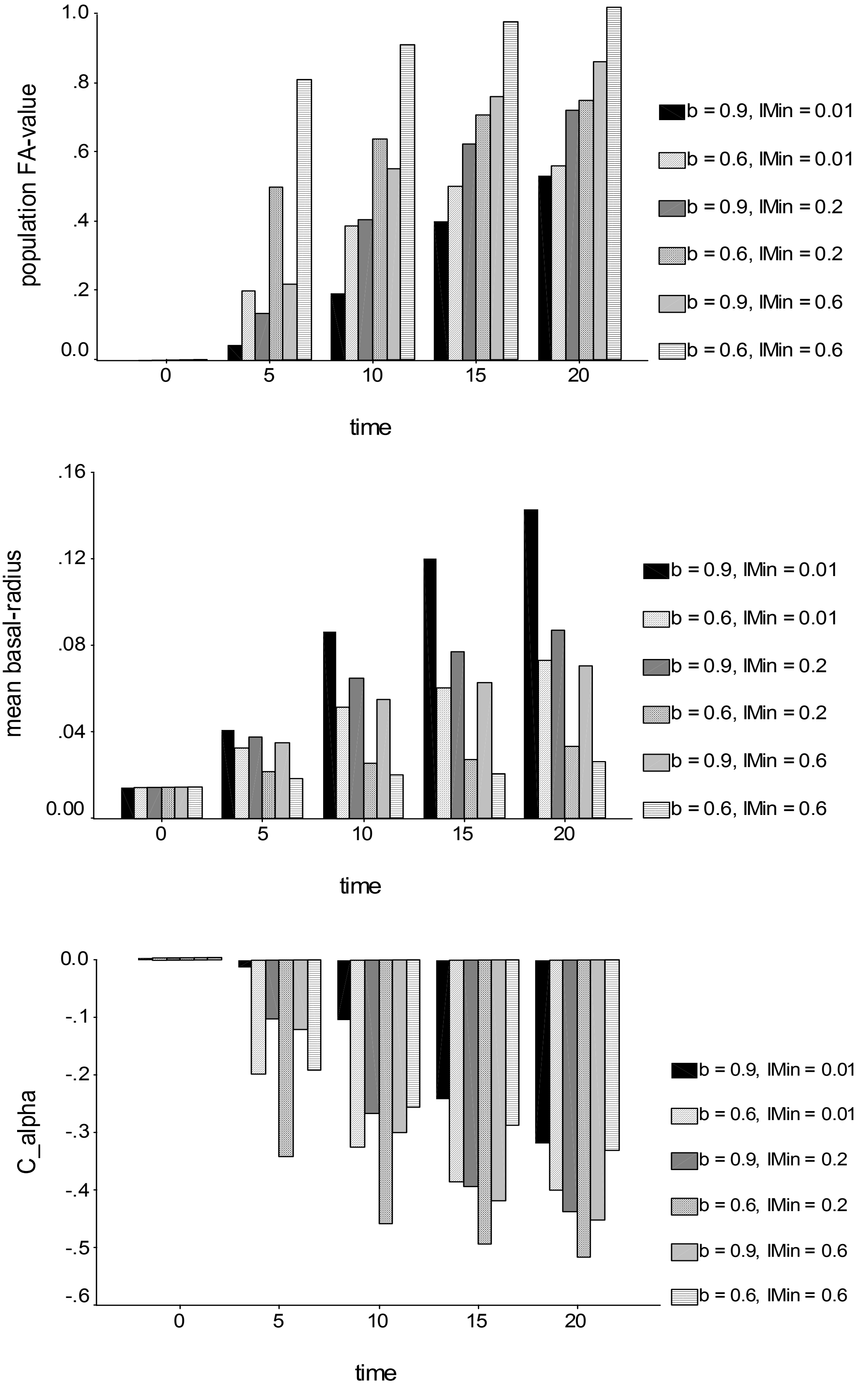
population FA-value
1.0
.8
.6
.4
.2
0.0
0
5
10
15
20
time
b = 0.9, lMin = 0.01
b = 0.6, lMin = 0.01
b = 0.9, lMin = 0.2
b = 0.6, lMin = 0.2
b = 0.9, lMin = 0.6
b = 0.6, lMin = 0.6
mean basal-radius
.16
.12
.08
.04
0.00
0
5
10
15
20
time
b = 0.9, lMin = 0.01
b = 0.6, lMin = 0.01
b = 0.9, lMin = 0.2
b = 0.6, lMin = 0.2
b = 0.9, lMin = 0.6
b = 0.6, lMin = 0.6
C_alpha
0.0
-.1
-.2
-.3
-.4
-.5
-.6
0
5
10
15
20
time
b = 0.9, lMin = 0.01
b = 0.6, lMin = 0.01
b = 0.9, lMin = 0.2
b = 0.6, lMin = 0.2
b = 0.9, lMin = 0.6
b = 0.6, lMin = 0.6

fig. 4

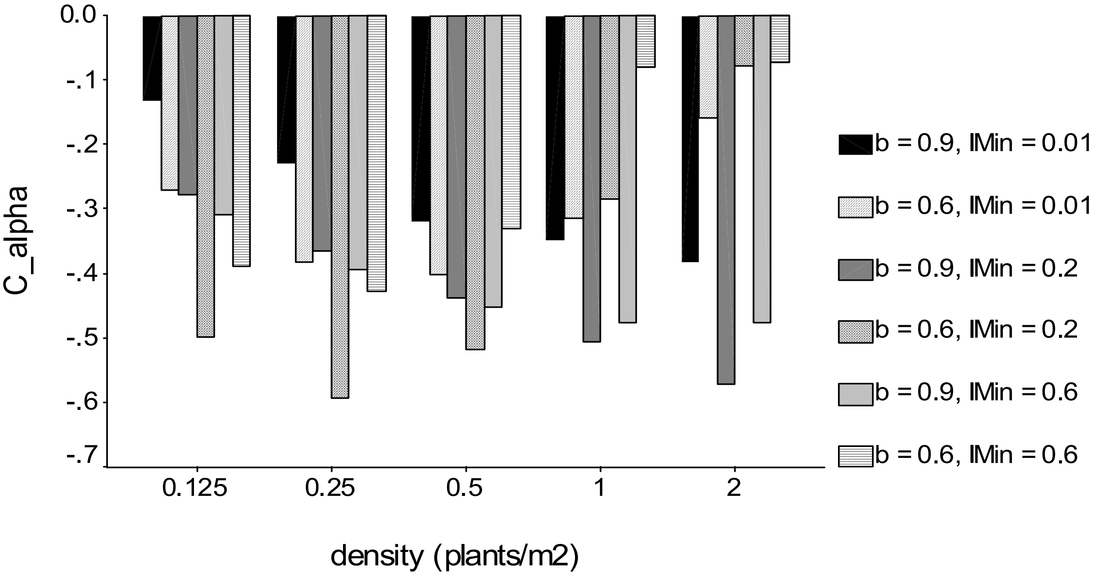
0.0
-.1
-.2
-.3
-.4
-.5
-.6
-.7
C_alpha
0.125
0.25
0.5
1
2
density (plants/m2)
b = 0.9, IMin = 0.01
b = 0.6, IMin = 0.01
b = 0.9, IMin = 0.2
b = 0.6, IMin = 0.2
b = 0.9, IMin = 0.6
b = 0.6, IMin = 0.6

fig. 5

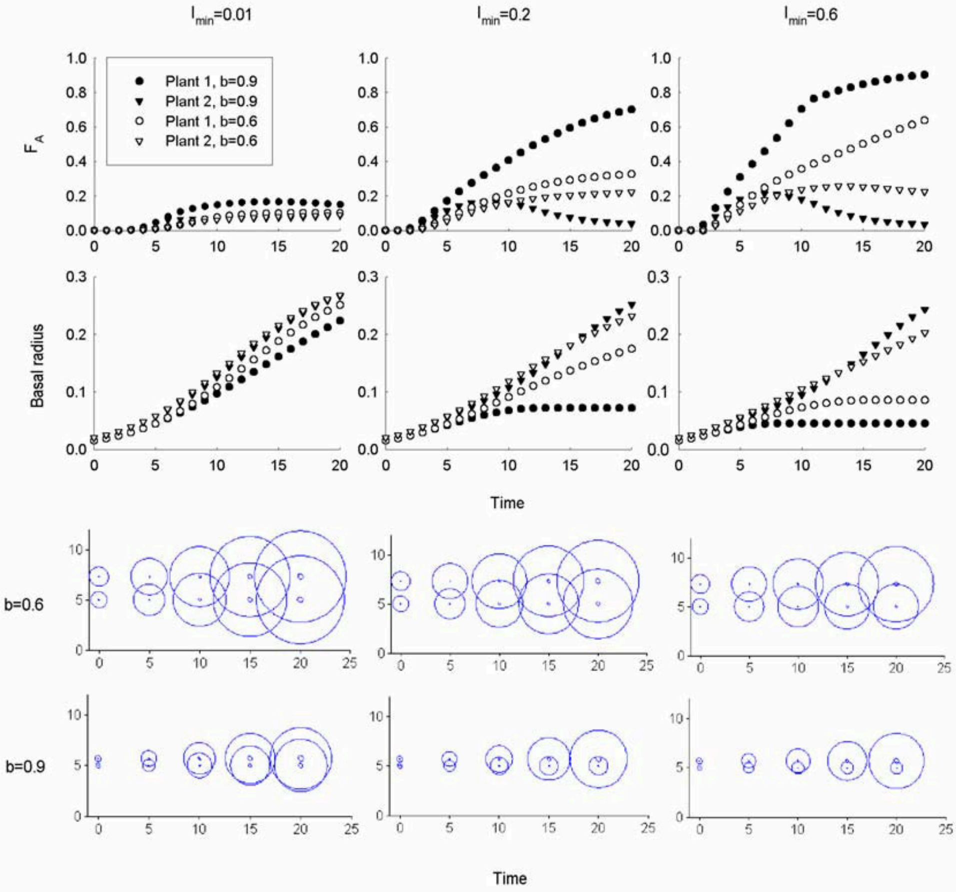
I_{min}=0.01
I_{min}=0.2
I_{min}=0.6
● Plant 1, b=0.9
▼ Plant 2, b=0.9
○ Plant 1, b=0.6
▽ Plant 2, b=0.6
F_A
1.0
0.8
0.6
0.4
0.2
0.0
0
5
10
15
20
Basal radius
0.3
0.2
0.1
0.0
Time
b=0.6
b=0.9
10
5
0
0
5
10
15
20
25
Time

fig. 6

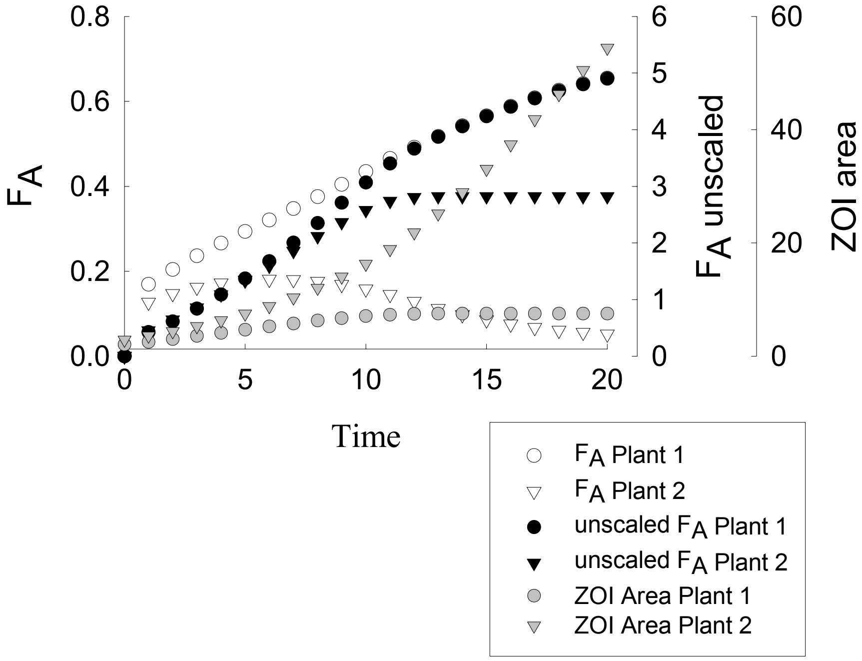
F_A
0.0
0.2
0.4
0.6
0.8
F_A unscaled
0
1
2
3
4
5
6
ZOI area
0
20
40
60
0
5
10
15
20
Time
F_A Plant 1
F_A Plant 2
unscaled F_A Plant 1
unscaled F_A Plant 2
ZOI Area Plant 1
ZOI Area Plant 2

Kapitel II,5

Towards a standard for the individual-based modeling of plant populations: self-thinning and the field-of-neighborhood approach

Uta Berger[1], Hanno Hildenbrandt[1] and Volker Grimm[2]

[1] Centre for Marine Tropical Ecology (ZMT), Bremen, Germany
[2] Centre for Environmental Research (UFZ), Leipzig-Halle, Germany

Natural Resource Modeling 15:39-54 (2002)

NATURAL RESOURCE MODELING
Volume 15, Number 1, Spring 2002

TOWARDS A STANDARD FOR THE INDIVIDUAL-BASED MODELING OF PLANT POPULATIONS: SELF-THINNING AND THE FIELD-OF-NEIGHBORHOOD APPROACH

UTA BERGER
Center for Tropical Marine Ecology
Fahrenheitstr. 1
28359 Bremen, Germany
E-mail: `uberger@zmt.uni-bremen.de`

HANNO HILDENBRANDT
Center for Tropical Marine Ecology
Fahrenheitstr. 1
28359 Bremen, Germany

VOLKER GRIMM
UFZ Centre for Environmental Research Leipzig-Halle
Department of Ecological Modelling
P.O. Box 500136
D-04301 Leipzig, Germany
E-mail: `vogri@oesa.ufz.de`

ABSTRACT. In classical theoretical ecology there are numerous standard models which are simple, generally applicable, and have well-known properties. These standard models are widely used as building blocks for all kinds of theoretical and applied models. In contrast, there is a total lack of standard individual-based models (IBM's), even though they are badly needed if the advantages of the individual-based approach are to be exploited more efficiently. We discuss the recently developed 'field-of-neighborhood' approach as a possible standard for modeling plant populations. In this approach, a plant is characterized by a circular zone of influence that grows with the plant, and a field of neighborhood that for each point within the zone of influence describes the strength of competition, i.e., growth reduction, on neighboring plants. Local competition is thus described phenomenologically. We show that a model of mangrove forest dynamics, KiWi, which is based on the FON approach, is capable of reproducing self-thinning trajectories in an almost textbook-like manner. In addition, we show that the entire biomass-density trajectory (*bdt*) can be divided into four sections which are related to the skewness of the stem diameter distributions of the cohort. The skewness shows two zero crossings during the complete development of the population. These zero crossings indicate the beginning and the end of the self-thinning process. A characteristic decay of the positive skewness accompanies the occurrence of a linear *bdt* section, the well-known self-thinning line. Although the slope of this line is not fixed, it is confined in two directions, with morphological constraints determining the lower limit and the strength of neighborhood competition exerted by the individuals marking the upper limit.

KEY WORDS: Individual-based model, standard model, phenomenological description, plant population, field of neighborhood, self-thinning, skewed size distribution, mangrove forest.

Introduction. During the last decade, individual-based modeling (Huston et al. [1988], DeAngelis and Gross [1992], Grimm [1999]) has become established in ecology. Due to the enormous increase and general availability of computing power, it became possible to model aspects of populations which had previously to be ignored in population level models because of the constraints of mathematical methodology, the main ones being individual heterogeneity, random variation, space, and local interactions. However, the 'unification' of ecological theory, which Huston et al. [1988] predicted would emerge from the individual-based approach, failed to materialize. In a review of individual-based models (IBM's) of animal populations, Grimm [1999] discusses possible reasons for this situation. He concludes that a lack of appropriate modeling strategies and strategies for analyzing individual-based simulation models is the main reason why more theories have not yet emerged.

We would like to emphasize an additional problem of the individual-based approach: in contrast to classical theoretical population ecology, there are to date no simple, generally applicable *standard* IBM's. In classical theory, there are many standard models which are widely used, e.g., the logistic equation, the Ricker model, the Lotka-Volterra models of competition and predator-prey interactions, and the Holling types of functional response. Even though after closer examination many of these classical standard models may be criticized or even rejected, they are still widely used because they are simple, generally applicable, and have well-known properties. They are generally accepted as building blocks for all sorts of models and thus provide a common framework for many different investigations.

By contrast, most IBM's are more or less developed from scratch. Time and again, modelers re-invent the wheel; they spend huge amounts of time and resources on developing, documenting, explain-ing and justifying their models. The major obstacle to unification is that the resulting models are hard to compare because of major differences between even the most basic model structures. We are not sure whether this unfortunate situation can in principle be overcome in animal population ecology because it seems hard to find a unified, general description of animals at the individual level (but see Lomnicki [1978], Grimm and Uchmanski [1994], Uchmanski [1999, 2000]). With plants, however, the prospect of a standard IBM seems more promising, because all plant species are sessile, and therefore the interactions between established plants are local and they basically require the same resources (Stoll and Weiner [2000]). A standard IBM of plant populations would have to describe interactions between neighboring plants in a sufficiently detailed but still general way.

In a recent review, Stoll and Weiner [2000] discuss key elements of modeling neighborhood interactions in plants: they should have an explicit location, a basal extension where no other plant can exist (i.e., stem, tussock, rosette), and a zone of influence on which interactions with other plants occur; moreover, the size and distance of neighboring plants should be taken into consideration. The two approaches taking account of these key elements are the 'zone of influence' (ZOI; Gates and Westcott [1978], Gates [1982], Wyszomirski [1983], Czárán and Bartha [1992], Czárán [1998]) and the 'ecological field' (EF; Wu et al. [1985], Walker et al. [1989]) approach. In ZOI models, individuals have a circular zone of influence whose resources they use. This zone grows as the plant grows. Competition between plants occurs when their zones of influence overlap. Although this approach is conceptually very simple, it has a number of snags: the division of resources on the overlapping area, i.e. the mode of interaction, has to be specified by the modeler (e.g., symmetric or asymmetric division of resources (Weiner [1990])), and thus does not emerge from the interaction (Railsback [2000]). And, for small plants, e.g., seedlings, which are completely inside the ZOI of another, adult plant, its position within the zone makes no differences with regard to its performance. Moreover, the resources for which plants compete are often not obvious, and in most cases competition will be for more than just one resource. Regarding this, ecological field models can be seen as improvements of ZOI models. They define a spatially explicit field within the zone of influence which indicates how strongly the plant modifies its environment, e.g. by resource use. This is more realistic than the ZOI approach that implicitly assumes a constant field, but the details of the EF approach are rather complicated, which may be why it has not yet been widely used.

To summarize, there seems to be no standard IBM approach in modeling plant populations. Yet such a standard is urgently needed, not only because of the theoretical unification which might emerge from such an approach, but also because many applied problems of natural resource modeling would benefit from an easy-to-use but still powerful approach. Berger and Hildenbrandt [2000] noticed the lack of such an approach when they started modeling mangrove forest dynamics within the Brazilian-German co-operation project MADAM (Berger et al. [1999], Lara et al. [1999], Thüllen and Berger [2000]). They could not use the grid-based (or cellular automaton) approach (Czárán [1998]), because this would have required more empirical knowledge about local interactions than is available for mangroves. Therefore, they developed a new approach from scratch, the 'field of neighborhood' (FON) approach, which combines the advantages of ZOI, EF and grid-based models while trying to avoid their drawbacks.

Although the FON approach was not designed to be a standard IBM approach for plants, it now seems as if it does indeed have some properties of such an approach: it is conceptually and computationally simple, it is realistic but still general, and, most importantly, it is phenomenological with regard to competition and thus very similar in philosophy to classical standard models which are also phenomenological with regard to the processes they describe.

The purpose of this article is to put forward evidence that, despite its phenomenological design, the FON approach is capable of reproducing realistic phenomena at the population level. To this end, one of the very few general patterns of ecology, the self-thinning line of plant monocultures, is analyzed with KiWi, a mangrove model using the FON approach (Berger and Hildenbrandt [2000]).

2. Self-Thinning. Yoda et al. [1963] have shown that during the so-called self-thinning stage of higher plant cohorts, the logarithms of the averaged biomass are linearly related to the logarithms of the stand density (Harper [1977], Westoby [1984], Silvertown [1992]). The proportionality factor between these two values, the 'self-thinning exponent,' was found to be $-3/2$. This finding was explained geometrically, i.e., by packing evenly sized plants with circular crowns in a plane, and its generality was postulated. Since then, numerous empirical and theoretical investigations have been presented which demonstrate that there are in fact other plant species for which the '$-3/2$ self-thinning rule' applies. However, many examples deviating from this rule have also been found (Weller [1987]). The current consensus is that a fixed value of the self-thinning exponent cannot be specified. However, whether there is a fixed boundary value that cannot generally be exceeded by the slopes of the self-thinning lines is still under discussion, with values of $-3/2$ or $-4/3$ being debated. An allometric explanation is provided for the latter, see, e.g., (White [1981], Enquist et al. [1998]).

The debate about self-thinning is controversial. The value of the thinning exponent is mainly questioned, but also whether the rule really merits this name or does not actually exist (Lonsdale [1990], Weller [1991]), whether the explanation of the linear section of the *bdt* is basically geometric or allometric (Westoby [1984]), and whether the 'line' really is a straight line or a concave curve (Zeide [1987]). Instead of taking up this debate here, we will focus on the following questions: Does the FON approach lead to self-thinning trajectories which can be observed in nature? And, can different parts of the *bdt* be attributed to different stages of development in the plant cohort, i.e., size hierarchies?

3. Methods. We use the KiWi simulation model (Berger and Hildenbrandt [2000]) which is an application of the FON approach. Since both KiWi and FON are described in detail in Berger and Hildenbrandt [2000], we confine our explanation in the following to the essentials.

3.1 The FON modeling approach. FON is the abbreviation for 'field of neighborhood.' This particular approach is based on the description of a 'zone of influence' (ZOI) according to which an individual is firstly characterized in terms of its (stem-) position. A circular zone whose diameter increases with the size of the individual surrounds this position. This zone defines the area within which the individual interacts with its environment and with potential neighbors. The extension of the FON approach as compared to the ZOI approach consists in a competition function of field that is defined within the ZOI. This field describes the location-dependent competition strength exerted by the individual on its neighbors and its environment. Assuming that the neighborhood fields of all individuals superimpose, two quantities are important (Figure 1): $F(x,y)$ quantifies the competition strength exerted by the established individuals at position (x,y), whereas F_A is a measure of the competition which an individual encounters from its neighbors. It is summarized from the overlapping parts of the neighborhood fields of all competitors and is related to the ZOI of the individual in focus, i.e., is normalized by the ZOI area A of the target plant. $F(x,y)$ and F_A thus indicate the neighborhood situation for a point and/or an individual defined in terms of the number of neighbors, their size and their spatial configuration.

3.2 The KiWi simulation model. KiWi applies the FON approach to the description of mangroves. The radius of the zone of influence is described by the expression:

$$a \cdot rbh^b \tag{1}$$

where rbh stands for the stem radius in breast height. The parameters a and b were first chosen arbitrarily. The neighborhood field within the stem is by definition equal to 1. Outside the stem, it decreases exponentially to the minimum value $FON_{\min}$, which is reached at the edge of the ZOI (Figure 1). KiWi uses only one level of description for all trees, regardless of size (Berger and Hildenbrandt [2000]). This compact handling is possible since the fields of neighborhood completely describe the competition effect on all demographic processes. Environmental factors such as pore water salinity or soil moisture are each described in separate description levels.

The growth of the trees is described according to Chen and Twilley [1998]: the annual increment in stem diameter is calculated using a sigmoid function which is valid for optimal environmental conditions. Damaging environmental factors are taken into account using correction factors. In addition to the salinity factor introduced by Chen and Twilley [1998], KiWi uses a correction factor for neighborhood competition (Berger and Hildenbrandt [2000]). It is equal to 1 if the tree has no competing neighbors. Otherwise, it decreases with increasing competition strength F_A. If $F_A \geq 0.5$, the correction factor is zero, which means the tree cannot grow. Obviously, growth is also influenced by

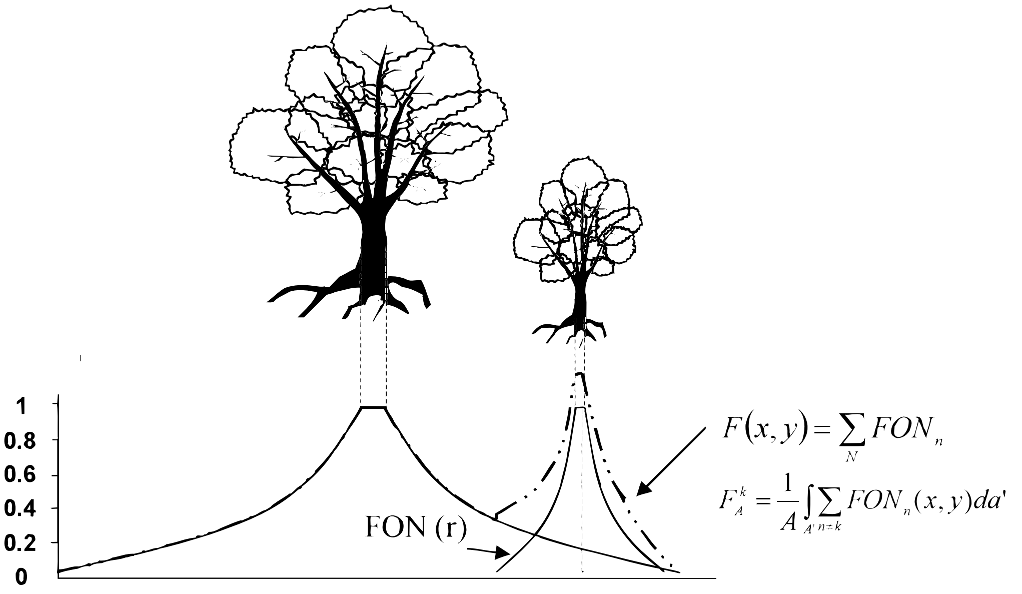

FIGURE 1. The *Field of Neighborhood* describes the competition strength that an individual exerts on its neighbors or on its environment. $F(x, y)$ indicates the competition strength of all established trees at the location (x, y). F_A records the competition that an individual encounters from its neighbors. A is the area of the zone of influence of the target plant.

other ecological factors such as salinity, nutrients and inundation. However, in this work we wish to concentrate on the effects of intra-specific competition. We therefore assume the dominant nutrients and moisture content of the sediment to be optimal. The pore water salinity may be benign, at ≤ 40 PSU.

Virtually nothing is known about the mean age of mangrove trees. References vary between 70 and 350 years for different species (Burns and Ogden [1985], Chen and Twilley [1998]). Therefore, mortality is not linked directly to the tree age in KiWi. Instead, we assume that the probability of dying will increase with reduced growth. In order to enable a tree to recover after a period of bad growth years, this relation is represented in a "memory function" (Berger and Hildenbrandt [2000]). According to this function, a tree dies if its mean stem diameter increase within 5 years is less than half the average increase it would have achieved under optimal conditions.

3.3 Simulations. Using the growth parameters of *Rhizophora mangle* (Chen and Twilley [1998]), the development of a mangrove cohort was simulated. The initial stem diameter of all trees was

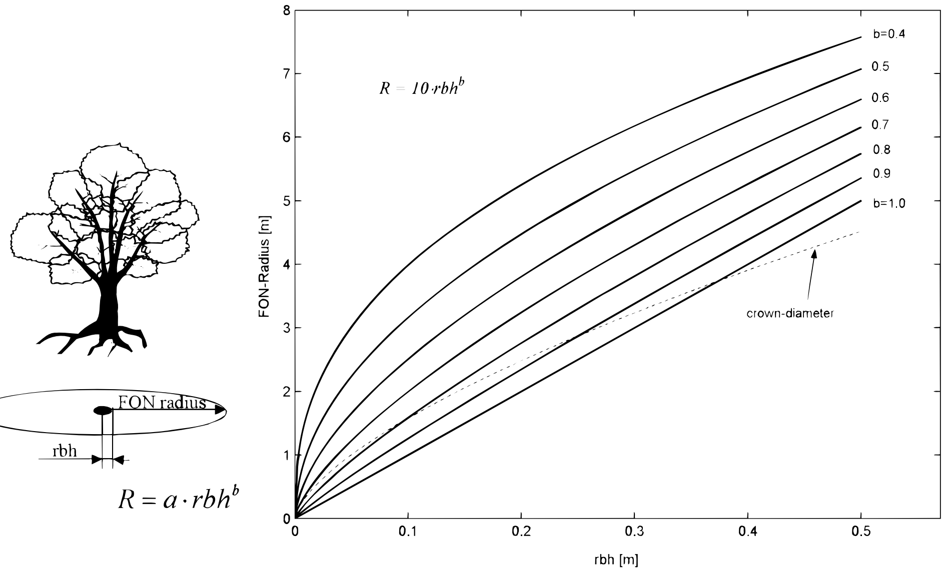

FIGURE 2. The FON radius (R) depends on the stem diameter of the tree. The curve of the crown diameter was calculated after Fromard et al. [1998].

1 cm. They were randomly distributed at a plot 1 ha in size. The initial density was 2,000 individuals per hectare. The influence of individual competition strength on the dynamics of the population was investigated. The competition strength was varied by the form and extension of the neighborhood field. For this, the parameter b of equation (1) was varied between 0.4 and 1.0, whereas $a = 10$ was held constant. Figure 2 shows that the FON radius increases if b decreases. Moreover, at a specific distance from the stem, the competition strength will be stronger the lower b is. For each b value, 50 simulations were carried out. The number of individuals and their stem diameter were registered in each simulation year. The biomass distribution of the trees was calculated on the basis of these data according to Fromard [1998]; Berger and Hildenbrandt [2000].

4. Results. As a result of the competition between the growing trees, the distribution of the stem diameters in breast height (*dbh*) widens in the course of development. Depending on their local neighborhood situations, some trees will be unobstructed at least for a while, and others will be slowed down. It was expected that a size hierarchy would develop, in which a few large trees would dominate many smaller ones as a result of this process. This characteristic of asymmetric com-

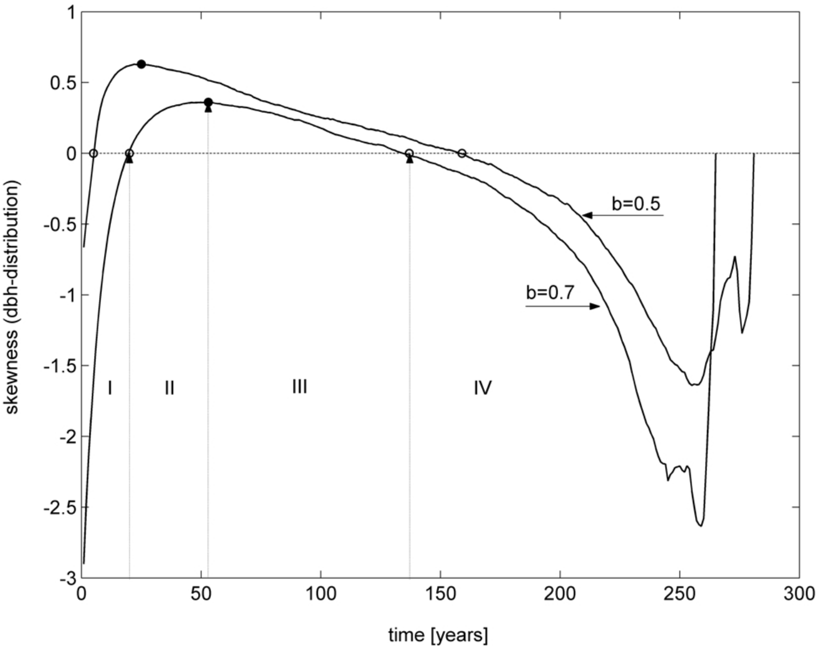

FIGURE 3. The skewness of the *dbh*, distribution over time. The curves for $b=0.5$ and $b=0.7$ were drawn as examples. The qualitative shape of the curves is the same for other values of b.

petition is regarded as typical of self-thinning populations, e.g., Adler [1996], Davie [1999]. It can be tracked by means of the skewness (third moment) of the stem diameter distribution. If skewness is negative there is a minority of small trees in the stand compared to a majority of larger ones. Positive skewness indicates that the cohort consists of a few large trees and many smaller ones.

Figure 3 shows the dynamics of the skewness for $b = 0.5$ and 0.7. The shape of these dynamics is identical for the entire range of b examined here. The first values were computed after one year of growth. They show that, at the beginning of the growth period, only a few trees are more strongly hindered in their growth than their neighbors. However, this negative skewness is quickly reduced during the growth process. A period follows in which the *dbh* distribution is positively skewed, as initially expected. The duration of this stage and the maximum skewness achieved increase with decreasing b which corresponds to, as explained above, increasing competition strength. An interpretation of the dynamics after 250 years is not feasible. The densities are so small here that any death of an individual can lead to a change of the skewness sign.

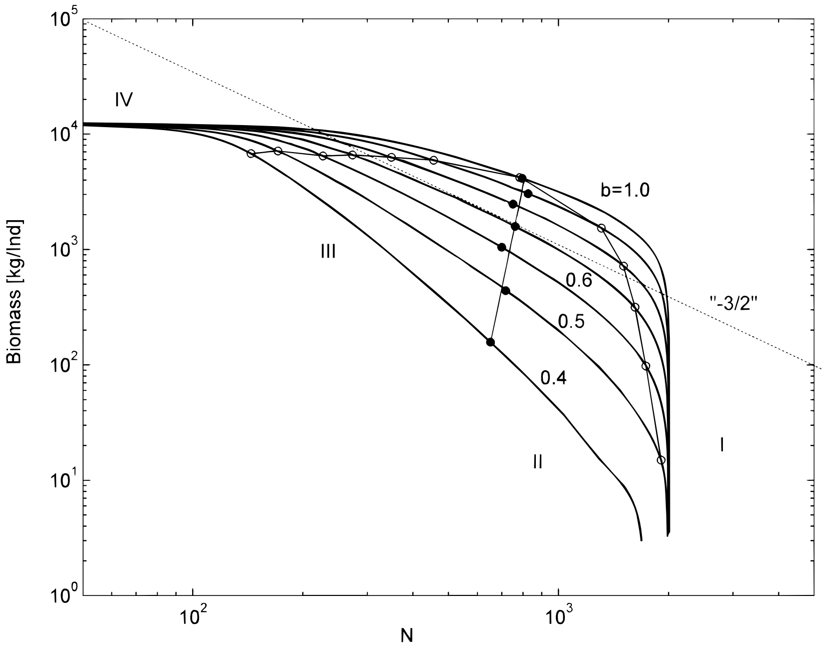

FIGURE 4. The biomass-density trajectories for different b values. The dots mark the crossover and the maximum skewness of the *dbh* distribution. They indicate different stages of the simulated development of the population, see Figure 3.

To relate the modification of the population structure presented in Figure 3 to the self-thinning of the cohort, the self-thinning trajectories for different competition strengths are plotted in Figure 4. The trajectories show the number of surviving individuals and their mean biomass during the development of the cohort. Since the first results were registered after one year, the *bdt* resulting from $b = 0.4$ does not originate from the same point as all others. Although all simulations were initialized with the same number of individuals, the high competition strength of the individuals realized in this case reduces the number of trees established compared to the scenarios with higher b values. In turn, the qualitative shape of the curves is similar for all b values examined and describes the stages of development of a cohort as they are described in textbooks, e.g., Begon et al. [1991], Silvertown [1992]. The direction of the trajectories, i.e., the course of time, is from bottom right to top left.

The first section is marked by a rapid increase in the biomass of the individuals. Mortality is not significant in the initial years because most plants do not experience any neighborhood at all. The onset of mortality due to the onset of local competition is indicated in the trajectory by the 'left turn,' and occurs more pronouncedly the greater the competition strength as specified by smaller b-values. The linear section of the trajectory that follows is the classical self-thinning line. For $b = 0.7$, a line with the 'classical' slope of $-3/2$ is attached to the trajectory. This line shows that stronger competition strength results in steeper slopes.

The trajectory bends away from the linear section as soon as the overall potential growth rate decreases to zero. Thus, the natural limitation of growth of the individuals becomes visible. The last curve section, parallel to the x-axis, indicates the maximum mean biomass that is attainable. Since the latter is determined by the growth parameters and not by the competition strength, it is identical for all b-values. However, the density at which the individuals can achieve this biomass increases with b. For this reason, the maximum absolute biomass increases if the individual competition strength becomes smaller. Assuming that there is no other resource limitation, the maximum absolute biomass consequently defines the optimal stand density of the area.

5. Discussion. We presented an analysis of self-thinning in a mangrove model, KiWi, which is based on a new approach to individual-based modeling of plant population dynamics, the FON ('field of neighborhood') approach. Since FON is a phenomenological approach, it was not clear whether it would produce realistic dynamics and structures at the population level. The results show that FON is indeed capable of reproducing such emergent properties. The self-thinning trajectory of growing plant monocultures was reproduced in an almost textbook-like manner.

To discuss the relationship between population structure and the development of the cohort, the crossover points (I and IV in Figure 3) and the maximum skewness of the *dbh* distribution (III) are marked in the *bdt* (Figure 4). They subdivide the trajectories into four characteristic sections. Section I contains the 'pure growth stage' of the cohort. Only a few trees are hindered in their growth such that they die by the end of this section. Sections II and III are defined by the crossover points and the maximum of the skewness dynamics. They mark the stage of 'asymmetric competition' and hence the process of self-thinning in the classical sense. However, whereas in Section II the logarithmic relation between the biomass increase and the density loss is not linear, Section III corresponds to the 'self-thinning line.' It is delineated by the maximum and the second crossover point of the skewness. The fourth section of the *bdt* is characterized by only little growth because the plants achieved almost maximum size.

Gates [1982] performs modeling experiments similar to those presented here, but uses the ZOI approach and does not consider mortality, i.e., self-thinning. Like us, he first finds negative skewness which then changes to zero and positive values. Weiner and Thomas [1986] review experiments on growth and self-thinning in plant monocultures and conclude that "during the development of an even-aged monospecific stand, size inequality increases over time until the onset of self-thinning, then inequality decreases as self-thinning progresses."

The results hitherto discussed can be summarized as follows:

1. The occurrence of self-induced mortality is not completely bound to a positive skewness of the stem diameter distribution.

2. In the first stage of asymmetric competition (Section II), the skewness of the size distribution increases despite the high mortality rate of the smallest trees. This explains the substantial differences in the growth rates of the residual trees.

3. The classical self-thinning line (Section III) is characterized by a decrease in the skewness of size distribution. Consequently, its occurrence is linked to the homogenization of the stem diameters of the surviving individuals.

4. The slope of the thinning line is determined by the individual competition strength. The greater the maximum (positive) skewness of the diameter distribution, the steeper the slope of the thinning line.

Since these results are of a qualitative nature, they are valid for all trajectories generated by the model. Now, by varying the FON parameter b, almost any slope of the self-thinning line could be achieved. At first, we chose its value arbitrarily but looked for a limitation of the range that could be adequate for the description of the development of *R. mangle* cohorts under optimal conditions. Since for this purpose no survey data are available, a direct parameter estimation is not possible. However, the field of the potentially possible curves is indirectly limitable. For this purpose, the crown diameter was drawn in Figure 2 depending on the stem radius (Fromard et al. [1998]). If we assume that this diameter determines the minimum space a tree requires, then b parameters which result in very small FON diameters are unrealistic, as they lead to tree densities per area which cannot naturally occur. For the biomass-density trajectories in Figure 4, this means that no curves are allowed for $b > 0.7$. For this reason, the following general hypothesis is produced with regard to the slope of the self-thinning line for cohorts that develop under natural, optimal conditions: the slope of the self-thinning line is downwardly limited by the physical extension of the individuals (and, therefore, morphological constraints of the species) and upwardly by the individual competition strength. In this case, the morphological boundaries need not always be directly perceptible. A limitation is possible over the entire root area, for example. The curves in Figure 4 refute the thesis of a universal, fixed self-thinning factor. Depending on competition strength and the minimum area claim of the individuals, different self-thinning lines must be expected.

Although FON and KiWi were not at all designed to perform theoretical studies like that of self-thinning presented here, we were surprised by how well essential features of self-thinning were reproduced and how easy it was to examine features of the self-thinning trajectories with regard to individual characteristics, e.g., competition strength. This 'natural' performance of our model led us to wonder whether FON could possibly be a candidate for a standard in the individual-based modeling of plant populations. It seems as if realism and the phenomenological description of local interactions are combined in just the right balance needed for a standard model. Of course, a model can never be declared a standard model by its constructors but has to be pronounced a standard by the scientific community. Therefore, our goal here was not to immodestly declare the FON approach as a standard model, but to pinpoint two essentials of individual-based modeling which have not previously been considered explicitly: First, individual-based modeling needs, besides models which are tailored to specific situations, standards. This is not only important for theoretical unification, but also for applied issues, such as modeling natural resources. Applied models could be constructed much more effectively if standard approaches with known properties existed. A model similar to KiWi could, for example, easily be constructed for grassland dynamics. And second, a standard model would, at least partly, have to rely on a phenomenological description of key processes in order to be generally applicable. What we tried to show is that such a description is possible not only in classical population level models, but also in individual-based models.

Acknowledgments. The authors are grateful to Jacob Weiner, Tomasz Wyszomirski and an anonymous reviewer for their helpful comments on an earlier version of the manuscript. This paper resulted from the cooperation between the Center for Tropical Marine Ecology (ZMT), Bremen, Germany, and the Universidade Federal do Pará (UFPa), Belém, Brazil, under the Governmental Agreement on Cooperation in the Field of Scientific Research and Technological Development between Germany and Brazil, financed by the German Ministry of Education, Science, Research and Technology (BMBF) [Project number: 03F0253A, Mangrove Management and Dynamics, MADAM], and the Conselho Nacional de Pesquisa e Tecnologia (CNPq). This is MADAM contribution number 30.

REFERENCES

F.R. Adler [1996], *A Model of Self-Thinning through Local Competition*, Proc. National Acad. Sci. **93**, 9980–9984.

M. Begon, J.L. Harper and C.R. Townsend [1991], *Ökologie: Individuen, Populationen und Lebensgemeinschaften*, Birkhäuser Verlag, Basel.

U. Berger and H. Hildenbrandt [2000], *A New Approach to Spatially Explicit Modelling of Forest Dynamics: Spacing, Ageing and Neighborhood Competition of Mangrove Trees*, Ecological Modelling **132**, 287–302.

U. Berger, M. Glaser, B. Koch, G. Krause, R. Lara, U. Saint-Paul, D. Schories and M. Wolff [1999], MADAM—*the Approach of an Integrated Project on Mangrove Dynamics and Management*, J. Coastal Conservation **5**, 125–134.

B.R. Burns and J. Ogden [1985], *The Demography of the Temperate Mangrove* Avicennia marina (*Forsk.*) *Vierh. at Its Southern Limit in New Zealand*, Austral. J. Ecology **10**, 125–133.

R. Chen and R.R. Twilley [1998], *A Gap Dynamic Model of Mangrove Forest Development along Gradients of Soil Salinity and Nutrient Resources*, J. Ecology **86**, 37–51.

T. Czárán and S. Bartha [1992], *Spatiotemporal Dynamic Models of Plant Populations and Communities*, Trends in Ecology & Evolution **7**, 38–42.

T. Czárán [1998], *Spatiotemporal Models of Population and Community Dynamics*, Chapman & Hall, London.

T.J.A. Davie [1999], *A Numerical Model to Quantify the Growth of a Canopy for a Forest Hydrology Model*, Appl. Geography **19**, 45–67.

D.L. DeAngelis and L.J. Gross [1992], *Individual-Based Models and Approaches in Ecology*, Chapman and Hall, New York.

B.J. Enquist, J.H. Brown and G.B. West [1998], *Allometric Scaling of Plant Energetics*, Nature **395**, 163.

F. Fromard, H. Puig, E. Mougin, G. Marty, J.L. Bétoulle and L. Cadamuro [1998], *Structure, Above-Ground Biomass and Dynamics of Mangrove Ecosystems: New Data from French Guiana*, Oecologia **115**, 39–53.

D.J. Gates [1982], *Competition and Skewness in Plantation*, J. Theoret. Biology **94**, 909–922.

D.J. Gates and M. Westcott [1978], *Zone of Influence Models for Competition in Plantations*, Adv. in Appl. Probab. **10**, 299–537.

V. Grimm [1999], *Ten Years of Individual-Based Modelling in Ecology: What Have We Learned, and What Could We Learn in the Future?*, Ecological Modelling **115**, 129–148.

V. Grimm and J. Uchmanski [1994], *Ecological Systems are not Dynamic Systems: Some Consequences of Individual Variability*, in *Predictability and Nonlinear Modelling in Natural Sciences and Economics* (J. Grasman and G. van Straten, eds.), Kluwer, Dordrecht, 248–260.

J.L. Harper [1977], *The Population Biology of Plants*, Academic Press, London.

M. Huston, D. DeAngelis and W. Post [1988], *New Computer Models Unify Ecological Theory*, BioScience **38**, 682–691.

R.J. Lara, U. Berger and M. Cohen [1999], *Mangrove Degradation by Sand Deposition in Bragança, North Brazil*, in *Tidal Action, Tidal Processes and Tidal Effects on Coastal Evolution* (J.M.L. Dominguez, L. Martin, V. Testa, and E. Koutsoukos, eds.), Porto Seguro, Brazil.

A. Lomnicki [1978], *Individual Differences between Animals and the Natural Regulation of Their Numbers*, J. Animal Ecol. **47**, 461–475.

W.M. Lonsdale [1990], *The Self-Thinning Rule: Dead or Alive?*, Ecology **71**, 1373–1388.

S.F. Railsback [2001], *Concepts from Complex Adative Systems as a Framework for Individual-Based Modelling*, Ecological Modelling **139**, 47–62.

J.W. Silvertown [1992], *Introduction to Plant Population Ecology*, Longman Scientific & Technical Publ., Essex, England.

P. Stoll and J. Weiner [2000], *A Neighborhood View of Interactions among Individual Plants*, *The Geometry of Ecological Interactions—Simplifying Spatial Complexity* (U. Dieckmann, R. Law and J.A.J. Metz, eds.), Cambridge Stud. Adaptive Dynamics, Cambridge Univer. Press, Cambridge, 11–27.

N. Thüllen and U. Berger [2000], *A Comparative Examination of Environmental Factors at Patchy Mangrove Seedling Stands at the Peninsula of Bragança, Northern Brazil*, Ecotropica **6**, 1–12.

J. Uchmanski [1999], *What Promotes Persistence of a Single Population: An Individual-Based Model*, Ecological Modelling **115**, 227–242.

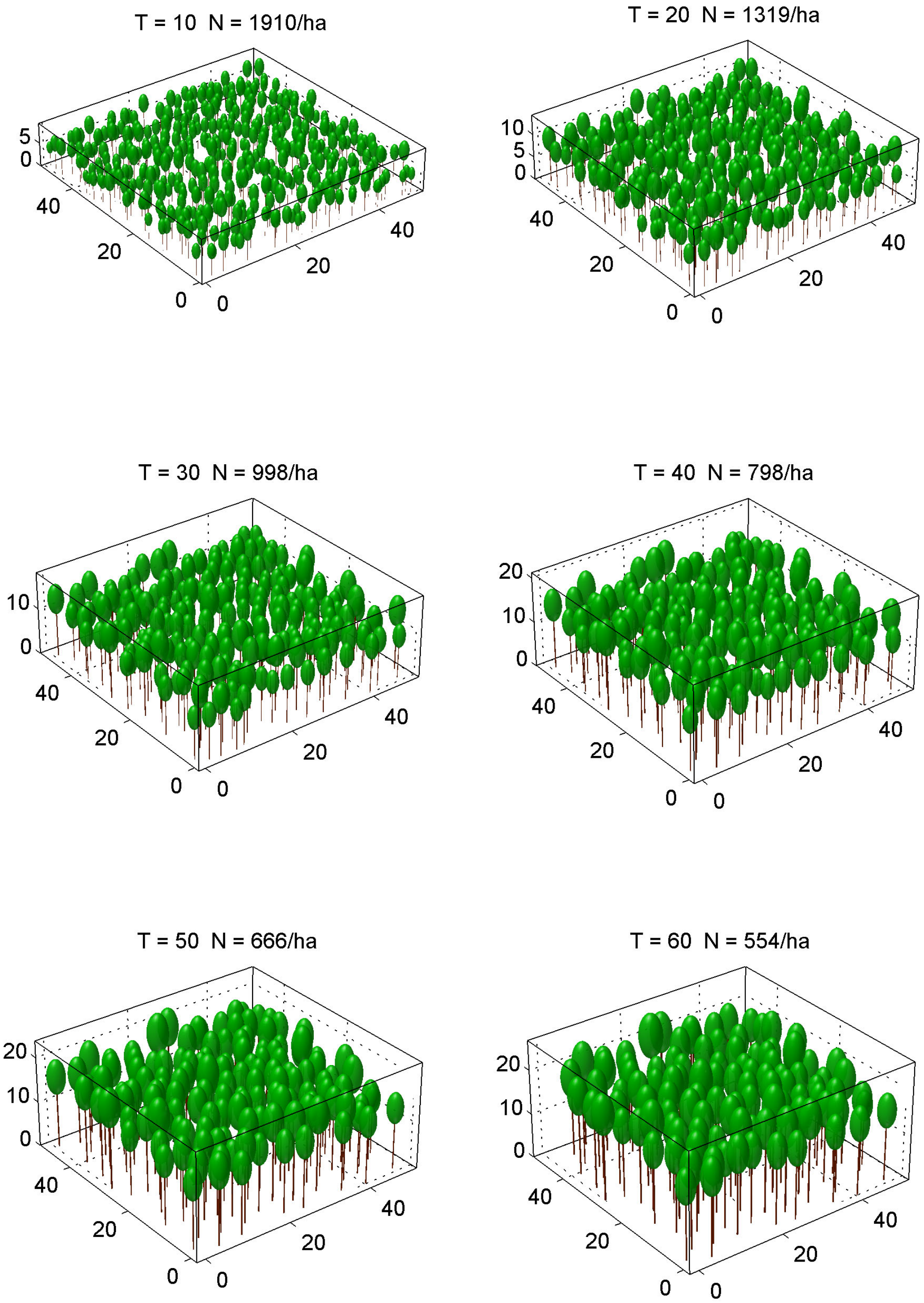

Tafel 1: Simuliertes Kohortenwachstum von *Rhizophora mangle* in KiWi. T ist der Zeitpunkt in Jahren nach der zufälligen Ansiedlung von N = 2000 Individuen auf einem Hektar. In den frühen Jahren der Selbstausdünnung bildet sich eine relativ breite Größenverteilung heraus.

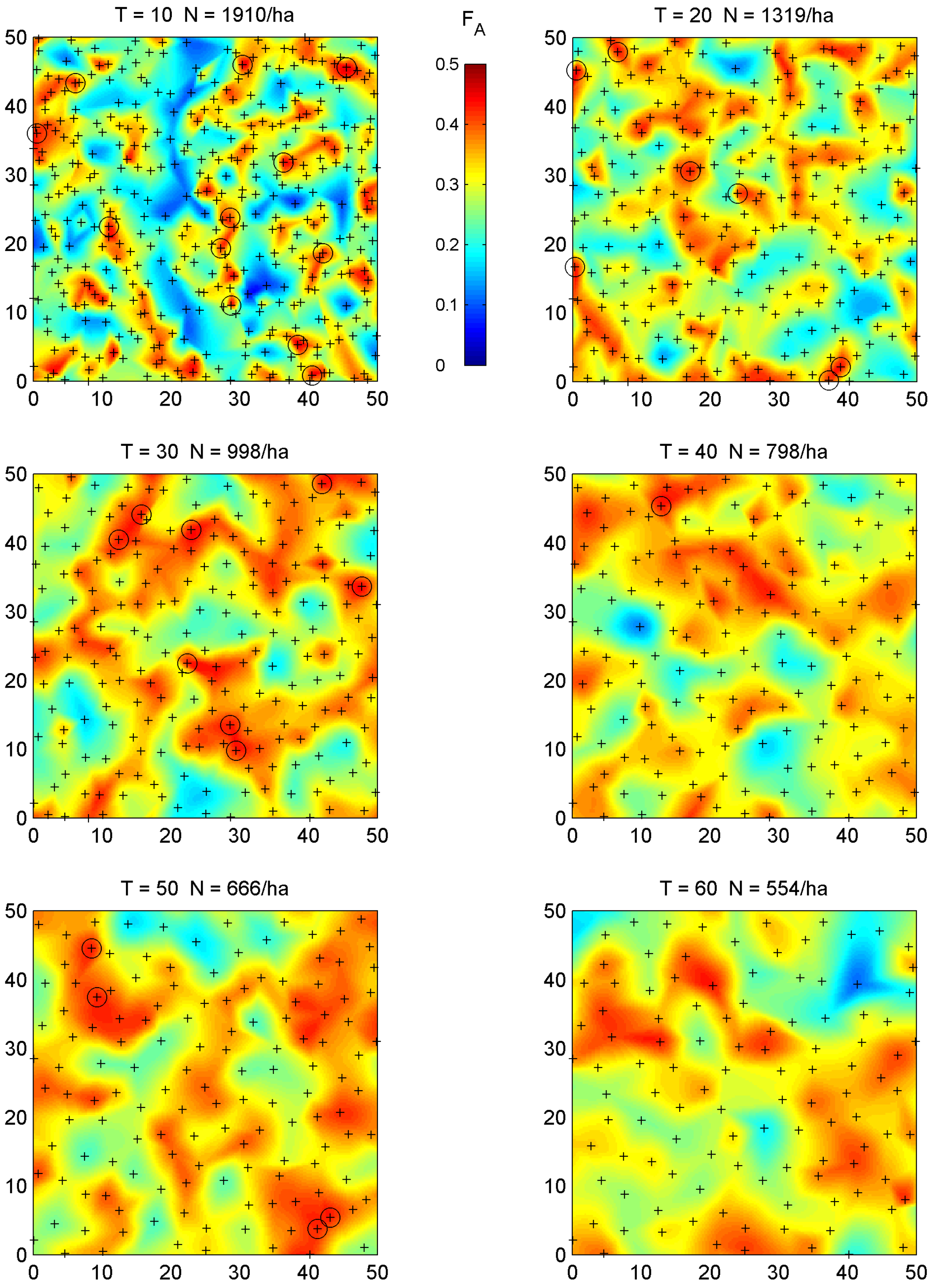
T = 10 N = 1910/ha

T = 20 N = 1319/ha

T = 30 N = 998/ha

T = 40 N = 798/ha

T = 50 N = 666/ha

T = 60 N = 554/ha

Tafel 2: Die gleichen Entwicklungszeitpunkte wie in Tafel 1. Die Farben stellen die (interpolierten) F_A-Werte der Pflanzen dar. In roten Bereichen herrscht erhöhter Konkurrenzdruck, der sich in geringerem Wachstum und erhöhter Mortälität auswirkt. Ein Kreuz markiert den Standort einer Pflanze, ein zusätzlicher Kringel zeigt an, dass die Pflanze das betreffende Jahr nicht überleben wird.

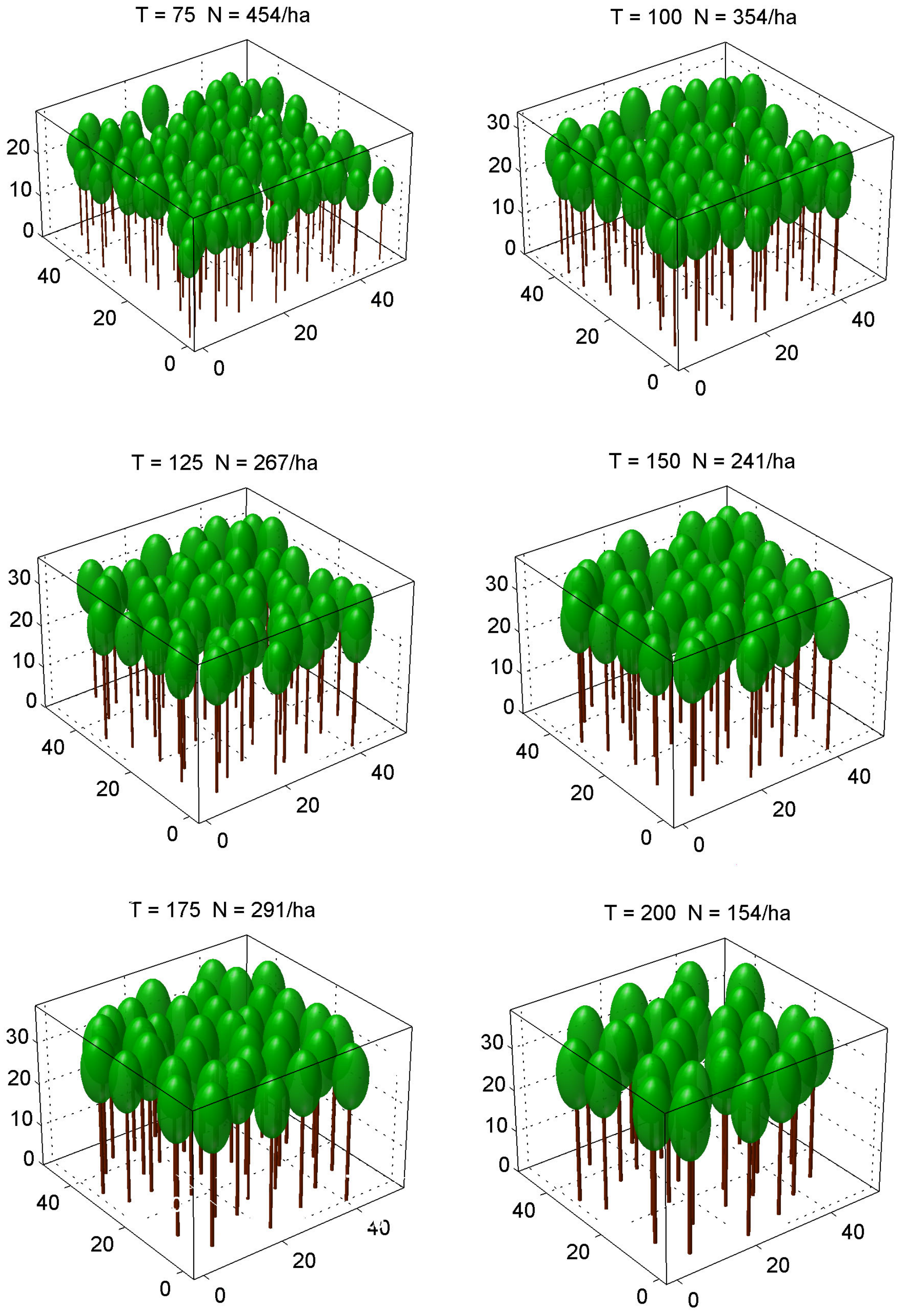
T = 75 N = 454/ha

T = 100 N = 354/ha

T = 125 N = 267/ha

T = 150 N = 241/ha

T = 175 N = 291/ha

T = 200 N = 154/ha

Tafel 3: Die späten Jahre der Bestandsentwicklung (s. Tafel 1 & 2). Gegen Ende bildet sich eine sehr regelmäßige Struktur heraus. Räumlich stehen die Bäume nun nahezu äquidistant. Die Größenverteilung wird immer schmaler bis die Bäume schließlich fast gleiche Größe erreichen.

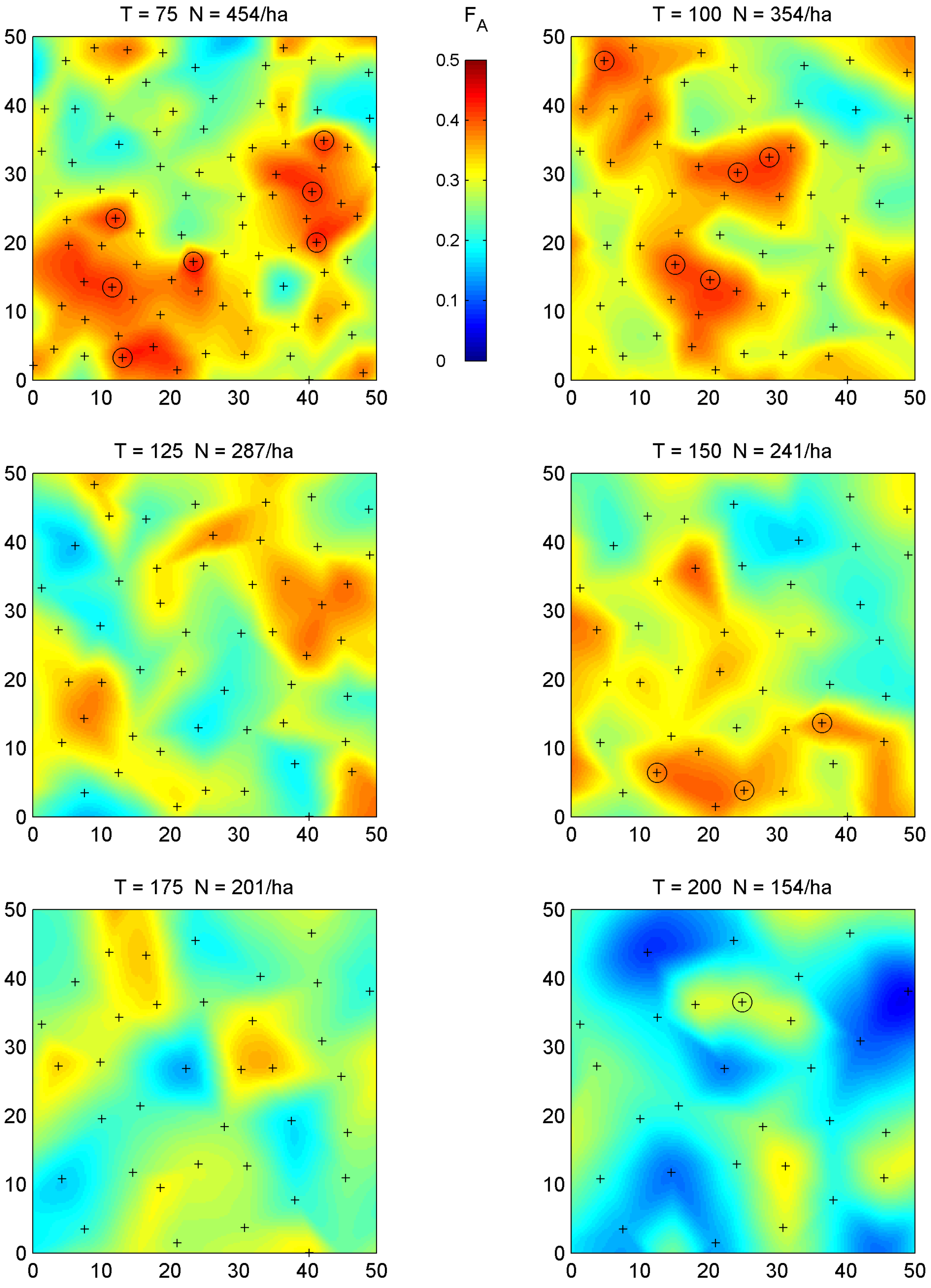

Tafel 4: Die gleichen Entwicklungszeitpunkt wie in Tafel 3 im Konkurrenz-Bild (F_A). Der Konkurrenz-Druck lässt ganz langsam nach (die Kringel markieren hier Bäume, die innerhalb der nächsten 10 Jahre absterben werden). Ab etwa T=175 Jahren ist der Endzustand der Selbstausdünnung erreicht. Später wirk hauptsächlich Altersmortalität.

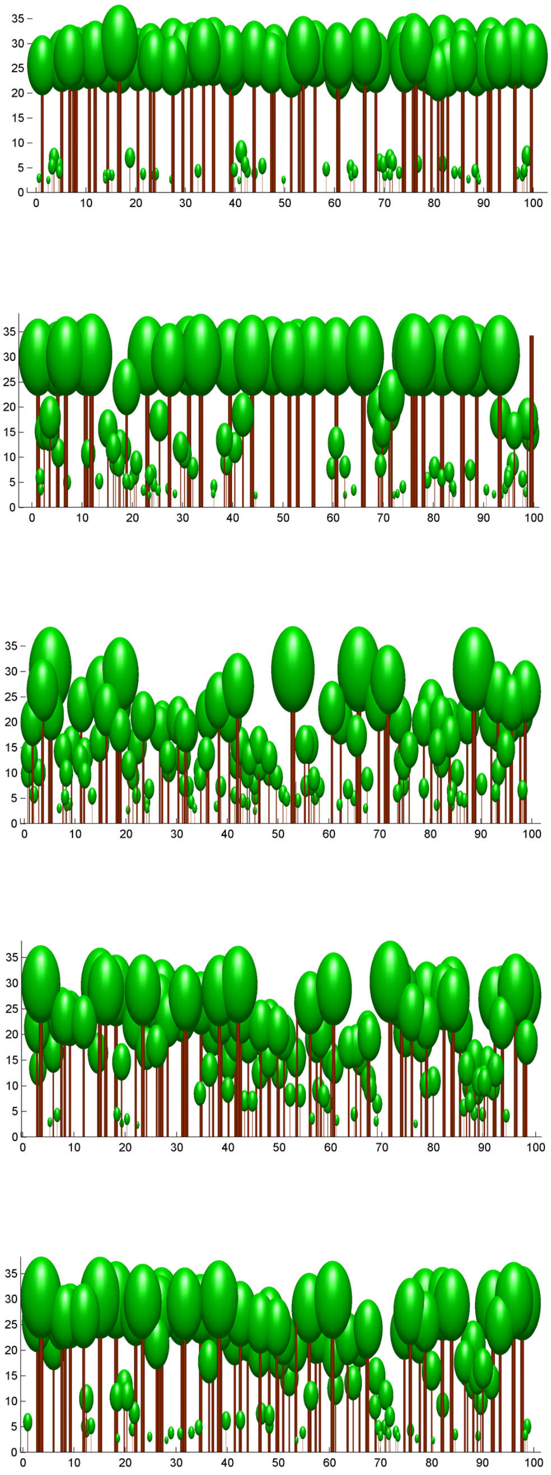

Tafel 5: Natürliche Verjüngung eines Bestandes von *Rhizophora mangle*. Gezeigt ist ein 100x10m Profil aus einer KiWi-Simulation, die auf einem Hektar ablief. Von oben (in der Terminologie der Theorie der Mosaikzyklen): Optimalstadium; beginnendes Zerfallsstadium; Übergang in das Heranwachsstadium; Heranwachsstadium; Übergang in neues Optimalstadium. Der gezeigte Zeitraum beträgt etwa 200 Jahre.